LIÈGE université
Gembloux
Agro-Bio Tech

PONTIFICIA
UNIVERSIDAD
CATÓLICA DE
VALPARAÍSO

UNIVERSIDAD TECNICA
FEDERICO SANTA MARIA

Development of metabolic engineering strategies in *Komagataella phaffii* for the reduction of cellular methanol requirements based on the cellular response to non-repressive compounds of the *pAOX1* promoter

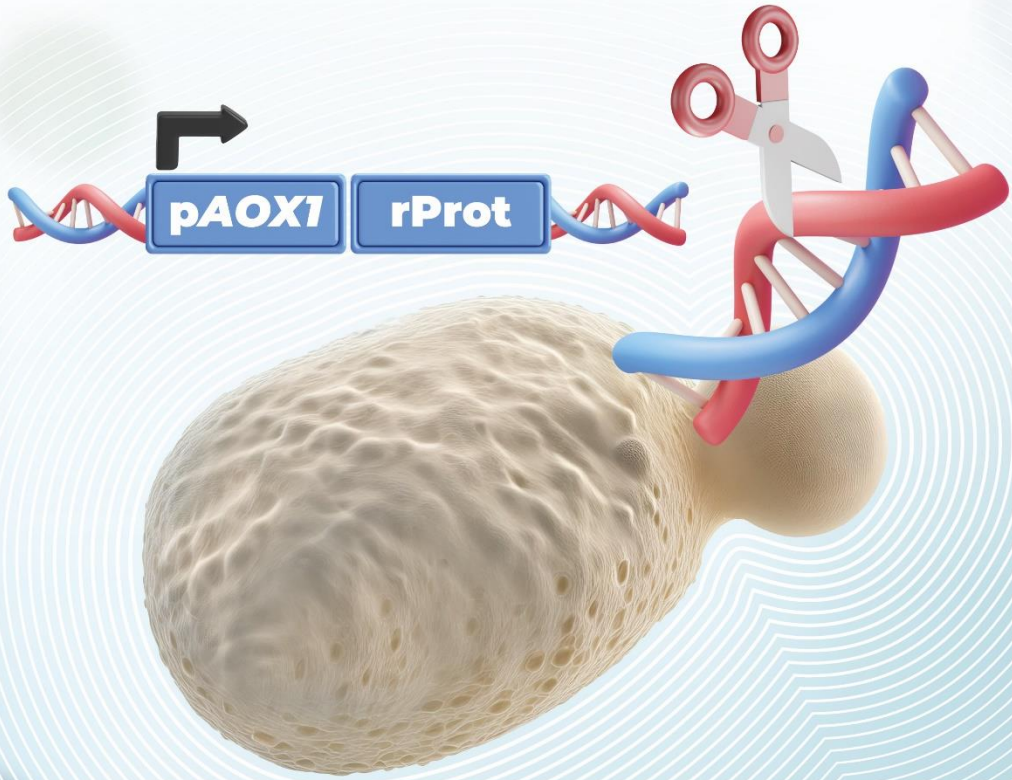

Author: Cristina Verónica Bustos Cosios

Supervisors: Prof. Dr. Patrick FICKERS and Prof. Dr. Julio BERRIOS.

Year 2025

COMMUNAUTÉ FRANÇAISE DE BELGIQUE
UNIVERSITÉ DE LIÈGE – GEMBLOUX AGRO-BIO TECH
PONTIFICIA UNIVERSIDAD CATÓLICA DE VALPARAÍSO
UNIVERSIDAD TÉCNICA FEDERICO SANTA MARÍA

Development of metabolic engineering strategies in *Komagataella phaffii* for the reduction of cellular methanol requirements based on the cellular response to non-repressive compounds of the *pAOX1* promoter

Cristina Verónica BUSTOS COSIOS

Dissertation submitted in partial fulfillment of the requirements for the degree of
Doctor of Philosophy in Agronomic Sciences and Biological Engineering - University of Liège
&
Doctor in Biotechnology – Pontificia Universidad Católica de Valparaíso – Universidad Técnica Federico Santa María

Supervisors: Prof. Dr. Patrick FICKERS and Prof. Dr. Julio BERRIOS

Year: 2025

Abstract

Cristina Verónica Bustos Cosios (2025). "Development of metabolic engineering strategies in *Komagataella phaffii* for the reduction of cellular methanol requirements based on the cellular response to non-repressive compounds of the *pAOX1* promoter" (PhD dissertation in English). Gembloux, Belgium, Gembloux Agro-Bio Tech, University of Liege. 103 pages, 25 figures, 9 tables

The methylotrophic yeast *Komagataella phaffii* (formerly *Pichia pastoris*) is widely recognized as a prominent platform for recombinant protein (rProt) production. This yeast is capable of oxidizing methanol to support energy production and biomass formation. In this non-conventional yeast, the methanol-regulated p*AOX1* promoter has been widely used to drive the expression of recombinant proteins. However, the use of methanol raises significant safety concerns due to its high flammability, particularly in large-scale industrial applications. Consequently, the main objective of this thesis was to explore alternatives to reduce or eliminate the reliance on methanol.

In this framework, disruption of the formate dehydrogenase gene (*FDH1*) was employed as a strategy to modify the p*AOX1* expression system. This genome edition successfully converted the system into a self-inducing platform for rProt synthesis, eliminating the need for methanol or other inducers to trigger gene expression. Further investigation revealed that this induction mechanism is mediated by cytoplasmic formate generated from THF-C1 metabolism, which cannot be converted to carbon dioxide in an *FDH1* knockout strain. Notably, this discovery showed that the p*AOX1* promoter could be induced under non-repressive conditions, such as in the presence of sorbitol. The efficacy of this system was demonstrated through the synthesis of two model proteins: intracellular eGFP and secreted CalB lipase from *Candida antarctica*.

Further into this investigation, metabolic engineering efforts focused on optimizing sorbitol uptake to enhance cell growth and rProt production in the *FDH1* knockout strain. Sorbitol metabolism was identified as the bottleneck, and overexpression of the sorbitol dehydrogenase gene (*SOR1*) significantly improved the growth in *K. phaffii*, leading to a 2.5-fold increase in specific cell growth rate. Despite these improvements, an unexpected impairment in p*AOX1* induction was observed. This study proposes several hypotheses to explain this issue, which are discussed in detail in this work.

Overall, this investigation lays the groundwork for a deeper understanding of p*AOX1* induction and highlights new avenues for exploring the underlying regulatory mechanisms. These insights will be pivotal in optimizing the system's potential for advancing biotechnological applications in this innovative methanol-free platform.

Keywords: *Pichia pastoris*, *Komagataella phaffii*, cell engineer, formate dehydrogenase, tetrahydrofolate-mediated one-carbon metabolism, methanol-free system, sorbitol dehydrogenase, sorbitol.

Résumé

Cristina Verónica Bustos Cosios (2025). "Développement de stratégies d'ingénierie métabolique chez Komagataella phaffii pour la réduction des besoins cellulaires en méthanol basées sur la réponse cellulaire aux composés non répressifs du promoteur p*AOX1*" (Thèse de doctorat en anglais).

Gembloux, Belgique, Gembloux Agro-Bio Tech, Université de Liège,103 pages, 25 figures, 9 tableaux

La levure méthylotrophe *Komagataella phaffii* (anciennement *Pichia pastoris*) est largement reconnue comme une plateforme de choix pour la production de protéines recombinantes (rProt). Cette levure est capable d'oxyder le méthanol pour soutenir la production d'énergie et la formation de biomasse. Dans cette levure non conventionnelle, le promoteur *pAOX1*, régulé par le méthanol, a été largement utilisé pour réguler la production de protéines recombinantes. Cependant, l'utilisation du méthanol présente quelques inconvénients, notamment en matière de sécurité en raison son inflammabilité, en particulier dans les applications industrielles à grande échelle. Par conséquent, l'objectif principal de cette thèse a été d'explorer des alternatives pour réduire ou éliminer la dépendance au méthanol.

Dans ce travail, la disruption du gène codant pour la formate déshydrogénase (*FDH1*) a été utilisée comme stratégie pour modifier le système d'expression *pAOX1*. Cette modification a permis de convertir le système en une plateforme auto-inductive, éliminant ainsi l'utilisation de méthanol comme inducteur de l'expression génique. Nos recherches ont révélé que ce mécanisme d'induction est médié par le formate cytoplasmique généré par le métabolisme du THF-C1 ; ce formate ne pouvant pas être converti en dioxyde de carbone dans une souche knockout *FDH1*. Cette découverte a montré que le promoteur *pAOX1* pouvait être induit dans des conditions non répressives, notamment en présence de sorbitol. L'efficacité de ce système a été démontrée par la synthèse de deux protéines modèles : l'eGFP intracellulaire et la lipase extracellulaire CalB de *Candida antarctica*.

Par la suite, notre stratégie d'ingénierie métabolique a été axé sur l'optimisation de l'absorption du sorbitol pour améliorer la croissance cellulaire et la production de rProt dans la souche knockout *FDH1*. Le métabolisme du sorbitol a été identifié comme un goulet d'étranglement, et la surexpression du gène de la sorbitol déshydrogénase (*SOR1*) a considérablement amélioré la croissance de *K. phaffii*, conduisant à une augmentation de 2,5 fois de la croissance cellulaire spécifique. Malgré ces améliorations, une réduction du niveau d'induction du *pAOX1* a été observée. Cette étude propose plusieurs hypothèses pour expliquer ce phénomène.

Ce travail jette les bases d'une compréhension plus approfondie de l'induction du promoteur *pAOX1* et met en lumière de nouvelles voies d'exploration des mécanismes de régulation sous-jacents. Ces connaissances seront essentielles pour optimiser le

potentiel de ce système dans l'avancement des applications biotechnologiques sur cette plateforme innovante sans méthanol.

Mots-clés : *Pichia pastoris*, *Komagataella phaffii*, ingénierie cellulaire, formate déshydrogénase, métabolisme à un carbone médié par le tétrahydrofolate, système sans méthanol, sorbitol déshydrogénase, sorbitol.

Resumen

Cristina Verónica Bustos Cosios (2025). "Desarrollo de estrategias de ingeniería metabólica en *Komagataella phaffii* para la reducción de los requerimientos celulares de metanol, basadas en la respuesta de celular a compuestos no represores del promotor p*AOX1*" (Tesis doctoral en inglés). Gembloux, Bélgica, Gembloux Agro-Bio Tech, Universidad de Liege. 103 páginas, 25 figuras, 9 tablas

La levadura metilotrófica *Komagataella phaffii* (anteriormente *Pichia pastoris*) es ampliamente reconocida como una plataforma destacada para la producción de proteínas recombinantes (rProt). Esta levadura es capaz de oxidar el metanol para sustentar la producción de energía y la formación de biomasa. En esta levadura no convencional, el promotor p*AOX1*, regulado por metanol, se ha utilizado ampliamente para controlar la expresión de genes que codifican proteínas recombinantes. Sin embargo, el uso de metanol plantea importantes preocupaciones de seguridad debido a su alta inflamabilidad, particularmente en aplicaciones industriales a gran escala. Por lo tanto, el objetivo principal de esta tesis fue explorar alternativas para reducir o eliminar la dependencia del metanol.

En este trabajo, la interrupción del gen que codifica la formiato deshidrogenasa (*FDH1*) se empleó como estrategia para modificar el sistema de expresión p*AOX1*. Esta modificación permitió convertir el sistema en una plataforma auto inducible, eliminando la necesidad de metanol u otros inductores. Nuestras investigaciones revelaron que este mecanismo de inducción está mediado por el formiato citoplasmático generado a partir del metabolismo del THF-C1; el cual no puede ser convertido en dióxido de carbono en una cepa con deleción de *FDH1*. Este descubrimiento demostró que el promotor p*AOX1* puede inducirse en condiciones no represivas, especialmente en presencia de sorbitol. La eficacia de este sistema quedó demostrada mediante la síntesis de dos proteínas modelo: la proteína fluorescente intracelular eGFP y la lipasa CalB de *Candida antarctica*, secretada al medio.

Posteriormente, nuestra estrategia de ingeniería metabólica se centró en optimizar la absorción de sorbitol para mejorar el crecimiento celular y la producción de rProt en la cepa con deleción de *FDH1*. Se identificó el metabolismo del sorbitol como el principal cuello de botella, y la sobreexpresión del gen de la sorbitol deshidrogenasa (*SOR1*) mejoró considerablemente el crecimiento en *K. phaffii*, lo que llevó a un aumento de 2.5 veces en la tasa específica de crecimiento celular. A pesar de estas mejoras, se observó una reducción en el nivel de inducción del promotor p*AOX1*. Este estudio propone varias hipótesis para explicar este fenómeno, las cuales se discuten en detalle en este trabajo.

En general, esta investigación establece las bases para una comprensión más profunda de la inducción del promotor p*AOX1* y destaca nuevas vías para explorar los mecanismos reguladores subyacentes. Estos hallazgos serán fundamentales para

optimizar el potencial del sistema en el avance de aplicaciones biotecnológicas en esta innovadora plataforma libre de metanol.

Palabras clave: *Pichia pastoris*, *Komagataella phaffii*, ingeniería celular, formiato deshidrogenasa, metabolismo de un carbono mediado por tetrahidrofolato, sistema libre de metanol, sorbitol deshidrogenasa, sorbitol.

Acknowledgments

The completion of a doctoral program represents both a challenging journey and a deeply rewarding period of professional and personal growth. Throughout this process, the guidance of an inspiring and dedicated advisor has been instrumental in shaping and realizing this research. I would like to extend my deepest gratitude to Professor Patrick Fickers. I am immensely grateful for his support from my very first day at TERRA. From basic training in the laboratory to fruitful discussions exploring the behavior of the *Komataella phaffii* yeast and his valuable advice on publications, his unwavering commitment to this project has been a cornerstone of its success, providing direction and encouragement at every stage. I would like to express my gratitude that his guidance marks the before and after of my professional scientific career.

I would like to express my sincere gratitude to Professor Julio Berrios for the opportunity to join his team and for introducing me to *Komagataella phaffii*, the focus of this research. Despite the challenges posed by the pandemic, Professor Berrios motivated me to develop a new research project, which I am now honored to present as a contribution to the yeast research scientific community. I also extend my heartfelt thanks to my thesis committee for their unwavering support and valuable guidance.

This doctoral journey began in Chile with dear friends who share a love for science and a commitment to helping others. My cherished friends: Ximena Báez, Manuel Arce, Darlyn Riquelme, and Esli Lobaina. I hold close to my heart the moments we shared during our first year of the program, and I will always treasure them fondly.

At TERRA, I had the opportunity to meet remarkable scientists from around the world. I am grateful to Vincent Vandenbroucke, Adrian Anckaert, Mateo Delvenne, Juan Andrés Martínez, and Lucas Henrion for the long discussions that broadened my perspective and helped me overcome many of the challenges faced in this thesis. I also had the pleasure of working with Sebastien Steels, whose guidance was indispensable as I took my first steps in the Molecular Biology lab. Olivia Denies, thank you for your kindness and charisma in the lab. I also acknowledge Romain Thomas and Samuel Telek for all the help they provided in the quest to identify the elusive key compound in this work, sodium format. Furthermore, I would also like to extend my heartfelt thanks to Marina Chanet, Marguerite Demi, and Danielle Duballet for their unwavering support, kindness, and readiness to help throughout this journey.

Being in a place where you can recharge alongside friends is invaluable, especially during a process filled with highs and lows; thank you, Mümine Guruk, Aparna Padmanabhan, Sandeep Kumar, Sigrid Gorgen, Andrea Kerezsi, Arpita Chakraborty and Andrea Chacon. I am especially grateful to have found a good friend in Rocio Cozmar; through you, everyone in the lab has learned valuable lessons, and I deeply appreciate your genuine friendship.

To my dear friends who encouraged me from afar with notes, messages, and calls, thank you so much, Johanna Fiallos, Jenny Sevilla, Vanessa Moya, Maura Fiallos, Taty Ortiz, Nicole Vásconez. Special thanks to Maximiliano Munckel for his invaluable support with his artistic work on the cover of this thesis, thank you dear

friend. I am also grateful to my friends back in Ecuador, who have been a great source of support and motivation along this journey. Thank you Kevin V.

My deepest thanks go to my family, who welcomed me into their home and hearts in Belgium. Martha, José, Milton, and Gloria, thank you for guiding me through my first months in this country. Dearest Jessica, thank you for your care and for always checking in on me. To my family back in Ecuador, Rodrigo Bustos, Nalda Ontaneda, Andréa Cosios, Selene Cosios, Patricia Cosios, Luis Cosios, Soledad Cosios and my dear grandfather Salomón Cosios.

Home is where our hearts smile, and my beloved Jonathan, words cannot fully express my gratitude for your support these past years. A cup of tea and a long conversation with you have always cleared my mind and helped me move forward. You, along with your family, have given me love and support at every moment.

Since leaving my country to embark on this PhD journey, my parents, Luis Bustos, Carmen Cosios, and my siblings Karla, Luis Andrés, and Jordy have been a constant source of comfort through calls filled with encouragement. On days when my resilience wavered, you were my pillar and my strength to keep pursuing my dreams. Thank you for your inspiration and love, my dear family. It would have brought me great joy to share this achievement and celebrate with my grandfather Hector, but life took a different path. Now, his soul rests in peace alongside my other angels, my grandmothers Hilda and Clemencia. My deepest thanks reach up to heaven for you, my beloved grandparents.

I am grateful to everyone who has supported me directly or indirectly throughout these years, encouraging and guiding me along this path of professional and personal growth, fueling my innate curiosity for science, the courage to start from scratch, and the resolve to overcome each obstacle. My deepest thanks to you all.

January 2025, Cristina Bustos

List of publications

- Bustos, C., Fickers. P., & Berrios., J. (2024). "Formate from THF-C1 metabolism induces the *AOX1* promoter in formate dehydrogenase-deficient *Komagataella phaffii*". This paper was published in *Microbial Biotechnology*, ***17*** (10), e70022. (https://doi.org/10.1111/1751-7915.70022)

- Berrios, J., Theron, C., Steels, S., Ponce, B., Velastegui, E., Bustos, C., Altamirano, C., & Fickers, P. (2022). "Role of Dissimilative Pathway of *Komagataella phaffii* (*Pichia pastoris*): Formaldehyde Toxicity and Energy Metabolism". This paper was published in *Microorganisms* ***10:*** *1466.* (https://doi.org/10.3390/microorganisms10071466)

- Bustos, C., Quezada, J., Veas, R., Altamirano, C., Braun-Galleani, S., Fickers. P., & Berrios., J. (2022). "Advances in Cell Engineering of the *Komagataella phaffii* Platform for Recombinant Protein Production". This paper was published in *Metabolites* ***12:*** *346.* (https://doi.org/10.3390/metabo12040346)

List of communications during scientific events

- Oral communication:
  "Cell engineering of the *Komagataella phaffii* for co-substrate metabolism" (1st Yeast Conference held in Rzeszow, Poland, June 2022)

- Oral communication:
  "Development of metabolic engineering strategies in *Pichia pastoris* for the reduction of cellular methanol requirements, for the production of recombinant protein" (UMRt Seminar, Belgium, November 2022)

- Poster:
  "Cell engineering of the *Komagataella phaffii* for co-substrate metabolism" (Belgian Society for Microbiology. Annual Symposium 2023: Amazing Microbes, Belgium, February 2023)

- Poster:
  "Regulation of p*AOX1* promoter in a *Komagataella phaffii* disrupted for gene encoding formate dehydrogenase" (Belgian Society for Microbiology. Annual Symposium 2024: Milestones in Microbiology, Belgium, March 2024)

Table of contents

List of Figures

Figure 3-5. Relative expression level of eGFP gene in Fdh eGfp strain (green) and FdhKO eGfp strain (blue) in minimal medium containing sorbitol (YNBSC). Samples were collected after 18 h and 24h. Displayed values were normalized to that of the actin gene and corresponded to means and standard deviations from three independent replicates conducted in flake flasks.

Figure 3-6. Observation of *Komagataella phaffii*, Fdh eGfp strain and FdhKO eGfp strain after 18h and 24 h of growth in minimal medium containing sorbitol (YNBSC) by fluorescent microscopy. A representative sample from the triplicate cultures conducted in flake flask are shown. Observation and image processing are detailed in material and methods.

Figure 3-7. eGFP fluorescence of Fdh eGfp strain (green); FdhKO eGfp strain (blue); FdhKO eGfp-FdhOE strain (yellow) after 18h and 24 h of growth in minimal medium containing sorbitol (YNBSC). Fluorescence was quantified by flow cytometry on 20,000 cells and expressed as TFU (total fluorescence, see materials and method for calculation details). Values are the means and standard deviation from biological triplicate cultures conducted in shake flasks.

Figure 3-8. Relative expression level of genes involved in the methanol dissimilation pathway *FLD* (PAS_chr3_1028), *FGH1* (PAS_chr3_0867), *FDH1* (PAS_chr3_0932) in the Fdh eGfp strain (green) and FdhKO eGfp strain (blue) in YNBSC medium**.** Samples were collected after 18 h of culture. The displayed values were normalized to that of the actin gene and corresponded to means and standard deviations from duplicates independent replicates cultures conducted in flake flasks.

Figure 3-9. Specific eGFP fluorescence of Fdh strain (black); Fdh eGfp strain (green); FdhKO eGfp strain (blue); Fdh&Shm2KO eGfp strain (orange) strains; during growth in YNB minimal medium containing sorbitol (YNBS, panel A), sorbitol and serine (YNBSS, panel B), and sorbitol and glycine (YNBSG, panel C). Cells were grown in BioLector and specific fluorescence values are means and standard deviation on four cultures replicates. sFU: specific fluorescence unit.

Figure 3-10. Biomass and specific lipase activity during growth of strains Fdh CalB strain (green squares) and FdhKO CalB strain (blue triangles) in the presence of glycerol (YNBG, panels A and B), methanol-sorbitol (YNBMS, panels C and D) and sorbitol (YNBS, panels E and F). Data are mean and standard deviation from cultures were performed in triplicate in shake flasks. Lipase assays were performed in triplicates.

Figure 3-11. High-performance liquid chromatography (HPLC) chromatogram. Formate standard solutions at concentrations ranging from 0.01 mM to 0.08 mM (A); supernatant of Fdh CalB strain (black) and supernatant of Fdh CalB strain spiked with

formate standard solution (red, 0.08 mM final concentration of spiked formate) (B); supernatant of FdhKO CalB strain (blue) and supernatant of FdhKO CalB strain spiked with formate standard solution (red, 0.08 mM final concentration of spiked formate) (C). Supernatant samples from cultures performed on sorbitol medium (YNBS) were collected after 15 hours. The absorbance value was set at zero after 11.5 min.

Figure. A3-2. Specific eGFP fluorescence of strain Fdh eGfp strain; Fdh eGfp strain; Fdh&Shm2KO eGfp strain; Fdh&Shm1KO eGfp strain; Fdh&Shm1,2KO eGfp strain. **Appendix 2**.

Figure 4-1. Schematic diagram illustrating the sorbitol assimilation pathway in a formate dehydrogenase-deficient *K. phaffii*. Formate from THF-C1 metabolism induces the p*AOX1* promoter. The overexpression of the sorbitol dehydrogenase *SOR1* gene increases biomass and energy production.

Figure 4-2. Schematic representation of the genotype of the strains presented in this chapter.

Figure 4-3. Biomass and specific fluorescence of strain RIY540 (FdhKO eGfp) in various carbon sources. Carbon sources: glycerol (green); glucose (brown); fructose (purple); Mannitol (red); Lactate (black); sorbitol (blue). Data are mean and standard deviation from cultures were performed in triplicate in shake flasks.

Figure 4-4. Comparative impact of enhanced sorbitol catabolism through *SOR1* gene overexpression in FdhKO eGfp strain vs. FdhKO-SdOE eGfp strain at different sorbitol concentrations. **A & B**: FdhKO eGfp strain; **C & D**: FdhKO-SdOE eGfp strain. G: 1.75g L^{-1} glycerol; GS2: 1.75 g L^{-1} glycerol + 1.75 g L^{-1} sorbitol; GS4: 1.75 g L^{-1} glycerol + 3.5 g L^{-1} sorbitol). Cells were grown in BioLector, and specific fluorescence values are the means and standard deviation of three culture replicates. sFU: specific fluorescence unit; a.u: arbitrary units

Figure 4-5. Comparative impact of enhanced sorbitol catabolism through *SOR1* gene overexpression. **A:** cell density; **B:** total lipase CalB; **C:** specific lipase CalB. Fdh CalB (black); FdhKO CalB (blue); FdhKO-SdOE CalB (orange). Data are mean and standard deviation from cultures, which were performed in triplicate in shake flasks.

Figure 4-6. Growth rate and eGfp fluorescence in *K. phaffii* mutants cultured under different K_La values in shake-flask cultures. **A:** growth rate; **B:** eGfp fluorescence (TFU). FdhKO eGfp strain (blue), FdhKO-SdOE eGfp strain (orange). Numbers in the figure legend indicate the K_La parameter value in (h^{-1}). Data are the mean and standard deviation of biological triplicate cultures at 22 h in YNB20S.

Figure 4-7. Formate concentration in the supernatant of *K. phaffii* mutants cultured under different K_La in shake flask cultures. FdhKO eGfp strain (blue), FdKO-SdOE eGfp strain (orange). Data are the mean and standard deviation from biological triplicate cultures at 22 h in YNB20S.

Figure. A4-2. Substrate consumption profile of FdhKO eGfp (A) and FdKO-SdOE eGfp (B) strains in a glycerol-sorbitol mixed culture media. **Appendix 5.**

Figure. A4-3. Residual sorbitol profile. FdhKO eGfp strain (blue) and FdKO-SdOE eGfp strain (orange). Data are the mean and standard deviation from biological triplicate cultures at 22 h in YNB20S.**Appendix 6.**

List of tables

List of abbreviations

***AOX1*:**	alcohol oxidase 1 gene
a.u:	arbitrary units
Adh:	alcohol dehydrogenase
Aox1:	alcohol oxidase1
Aox2:	alcohol oxidase 2
BLAST:	basic local alignment search tool
BlastX:	basic local alignment search tool - translated nucleotides to proteins
CalB:	Candida antarctica lipase B
Cat:	catalase
Das:	dihydroxyacetone synthase
gDCW:	grams of dry cell weight
e*GFP*:	gene encoding the green fluorescent protein
eGfp:	enhanced green fluorescent protein
Fdh:	formate dehydrogenase
FDH1	gene encoding the formate dehydrogenase enzyme
Fdh1Δ:	FDH1 gene disruption
Fgh:	S-formylglutathione hydrolase
Fld:	formaldehyde dehydrogenase
FU:	fluorescence units
HPLC:	High performance liquid chromatography
LB:	Luria-Bertani medium
Mis1-1:	Trifunctional enzyme formate-tetrahydrofolate ligase, methenyltetrahydrofolate cyclohydrolase and methylenetetrahydrofolate reductase
Mis1-2:	formate-tetrahydrofolate ligase
Mis1-3:	methylenetetrahydrofolate dehydrogenase & methenyltetrahydrofolate cyclohydrolase
MUT:	methanol utilization pathway
Mut^+:	plus methanol utilization phenotype
Mut^-:	minus methanol utilization phenotype
Mut_s:	slow methanol utilization phenotype
OD_{600}:	Optical density at 600 nm
p-NPB:	p-nitrophenylbutyrate
PpHXT1:	Putative protein hexose transporter 1

Pp*HXT1*:	gene encoding the putative protein hexose transporter 1
rProt:	recombinant protein
sFU:	specific fluorescence units
Shm1:	mitochondrial serine hydroxymethyltransferase
***SHM1*:**	gene encoding the mitochondrial serine hydroxymethyltransferase
Shm1Δ:	*SHM1* gene disruption
Shm2:	cytosolic serine hydroxymethyltransferase
***SHM2*:**	gene encoding the cytosolic serine hydroxymethyltransferase
Shm2Δ:	*SHM2* gene disruption
sor1:	sorbitol dehydrogenase
***SOR1*:**	gene encoding the sorbitol dehydrogenase
TFU:	total fluorescence unit
THF:	tetrahydrofolate
THF-C1:	tetrahydrofolate-mediated one-carbon metabolism
YNB:	yeast nitrogen base
YNB20S:	yeast nitrogen base – 20 g L^{-1} sorbitol
YNBF:	yeast nitrogen base – fructose
YNBG:	yeast nitrogen base - glycerol
YNB-G:	yeast nitrogen base – 1.75 g L^{-1} glycerol
YNBGS2:	yeast nitrogen base – 1.75 g L^{-1} glycerol and 1.75 g L^{-1} sorbitol
YNBGS4:	yeast nitrogen base – 1.75 g L^{-1} glycerol and 3.75 g $^{L-1}$ sorbitol
YNBGu:	yeast nitrogen base – glucose
YNBL:	yeast nitrogen base – sodium lactate
YNBMS:	yeast nitrogen base – methanol and sorbitol
YNBMt:	yeast nitrogen base – mannitol
YNBS:	yeast nitrogen base -sorbitol
YNBSC:	yeast nitrogen base-sorbitol and casamino acids
YNBSFC:	yeast nitrogen base-sorbitol, sodium formate and casamino acids
YNBSG:	yeast nitrogen base - sorbitol and glycine
YNBSMC:	yeast nitrogen base- sorbitol, methanol and casamino acids
YNBSS:	yeast nitrogen base -sorbitol and serine
YPD:	yeast peptone dextrose
$Y_{S/P}$:	substrate-product conversion yield
μ:	specific growth rate

Chapter 1

General introduction

Chapter 1. General introduction

1. Context and objectives

1.1. Context

Komagataella phaffii, a methylotrophic yeast, is among the Ascomycota yeasts from the Saccharomycetes class (Ata *et al.*, 2021). It was first described in the 1920s as *Zygosaccharomyces pastori* by the French mycologist and cytologist Alexandre Guilliermond(Peña *et al.*, 2018). In the 1950s, Herman Phaff renamed it *Pichia pastoris* after isolating several related strains from oak trees in California (Phaff *et al.*, 1956). Initially, due to its ability to utilize methanol, it was considered as a source of cellular protein. However, this objective was abandoned in the 1970s due to the rising cost of methane (the source of the methanol) caused by the oil crisis (Macauley-Patrick *et al.*, 2005). This shift in focus promoted its use in academic research and for the generation of value-added compounds. Today, the *K. phaffii*-based expression system is one of the most popular for producing heterologous proteins, including biopharmaceutical proteins and other recombinant proteins used in research and industry (Rebnegger *et al.*, 2024). By the end of 2018, approximately 16.7% of all approved biopharmaceutical proteins were produced using yeast expression systems, including *K. phaffii* and *Saccharomyces cerevisiae* (Rußmayer *et al.*, 2023). *K. phaffii* possesses several physiological characteristics that distinguish it from *S. cerevisiae*, such as faster growth on inexpensive carbon sources, the capability to perform post-translational modifications, efficient production and secretion of heterologous proteins in high yields, and low secretion of endogenous proteins, thereby reducing purification costs (Khlebodarova *et al.*, 2024).

The methylotrophic nature of *K. phaffii* enables it to use methanol as the main carbon and energy source. Methanol metabolism involves its oxidation by the enzymes encoded by the alcohol oxidase genes (*AOX1* and *AOX2*). *AOX1* is responsible for producing the major enzyme, which can constitute up to 30% of the total soluble proteins in yeast extracts grown on methanol as the sole carbon source, which makes the *AOX1* promoter one of the strongest known promoters (Juturu and Wu, 2018).

In *K. phaffii*, methanol is metabolized through the methanol utilization pathway (MUT) Figure 1-1, which occurs in the peroxisome and the cytosol. In the peroxisome, methanol is initially oxidized to formaldehyde and hydrogen peroxide by the alcohol oxidase enzymes. Formaldehyde then follows two main pathways. In the dissimilative pathway, formaldehyde is further oxidized to carbon dioxide through the actions of formaldehyde dehydrogenase (Fld), formyl glutathione hydrolase (Fgh), and formate dehydrogenase (Fdh). In the assimilate pathway, formaldehyde is assimilated into central metabolism through several intermediate steps, contributing to biomass synthesis and energy production (Bustos *et al.*, 2022). The dissimilative pathway primarily protects cells from formaldehyde's toxic effects (Berrios *et al.*, 2022).

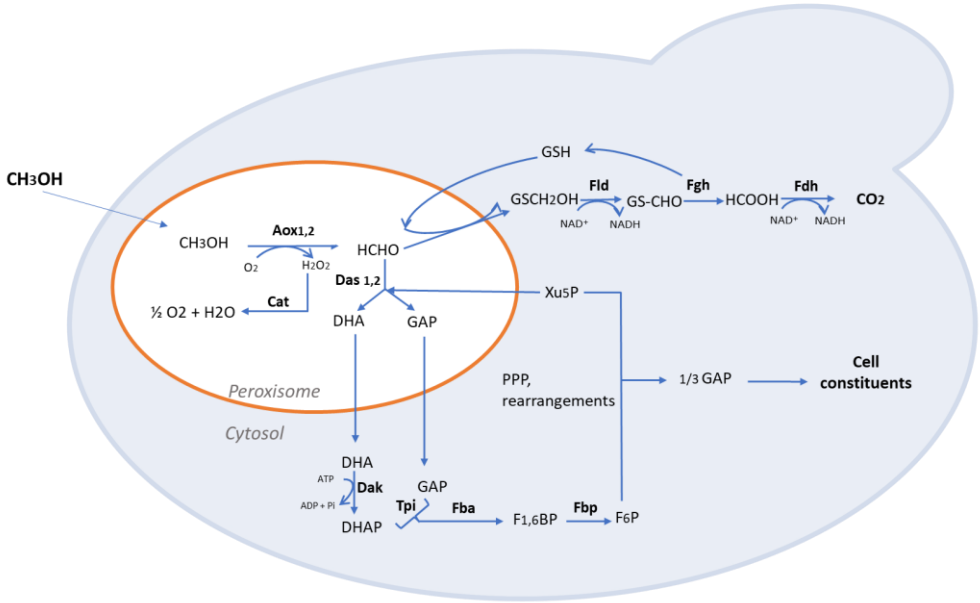

Figure 1-1. Methanol utilization pathway in *Komagataella phaffii*. Aox1, 2: alcohol oxidase1 and 2; Cat: catalase; Das1, 2: dihydroxyacetone synthase; Fld: formaldehyde dehydrogenase; Fgh: S-formylglutathione hydrolase; Fdh: formate dehydrogenase; Dak: dihydroxyacetone kinase; Tpi: triose phosphate isomerase; Fba: fructose-1,6-bisphosphate aldolase; Fbp: fructose-1,6-bisphosphatase; GS(H): glutathione; DHA: dihydroxyacetone; DHAP: dihydroxyacetone phosphate; GAP: glyceraldehyde-3-phosphate; F1,6BP: fructose-1,6-bisphosphate; F6P: fructose-6-phosphate; Xu5P: xylulose 5-phosphate.

The p*AOX1* has been extensively utilized for the expression of various proteins under methanol induction. The induction of p*AOX1* is principally mediated by three master transcription factors (TFs): methanol-induced transcription factor 1 (Mit1), methanol expression regulator 1 (Mxr1), and the positive regulator of methanol 1 (Prm1) (Vogl *et al.*, 2018). Mxr1 facilitates p*AOX1* de-repression, while Trm1 and Mit1 play crucial roles in promoter activation (Wang, Wang, *et al.*, 2016).

However, the use of methanol presents significant operational disadvantages. Among these are its toxicity, the high oxygen supply required for large-scale processes, the need for efficient heat removal, and the challenges associated with transporting and storing large quantities of methanol (Sales-Vallverdú *et al.*, 2024). These issues underscore the critical need for alternative methanol-free systems.

In recent years, significant efforts have been made to mitigate the toxic effects of methanol and enhance recombinant protein production using the p*AOX1* system. One widely used strategy involves co-feeding methanol with auxiliary carbon sources, including glycerol and glucose (Xie *et al.*, 2005; Berrios *et al.*, 2017; Zhu *et al.*, 2019).

The co-feeding approach reduces methanol's toxicity. However, certain carbon sources, such as glucose and glycerol, are known to strongly repress p*AOX1*, limiting their benefit (Thorpe *et al.*, 1999). The presence of glucose or glycerol leads to the action of catabolic repressors such as Mig1, Mig2, and Ngr1, which suppress the expression of p*AOX1*-controlled genes (Wang *et al.*, 2017).

In contrast, sorbitol, mannitol, alanine, lactic acid, and trehalose do not repress p*AOX1*, thereby allowing protein production to proceed without the need for stringent control over residual substrate levels (Inan and Meagher, 2001; Xie *et al.*, 2005).

Table 1-1. Repressive and non-repressive carbon sources for alcohol oxidase promotor p*AOX1* induction.

Classification	Carbon Source	Reference
Repressive	Glycerol	(Thorpe *et al.*, 1999)
	Glucose	(Thorpe *et al.*, 1999)
	Ethanol	(Brierley *et al.*, 1990)
	Fructose	(Zhang *et al.*, 2010)
Non-repressive	Alanine	(Inan and Meagher, 2001)
	Sorbitol	(Inan and Meagher, 2001)
	Mannitol	(Inan and Meagher, 2001)
	Trehalose	(Inan and Meagher, 2001)
	Lactic acid	(Xie *et al.*, 2005)
	Formate	(Jayachandran *et al.*, 2017)

Sorbitol has been widely utilized as a non-repressive carbon source for the *AOX1* promoter, with the advantage that its accumulation during the induction phase does not impact recombinant protein expression levels (Çelik *et al.*, 2009; Niu *et al.*, 2013; Carly *et al.*, 2016). Recent studies have highlighted sorbitol's suitability for providing energy in methanol-free systems (Liu, et al., 2022a; Liu et al., 2022b).

Other non-repressive carbon sources, such as formate, have shown promise in co-feeding along with methanol, enhancing cellular energy levels and recombinant *Candida antarctica* Lipase B (CALB) secretion (Jayachandran *et al.*, 2017). Additionally, Singh and Narang, (2020) have reported the use of formate and formaldehyde as inducers. The disruption of the methanol pathway, achieved by knocking out the formaldehyde dehydrogenase (*FLD1*) gene to prevent the conversion of formate into methanol, has revealed that formate can activate the p*AOX1*, achieving approximately 35% of the expression level compared to methanol induction (Tyurin and Kozlov, 2015). Although recent research has explored formate as an alternative inducer for p*AOX1*, challenges remain, including energy supply limitations and the need to maintain low formate concentrations due to formaldehyde's toxicity, which

inhibits cell growth (Feng *et al.*, 2022; Liu, Li, *et al.*, 2022; Liu, Zhao, *et al.*, 2022; Singh and Narang, 2023).

In *Komagataella phaffii*, formate dehydrogenase (Fdh) primary role has been identified as formate detoxification rather than energy generation (Guo *et al.*, 2021), and its disruption in other methylotrophic yeast, such as *Candida boidinii*, has been reported not to be essential for cell survival (Sakai *et al.*, 1997).

Considering the challenges associated with methanol use, there is a pressing need to develop methanol-free systems. This work addresses the limitations of current p*AOX1*-based systems and presents a new *Komagataella phaffii* methanol-free system. Additionally, it provides a detailed explanation of the underlying mechanisms driving these advancements.

1.2. Objectives

The main objective of this thesis was to develop metabolic engineering strategies in *Komagataella phaffii* to reduce methanol requirements and, thus, the drawbacks associated with its use by targeting the metabolism of formate and sorbitol known as non-repressor compounds of the p*AOX1* promoter. To accomplish this objective, it was first necessary to evaluate the behavior of *K. phaffii* in response to sorbitol and formate in terms of cell growth and induction of the p*AOX1*. Based on the cellular response to these non-repressive compounds, genetic modifications were performed in *K. phaffii*. The recombinant protein production levels and cell growth rate were evaluated as key criteria for further cellular engineering. The effect of the genetic modifications on the dissimilative pathway was evaluated, and the impact of cellular engineering in *K. phaffii* was analyzed using two model proteins: intracellular enhanced green fluorescence protein (eGFP) and extracellular *Candida antarctica* lipase B (CalB).

The strategy to achieve these objectives is outlined in Figure 1-2. *K. phaffii* cultures were evaluated using sorbitol, a mixture of methanol and sorbitol, and formate and sorbitol, demonstrating the potential of formate as an inducer of the *pAOX1* promoter. Genetic manipulation was employed to delete the gene encoding formate dehydrogenase (*FDH1*) in *K. phaffii*, thereby increasing intracellular formate availability and inducing *pAOX1*. Under sorbitol culture conditions, genetic modifications in the THF-C1 pathway were evaluated in the *K. phaffii* FdhKO strain, which is deficient in formate dehydrogenase, to investigate the origin of formate. Finally, metabolic engineering efforts were performed to enhance sorbitol metabolism and identify bottlenecks in its utilization, aiming to improve the recombinant protein production performance of the *K. phaffii* FdhKO strain.

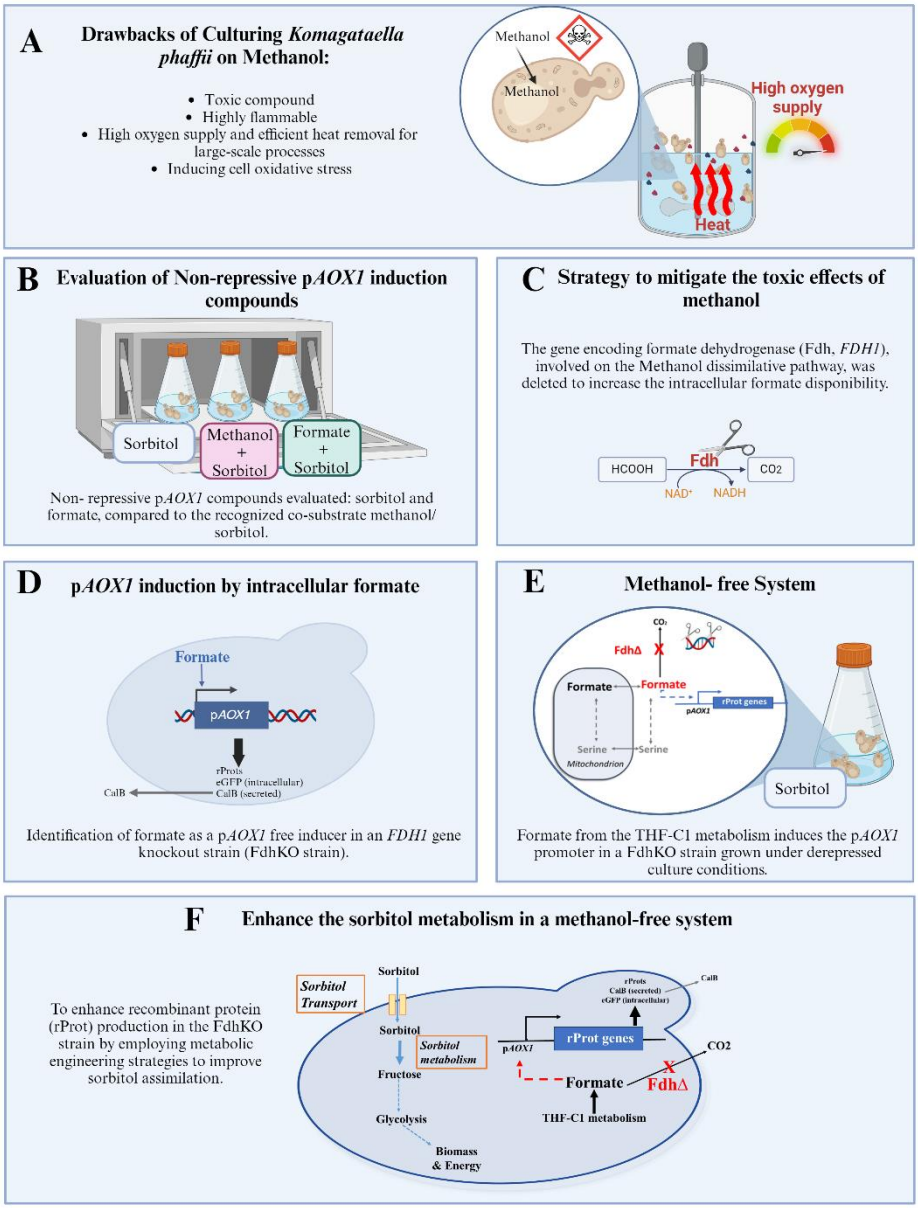

Figure 1-2. A schematic overview of the development of the *Komagataella phaffii* methanol-free system was performed in this investigation. **A:** Description of the drawbacks of using methanol in *Komagataella phaffii* for recombinant protein production; **B:** Evaluation of sorbitol and formate as carbon sources, recognized as non-repressive for p*AOX1*; **C:** Development of metabolic engineering strategies to accumulate formate in *K. phaffii* through deletion of the *FDH1* gene; **D:** Identification of formate as a p*AOX1* free inducer in an *FDH1* gene knockout strain; **E:** Unraveling the origins of formate in a methanol-free environment; **F:** Enhancement of sorbitol catabolism through metabolic

engineering of the sorbitol pathway. *Abbreviations:* Fdh: formate dehydrogenase; *FDH1*: formate dehydrogenase gene; eGFP: enhanced green fluorescent protein; CalB: *Candida antarctica* lipase B.

2.2. Outline

Chapter 1 introduces the thesis with a general overview, including the context, objectives, roadmap, and outline.

Chapter 2 presents a literature review, highlighting the characteristics that make *K. phaffii* one of the most significant yeast strains for heterologous protein production. It describes recent advances in cell engineering, focusing on improvements in metabolism and energy supply, as well as the development of new systems to reduce dependence on methanol for induction by the AOX1 promoter in methanol-free media.

Chapter 3 details the first part of this research, which aimed to reduce the use of methanol to induce the p*AOX1* in *K. phaffii*. This section discusses how deleting the formate dehydrogenase gene *FDH1* improves recombinant protein production, providing new insights into the induction of the p*AOX1* and highlighting the crucial role of the THF-C1 pathway in this process.

Chapter 4 presents the findings on the behavior of the new methanol-free system developed in this thesis using various p*AOX1* non-repressive carbon sources. Metabolic engineering efforts focused on optimizing a non-repressive carbon source to enhance cell growth in this new system. The chapter discusses the impact of these genetic modifications based on the production of two reporter proteins: the intracellular eGFP and the extracellular lipase CalB.

Chapter 5 provides a general discussion of the research in this thesis. It consolidates the key findings, integrating the insights from the previous chapters to offer a cohesive understanding. It discusses their implications and highlights the advancements made in this new methanol-free system.

Chapter 6 presents the conclusions and future perspectives of this thesis. This section highlights the significance of the findings and the novelty of the research and provides suggestions for future investigations to improve the novel methanol-free system.

Chapter 7 presents the appendices containing additional information regarding the primers used in this investigation, complementary information, and the scientific contribution made during the PhD thesis.

Chapter 2

Literature Review

Advances in cell engineering of the Komagataella phaffii - Platform for recombinant protein production

Description of Chapter 2

This chapter aims to provide a detailed description of recent advancements in cell engineering approaches, including metabolic engineering and energy supply optimization. These topics will be thoroughly discussed and evaluated based on the results of this investigation in the subsequent chapters.

This work is an original contribution adapted from:

- Bustos, C., Quezada, J., Veas, R., Altamirano, C., Braun-Galleani, S., Fickers. P., & Berrios., J. (2022). "Advances in Cell Engineering of the *Komagataella phaffii* Platform for Recombinant Protein Production". This paper was published in *Metabolites* ***12:*** *346.* (https://doi.org/10.3390/metabo12040346).
- Berrios, J., Theron, C., Steels, S., Ponce, B., Velastegui, E., Bustos, C., Altamirano, C., & Fickers, P. (2022). "Role of Dissimilative Pathway of *Komagataella phaffii* (*Pichia pastoris*): Formaldehyde Toxicity and Energy Metabolism". This paper was published in *Microorganisms* ***10:*** *1466.* (https://doi.org/10.3390/microorganisms10071466).

Chapter 2. Advances in cell engineering of *Komagataella phaffii* platform for recombinant protein production

1. Introduction

The methylotrophic yeast *Komagataella phaffii* (formerly *Pichia pastoris*) (Kurtzman, 2009), is one of the most prominent recombinant protein (rProt) production platforms (Ahmad *et al.*, 2014; Zhu *et al.*, 2019). As a methylotrophic yeast, it can oxidize methanol for energy production and biomass formation (Peña *et al.*, 2018). Given its ability to grow readily on relatively inexpensive culture medium, it was initially used as a cellular protein source (SCP, single-cell protein). Over the years, it has become an attractive host system to produce rProt from bacterial, fungal, plant, and mammalian/human origins (Maccani *et al.*, 2014; Zhu *et al.*, 2019; He *et al.*, 2020; Raza *et al.*, 2020).

K. phaffii stands out among other yeasts and microorganisms due to several non-conventional features (Ata *et al.*, 2021). In addition to its ability to metabolize methanol through the methanol utilization (MUT) pathway, *K. phaffii* can grow on inexpensive media at high cell density, reaching a biomass concentration exceeding 100 g L^{-1} of dry cell weight (DCW) (Braun-Galleani, Henríquez, *et al.*, 2019; Heistinger *et al.*, 2020; Henríquez *et al.*, 2020) Genetic manipulation tools for transgene expression in this species are well-established, resulting in the targeted and stable integration of rProt genes. Proteins carrying a suitable secretion signal, such as the widely utilized alpha mating factor (MATα) secretion signal, can be accumulated in the culture supernatant due to its efficient secretory machinery in an environment relatively free from other proteins and contaminants, as less than 10 % of the endogenous proteins are secreted (Zhu *et al.*, 2019; Burgard *et al.*, 2020). In addition, *K. phaffii* can perform diverse protein processing and post-translational modifications typical of higher eukaryotes, such as glycosylation, disulphide bond formation (Ahmad *et al.*, 2014; Raschmanová *et al.*, 2021) , and it lacks other known disadvantages that are present in bacterial systems (formation of inclusion bodies and presence of endotoxins) or mammalian cell systems (high cultivation and handling costs) (O'Flaherty *et al.*, 2020). Using this host system, rProt can be produced in either a constitutive or induced manner, depending on the type of promoter used to drive recombinant gene expression.

The success of *K. phaffii* for rProt synthesis has been facilitated by strong methanol-inducible promoters from alcohol oxidase genes (alcohol oxidase 1, *AOX1*, and to a lesser extent, alcohol oxidase 2, *AOX2*), and also from the glyceraldehyde 3-phosphate dehydrogenase (*GAP*) promoter p*GAP*, which exhibits strong constitutive expression in the presence of glucose and glycerol (Türkanoğlu Özçelik *et al.*, 2019). Notwithstanding the efficiency, tight control, and rProt productivity obtained when

using p*AOX1* to drive transgene expression, this production system presents some drawbacks associated with methanol utilization. Indeed, methanol is toxic to cells, inducing cell oxidative stress, and its use comes with a subsequent high oxygen demand for catabolism (Jia *et al.*, 2021). Additionally, as methanol is highly flammable, its use can imply safety issues, especially at an industrial scale. Taking these drawbacks into consideration, current research is being undertaken to evaluate alternatives in order to reduce or discard methanol use.

Important efforts have been carried out to improve the understanding of the physiology and cell response of *K. phaffii* under various genetic backgrounds (engineered strains) and bioprocesses operation (Riley *et al.*, 2016; Heistinger *et al.*, 2018; Braun-Galleani, Dias, *et al.*, 2019) with the goal of increasing rProt productivity, cell capabilities, and metabolic performance. These advancements have been reported in exhaustive reviews that focus on bioreactor process (W. C. Liu *et al.*, 2019; Nieto-Taype *et al.*, 2020), genetic manipulation techniques (Yang and Zhang, 2018; Bernauer *et al.*, 2021; Gao *et al.*, 2021), and metabolic engineering (Schwarzhans *et al.*, 2017). This chapter highlights and summarises the latest cell engineering approaches regarding engineering the methanol pathway, co-factor metabolism, catabolism of alternative carbon sources, and the development of methanol-free pAOX1 systems as illustrated in Figure 2-1, and their contribution to *K. phaffii*'s promising future as a robust and highly efficient host for the production of a huge variety of recombinant proteins.

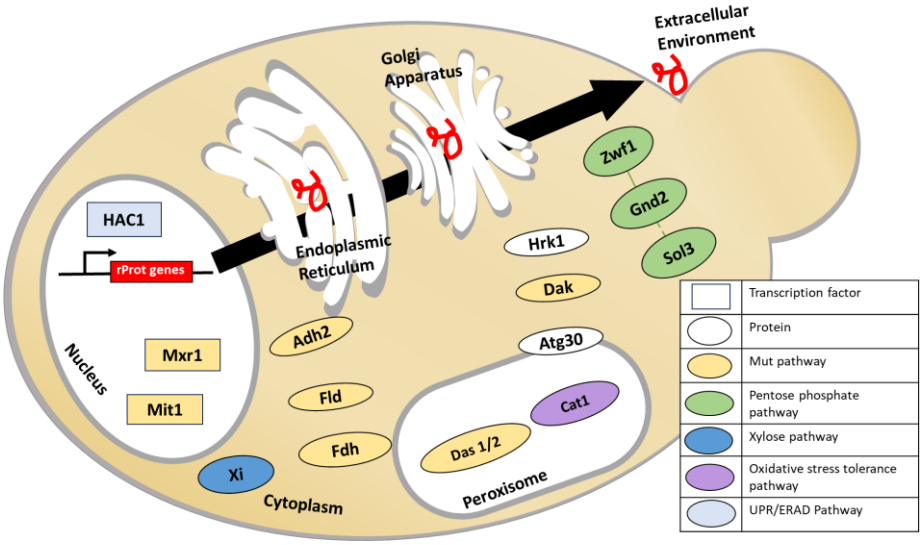

Figure 2-1. Schematic overview of the main pathways, proteins, and transcription factors involved in cellular engineering strategies for the improvement of recombinant protein production in *Komagataella phaffii*. Abbreviations: Hac1: UPR-regulating transcription factor; Mxr1: methanol expression regulator 1; Mit1: methanol-induced transcription factor

1; Cat1: catalase; Adh2: alcohol dehydrogenase; Das1/2: dihydroxyacetone synthase 1 and 2; Fld: formaldehyde dehydrogenase; Fdh: formate dehydrogenase; Zwf1: glucose-6-phosphate dehydrogenase; Sol3: 6-gluconolactonase; GND2: 6-phosphogluconate dehydrogenase; Hrk1: putative serine/threonine protein kinase; Dak: Dihydroxyacetone kinase; Atg30:autophagy-related protein 30; Xi: xylose isomerase.

2. Metabolic engineering for improved metabolism and energy supply

rProt production and secretion generate a high metabolic burden, as protein synthesis leads to increased nutrient and energy demands (Kafri *et al.*, 2016) . In addition, production of rProt can often trigger endoplasmic reticulum (ER) stress and oxidative stress, causing (NAD(P)H) co-factor unbalance (Tomàs-Gamisans *et al.*, 2020). As stated above, *K. phaffii* can metabolize methanol as the sole carbon source; however, it can also metabolize other non-frequently used alkylated nitrogen sources, such as methylamine and choline. The main metabolic drawback of methanol catabolism is the production of toxic metabolites such as formaldehyde and hydrogen peroxide (Jia *et al.*, 2017) . At high methanol concentration (above 5% vol/vol), disruption of the peroxisome can occur, thus impairing methanol catabolism (Cai *et al.*, 2021; Wang *et al.*, 2022). Furthermore, methanol catabolism requires high oxygen consumption that can limit the productivity of the bioreactor process, especially at large scale where the oxygen transfer capacity is lower (Carly *et al.*, 2016) . Therefore, the methanol concentration control in the culture medium is crucial to obtain high productivity of rProt.

In processes based on the p*AOX1* expression system, co-substrates such as sorbitol can be used with the goal of dedicating methanol mainly as the inducer for the expression system, while sorbitol is used for biomass and energy formation (Azadi *et al.*, 2017; Berrios *et al.*, 2017; Zepeda *et al.*, 2018). This has been evidenced by metabolic flux analysis of a simplified metabolic network describing cell growth, methanol and sorbitol catabolism, and energy formation, which was subsequently confirmed in a bioreactor culture (Niu *et al.*, 2013). In this case, it was observed that an appropriate methanol/sorbitol mixture ratio (methanol fraction 0.60 C-mol/C-mol) could increase the p*AOX1* induction level (β-galactosidase activity of 8.6 ± 0.8 × 103 Miller unit), compared to cultures with 100% methanol supplementation (7.8 ± 0.7 × 103 Miller unit) (Niu *et al.*, 2013) . Glycerol has also been widely used as a co-substrate, and different culture strategies have been implemented. Recently, a combined µ-stat (constant exponential feeding rate) and m-stat (constant methanol concentration) feeding process was developed for β-glucosidase FBG1 production in a 5 L bioreactor. This co-stat feeding strategy allowed reaching a productivity of 403 mg L^{-1} of β-glucosidase, which was 2.6- and 4.4-fold higher than the titer obtained in µ-stat and m-stat modes, respectively (Liu *et al.*, 2020) . Metabolic engineering of the host cell has also been considered, aiming at improving rProt productivity. Recent published work on engineering of the catabolic pathway of methanol and alternative

carbon sources, along with co-factor engineering, is described in the following sections and summarized in Table 1.

2.1 Engineering of the methanol catabolic pathway

The MUT pathway can be divided into two main stages. First, methanol is oxidized by two alcohol oxidases (Aox1, Aox2) into formaldehyde in the peroxisome, before being further metabolized in two distinct metabolic routes. In the assimilatory branch, formaldehyde is converted into Dihydroxyacetone (DHA) and GAP by the peroxisomal dihydroxyacetone synthase (Das). This pathway ends in the cytosol with the generation of fructose 1,6-biphosphate. In the dissimilatory branch, formaldehyde is oxidized to carbon dioxide in three steps by the enzymatic route formed by formaldehyde dehydrogenase (Fld), formyl glutathione hydrolase (Fgh), and formate dehydrogenase (Fdh), with the release of NADH (Cereghino and Cregg, 2000), as illustrated in Figure 2-2.

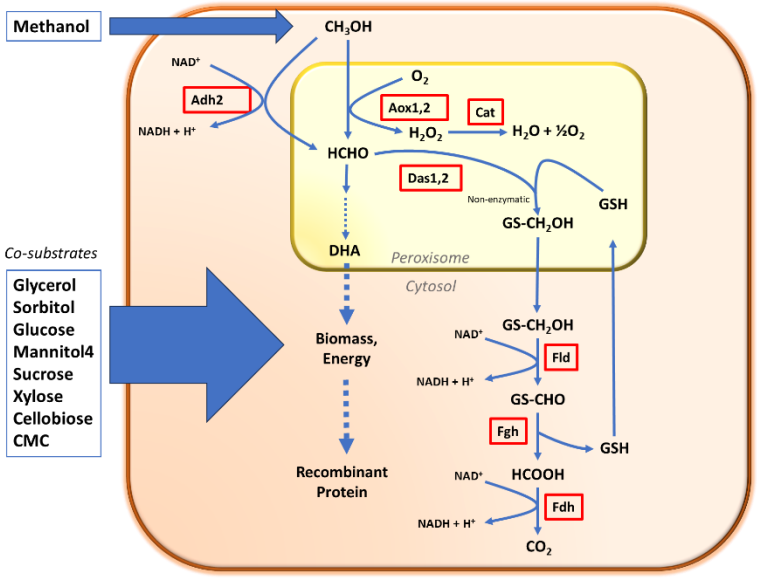

Figure 2-2. Diagram illustrating the main steps in the MUT pathway and co-substrate alternatives for enhancement of biomass and energy supply in *Komagataella phaffii*. Aox1, 2: alcohol oxidase1 and 2; Cat: catalase; Das: dihydroxyacetone synthase; Fld: formaldehyde dehydrogenase; Fgh: S-formylglutathione hydrolase; Fdh: formate dehydrogenase; Adh: alcohol dehydrogenase; GS(H): glutathione; CMC: carboxymethyl cellulose.

Engineering of the MUT pathway has led to higher substrate-product conversion yield ($Y_{S/P}$) and rProt productivity. In a MutS strain (strain with disrupted *AOX1*), the overexpression of *DAS* resulted in a 2- to 3-fold increase in $Y_{S/P}$ from methanol to produce horseradish peroxidase (Hrp) and *Candida antarctica* lipase B (CalB), with

reported values of 3.06 U $mmol^{-1}$ and 2.05 U $mmol^{-1}$, respectively, in comparison with the reference strains for each case (~1 U $mmol^{-1}$). Meanwhile, the overexpression of *FLD* with the same reporter proteins exhibited a 2-fold increase in $Y_{S/P}$ from methanol (1.65 UHRP $mmol^{-1}$ and 2.13 UCalB $mmol^{-1}$) (Krainer *et al.*, 2012). On the other hand, the deletion of both *DAS* isoforms (*DAS1* and *DAS2*) has increased green fluorescent protein (GFP) expression in single and double knockout strains. The highest rProt production was observed in the *DAS1* deletion strain, which produced 30% more GFP than the control strain. This yield was followed by the *DAS2* deletion strain and finally the double mutant *DAS1-DAS2*, with *GFP* expression levels of ~22% and ~15% in each case, both higher than the wild-type strain (Geier *et al.*, 2015).

An alternative methanol metabolism implemented for recombinant protein production has been presented by Zavec et al. (2020) with the recent reassessment of the Mut- strain (strain with *AOX1* and *AOX2* disruption), which, contrary to its generally recognized inability for methanol metabolization (Chiruvolu *et al.*, 1997), showed that it is indeed able to metabolize methanol with a similar rProt yield when compared to a MutS strain, due to the promiscuous activity of the alcohol dehydrogenase enzyme Adh2. Based on these results and using metabolic engineering, the overexpression of *ADH2* revealed a significant increase in the productivity (qP) of the camelid antibody fragment vHH (237 µg $g^{-1}h^{-1}$) in the Mut-p*AOX1*v*HH*p*FLD1*Adh2 strain compared to the Mut-p*AOX1*v*HH* parent strain (88 µg $g^{-1}h^{-1}$), and a slightly higher increase with the strain MutSp*AOX1*v*HH* (205 µg $g^{-1}h^{-1}$). It is worth noting that despite the similarity in productivity between the Mut- improved strain and the MutS strain, the latter showed an additional advantage by having lower rates of oxygen uptake and heat production (Zavec *et al.*, 2021)

As far as the main mechanism for induction of the p*AOX1/2* promoters is concerned, few studies have ventured to question whether methanol could be the sole inducer of the system. Tyurin and Kozlov (2015) discussed the exclusive inducing activity of methanol and proposed the use of formate as a possible inducer of the p*AOX1/2* system. Thus, to rule out the possibility of intracellular methanol reduction using potassium formate salt as an inducer, *FLD* was deleted. With this modification, the expression levels of β-galactosidase were increased by 2-fold (~4500 Miller units) compared to the wild-type strain (~2200 Miller units) (Tyurin and Kozlov, 2015). Modifying the MUT pathway and the redistribution of metabolic flux for rProt expression in key metabolic steps directed to a target product has also been successful (Krainer *et al.*, 2012; Geier *et al.*, 2015; Tyurin and Kozlov, 2015; Zavec *et al.*, 2021). However, little attention has been paid in recent years to modifying this pathway to improve the production of different recombinant proteins than those abovementioned, and some high-value compounds, such as malic acid and S-adenosylmethionine, have been produced when a knockout of *FDH* and *DAS*, respectively, was introduced (Guo *et al.*, 2021; Liu *et al.*, 2021).

Thus, the work presented by Zavec et al., (2021) and Tyurin & Kozlov, (2015) highlights the need to question the previously acknowledged and accepted premise of

the MUT pathway behavior and re-evaluate methanol metabolism from different perspectives.

2.2 Engineering of co-substrate catabolic pathways

Due to the already described problems with the use of methanol in rProt production, co-feeding strategies of methanol with auxiliary carbon sources have been studied to mitigate this problem. Based on the results of Inan and Meagher, (2001), it was identified that substrates such as alanine, trehalose, sorbitol, and mannitol could be used as co-substrates in combination with methanol, as these do not repress the p*AOX1*, while glycerol and glucose do exert repression of this inducible promoter. Nevertheless, glycerol is mainly used in co-feeding strategies with methanol because it generates higher biomass yield, higher growth rate, and improved productivity (Berrios *et al.*, 2017). The use of glucose has been favored due to the deletion of the hexose transporter gene *HXT1*, which made it possible to obtain a strain for the expression of rProt in a methanol-free medium (Zhang *et al.*, 2010). On the other hand, the co-feeding with sorbitol positively affects cell growth and energy supply for heterologous protein production, which makes it one of the most widely used co-substrates to produce rProt in methanol-inducing media (Carly et al., 2016; Berrios et al., 2017a; Chen et al., 2017). In order to improve xylanase expression under sorbitol-methanol co-feeding conditions, the gene identified in *K. phaffii* as the initial acceptor of the pexophagy process (*ATG30*) was deleted to favor peroxisome retention in cells under the influence of the addition of carbon sources that trigger this cellular response. This modification improved xylanase production, reporting an activity of ~1140.7 U mL^{-1} in cultures supplemented with 2% sorbitol, representing an increase of ~11.4% compared to the control culture containing 0.5% sorbitol (Liu et al., 2019). This demonstrates that by employing cell engineering strategies, the production of a highly in-demand enzyme in the food and paper industry can be successfully increased (Moreira et al 2016).

K. phaffii does not normally metabolize sucrose because of the absence of an invertase enzyme (Çalik *et al.*, 2015). However, a study evaluating the influence of the carbon source on cell size and production of an anti-LDL-single-chain variable fragment (scFV) (Diaz Arias *et al.*, 2019), expressed in *K. phaffii* the Suc2 invertase enzyme from *Saccharomyces cerevisiae* (Boehm *et al.*, 1999) under the control of p*AOX1*.When this strain was grown in sucrose-supplemented medium, both the antibody fragment concentration (93.7 mg L^{-1}) and the specific yield on biomass (3.96 mg g^{-1} DCW^{-1}) showed comparable values to glycerol-supplemented cultures (72.7 mg L^{-1} and 3.04 mg g^{-1} DCW^{-1}, respectively). Additionally, when evaluating the use of glucose, this condition showed the lowest productivity (63.3 mg L^{-1}), even though using this medium generated a higher cell volume compared to sucrose or glycerol (0.766 µm3 in glucose, 0.214 µm3 in sucrose, 0.202 µm3 in glycerol) (Arias *et al.*, 2017; Diaz Arias *et al.*, 2019). This suggests that high production of this heterologous protein in *K. phaffii* in sucrose-based cultures may be mainly related to cell number rather than cell concentration, in addition to the repressive effect on the p*AOX1* from both glycerol and glucose (Arias *et al.*, 2017; Diaz Arias *et al.*, 2019).

The study of these auxiliary carbon sources in recent years has mainly focused on managing the conditions and operating parameters in culture systems (Niu *et al.*, 2013; Arias *et al.*, 2017; Zepeda *et al.*, 2018; Nieto-Taype *et al.*, 2020) therefore, an interesting and complementary scope of study could be carried out looking into the modification in their respective metabolic pathways, in conjunction with the manipulation and optimization of these cultivation parameters.

2.3 Engineering of turnover co-factor metabolism

The metabolic burden that arises from processes rProt folding, posttranslational modifications, and secretion have shown that regeneration of the oxidised cofactor significantly affects energy metabolism, becoming a bottleneck(Geertman *et al.*, 2006; Kim and Hahn, 2015; Nocon *et al.*, 2016). The overexpression of genes encoding enzymes catalysing NADPH-producing reactions has proven its usefulness to overcome redox unbalance. The overexpression of the *Saccharomyces cerevisiae POS5*-encoded NADH kinase increased 2-fold the specific productivity of Fab antibody fragment (Tomàs-Gamisans *et al.*, 2020).

Constitutive overexpression of the genes encoding the glucose-6-phosphate dehydrogenase (*ZWF1*) and 6-gluconolactonase (*SOL3*) that catalyse NADPH generating reaction led to a 3.8-fold increase in the productivity of human superoxide dismutase (hSOD) (Nocon *et al.*, 2016). Beside this, overexpression of SOL3 and the gene encoding 6-phosphogluconate dehydrogenase (*GND2*), resulted in 2.2- fold increase (~6.5 mg L^{-1}) in recombinant human interferon-gamma (hIFN-γ) in comparison with the control strain GS115/hIFN-γ (2.5 mg L^{-1}) (Prabhu and Veeranki, 2018).

Table 2-1. Improving heterologous protein production by modifying metabolism and energy supply

Auxiliary Gene	Modification	Pathways Involved	Heterologous Product	Production (Fold change)	Operation Mode	Scale	Strain	Reference
A. Engineering of the MUT pathway								
p*AOX DAS*	OE	MUT	HRP (S) CalB (S)	+0.94 +0.56	Batch	5 L Bioreactor	CBS7435 (Muts)	(Krainer *et al.*, 2012)
p*AOX FLD*	OE	MUT	HRP (S) CalB (S)	+1.21 +1.07				
DAS1			CalB (S)	+1.3				
DAS2	Del	MUT	eGFP	+1.2	Batch	Flask	CBS7435 (Muts)	(Geier *et al.*, 2015)
DAS1/2				+1.15				
p*FLD1*	OE	MUT	cFab-vHH(S)	+2.69	Fed-batch	1L Bioreactor	CBS2612(Mut-)	(Zavec *et al.*, 2021)
ADH2								
FLD	Del	MUT	β-galactosidase	+2	Batch	Flask	GS115 (Mut+)	(Tyurin and Kozlov, 2015)
B. Engineering of co-substrate catabolic pathways								
ATG30	Del	MUT	Xylanase (S)	+3	Batch	Flask	GS115 (Mut+)	(Liu et al., 2019)
C. Engineering of co-substrate catabolic pathways								
p*GAPPOS5*	OE	PPP	Fab (S)	+2	Chemostat	2 L Bioreactor	X-33 (Mut+)	(Tomàs-Gamisans *et al.*, 2020)
p*GAPZWF1*-p*GAPSOL3*	OE	PPP	Hsod	+3.8	Batch	Flask	SMD1168H	(Nocon *et al.*, 2016)
p*AOXSOL3*-p*AOXGND2*	OE	PPP	hIFN- γ	+2.2	Fed-batch	1 L Bioreactor	GS115(Mut+)	(Prabhu and Veeranki, 2018)
D. Synthetic biology for alternative carbon source catabolism								
p*GAP XI*	Ex	Xylose path	β-mannanase(S)	+1.36	Batch	Flask	GS115 (Mut+)	(Li *et al.*, 2015)

Abbreviations: HRP: horseradish peroxidase; CalB: *Candida antarctica* lipase B; eGFP: enhanced green fluorescent protein; *DAS1*: dihydroxyacetone synthase 1; *DAS2*: dihydroxyacetone synthase 2; *FLD*: formaldehyde dehydrogenase; cFab-vHH: camelid antibody fragment; *ADH*: alcohol dehydrogenase; *FDH*: formate dehydrogenase; *XI*: xylose isomerase; MUT: methanol utilization pathway; PPP: pentose phosphate pathway; hSOD: cytosolic human superoxide dismutase; IFN-γ: recombinant human interferon gamma; (S) secreted protein; OE: gene overexpression; Del: gene deletion; Ex: expression by insertion.

2.4 Engineering for alternative carbon source catabolism

In the context of circular economy, the trend has been the valorization or increased added value of renewable raw materials, such as agricultural, forestry, food and industry bioproducts and/or waste streams. This goal would require *K. phaffii* to incorporate additional metabolic skills in order to metabolise substrates such as xylose, cellobiose, and cellulose (Li *et al.*, 2015; Kickenweiz *et al.*, 2018).

The heterologous expression of genes involved in xylose catabolism, namely the xylose isomerase (*XI*) from *Orpinomyces spp*. and an endogenous xylulokinase, allowed xylose conversion resulting in a yield ($Y_{x/s}$) of 0.378 $g.g^{-1}$, nearly 2-fold higher than that of the parental strain GS115, reaching values comparable to those achieved with glucose or glycerol (0.310 $g.g^{-1}$ and 0.435~0.490 $g.g^{-1}$, respectively) (Li *et al.*, 2015). Using the same engineered strain, the β-mannanase production titer reached approximately 80 U. mL^{-1}. In a different research study, the expression of three heterologous cellulases, namely *Aspergillus niger* β-glucosidase (An*BGL1*), *A. niger* endoglucanase (An*EG-A*), and a *Trichoderma reesei exoglucanase* (Tr*CBH2*), allowed the resulting strain to grow on cellobiose and carboxymethyl cellulose (Kickenweiz *et al.*, 2018).

Another metabolic engineering strategy in the search for alternative carbon source metabolism consisted of increasing the acetate tolerance in *K. phaffii*. Indeed, acetate, which can be obtained from syngas by the hydrolysis of cellulosic biomass or by anaerobic fermentation of different agro-industrial wastes (Park *et al.*, 2022), is a cheap and largely available carbon source. This increased tolerance was conferred by the p*GAP*-driven overexpression of the native gene PAS_Chr3_1091 encoding the putative serine/threonine protein kinase Hrk1, together with the *S. cerevisiae* gene sc*ACS1** encoding acetyl-CoA (Xu *et al.*, 2019).

Recently, *K. phaffii* was engineered for CO metabolization through a reorganization of the MUT pathway as well as the xylulose monophosphate (XuMP) pathway, in order to generate a Calvin–Benson–Bassham resembling cycle. This modification was obtained by the expression of eight recombinant proteins from five different organisms: from *Ogataea polymorpha* (glyceraldehyde-3-phosphate dehydrogenase Tdh3, phosphoglycerate kinase Pgk1), *Ogataea parapolymorpha* (transketolase Tkl1, triosephosphate isomerase Tpi1), *Spinacia oleracea* (phosphoribulokinase Prk), *Thiobacillus denitrificans* (ribulose-1,5-bisphosphate carboxylase-oxygenase RuBisCO), and *Escherichia coli* (chaperones GroEL and GroES); and the deletion of three native genes (*AOX1, DAS1, DAS2*) (Gassler *et al.*, 2020). This strategy opens up new opportunities for rProt synthesis from alternative carbon sources.

3. Methanol-free systems and p*AOX1* induction

Recently, investigations have focused on developing methanol-free expression systems through alternative strategies, including identifying new promoters, engineering regulation of the p*AOX1*, and evaluating new p*AOX1* inducer metabolites.

The p*AOX1* is repressed in the presence of ethanol (Brierley *et al.*, 1990). Ergün et al., (2020), developed *AOX1* hybrid-promoter that are ethanol-inducible by replacing specific cis-actin DNA motifs. The ethanol-inducible p*AOX1*/Cat8-L3 variant, which integrates a single synthetic Cat8 cis-acting element, achieved 74% eGFP expression compared to the p*AOX1* methanol induce system. The p*AOX1*/Adr1-L3/Cat8-L3 variant, designed with single Cat8 and Adr1 cis-acting elements, reached 85% eGFP expression.

Studies on the activation or inactivation of the catabolic p*AOX1* repression pathway have improved our understanding of the p*AOX1* transcription factor regulation (Parua *et al.*, 2012; Wang, Cai, *et al.*, 2016; Wang, Wang, *et al.*, 2016; Wang *et al.*, 2017).

For instance, the deletion of three transcription repressors (Δmig1, Δmig2, and Δnrg1) and the overexpression of the transcription activator *MIT1* allow p*AOX1* induction in the presence of glycerol. Through a fermentation culture strategy named "Glucose – glycerol – shift," *K. phaffii* modified strain growth is supported by glucose, and induction starts when the culture shifts to glycerol after glucose is depleted. This strain produced 77% GFP levels compared to the wild type in methanol, even though it has the disadvantage of requiring more oxygen (Wang *et al.*, 2017). An effective retrofitting of p*AOX1*-based expression strains into glucose/glycerol-regulated systems was achieved by combining the p*AOX1* expression system with a cassette strategy involving *MIT1* or *MXR1* overexpression under the derepressed promoter of the peroxisomal catalase 1 gene (p*CAT1*), which is initiated when glucose in the medium is depleted (Vogl *et al.*, 2018). Another methanol-free system was developed by deleting the putative protein hexose transporter (Pp*HXT1)*, which leads to the induced expression of the *AOX1* gene in response to glucose or fructose. However, this system has the disadvantage of sharp expression drop during later growth phases due to rapid degradation by pexophagy in response to glucose or fructose (Zhang *et al.*, 2010).

In the research of new p*AOX1* inducer metabolites, the p*AOX1* was induced by dihydroxyacetone. The Δdak-DHA methanol-free system involves knocking out the PAS_chr3_0841 gene encodes a dihydroxyacetone kinase (Dak), involved in the p*AOX1* repression pathways. This modification led to protein expression levels that surpassed those of the p*GAP* system and reached 50-60% of the levels achieved by the traditional methanol-induced system (Shen *et al.*, 2016).

3.1 Formate as a pAOX1 inducer

In the last years, it has been reported that methanol is not the sole inducer of p*AOX1*, and metabolites downstream of methanol metabolism (*i.e.*, formaldehyde and formate) may also induce p*AOX1* (Tyurin and Kozlov, 2015; Singh and Narang, 2020). However, while formaldehyde can induce p*AOX1*, it significantly affects cell

growth. Therefore, it is not suitable for use in industrial cultures (Singh and Narang, 2020). On the other hand, using formate in combination with methanol was reported to increase cell yield by around 20% compared to using methanol alone (Hazeu and Donker, 1983).

Feng et al.(2022) evaluated different concentrations of ammonium formate (0.1%, 0.3%, 0.5%, 0.7%, 1%, and 1.5%) as inducers of the p*AOX1* in a medium with glycerol as the primary carbon source. They found that higher concentrations of ammonium formate inhibited growth, while the optimal p*AOX1* induction occurred at 0.7%, achieving 17.5% of the induction level obtained with methanol. Based on transcriptomic analysis, they identified a low energy generation pathway as the cause of the reduced GFP expression when ammonium formate was used. To address this, they tested a combination of 0.7% ammonium formate with either 2 g/L ATP, 4 g/L alanine, or 0.05% sorbitol. The best results in terms of GFP intensity were obtained with the addition of ATP and sorbitol (Feng *et al.*, 2022). However, using ATP on industrial scales increases the production cost, making sorbitol one of the most viable options.

The overexpression of transcription factors related to p*AOX1* regulation has been explored to enhance p*AOX1* induction by formate. Liu et al. (2022a) overexpressed the transcription factor Mit1 in a system engineered to express xylanase and evaluated four concentrations of ammonium formate (0.2%, 0.5%, 0.8%, and 1.1%). They found that higher formate concentrations (0.8% and 1.1%) reduced cell density and xylanase activity. The best results were achieved with Mit1 overexpression in combination with 0.2% ammonium formate and 0.05% sorbitol. To use formate as a p*AOX1* inducer and increase its conversion to formaldehyde to enter the central metabolism via the pentose phosphate pathway, Liu et al. (2022b) later constructed a formate assimilation pathway in *K. phaffii* that overexpresses the transcription factor Mit1 and expresses xylanase B. To develop this assimilative pathway, they expressed acetyl-CoA synthase (ACS) from *Escherichia coli* and acetaldehyde dehydrogenase (ACDH) from the non-pathogenic *Listeria innocua*. The optimal condition for increased xylanase expression was achieved by adding 0.2% sodium formate and 0.05% sorbitol, resulting in a yield of 580 U/mL, a 1.2-fold increase compared to the strain expressing only Mit1. However, this improvement did not reach the xylanase expression levels obtained when methanol was used as the p*AOX1* inducer (3925 U/mL) (Xia *et al.*, 2021). Therefore, research on using formate, a safe and sustainable compound, as a p*AOX1* inducer has become increasingly important in recent years. Investigations that enhance the efficacy of formate as an inducer are essential to reducing the reliance on methanol and mitigating the associated drawbacks of this toxic compound.

4. Conclusions

K. phaffii is a successful platform for producing biotechnologically and commercially attractive products (as shown in Table 1-1), primarily due to its ability to produce a diverse range of functionally active heterologous proteins, from bacterial

origins to complex eukaryotic proteins with various applications. Metabolic modifications have enabled the development of more robust strains. The creation of these strains has involved several strategic approaches, including gene codon optimization that enhances translation efficiency in *K. phaffii*. At the same time, promoter engineering allows precise control over gene expression levels, facilitating optimal production conditions. On the other hand, leveraging CRISPR-Cas9 and other synthetic biology tools, genomic engineering has been pivotal in introducing new metabolic pathways and optimizing existing ones. These approaches have improved cellular capabilities and fitness, leading to higher recombinant protein (rProt) productivity levels and mitigating issues related to methanol metabolism.

Previous research on non-repressing carbon sources has predominantly focused on optimizing operational parameters, leaving unnoticed the regulation of metabolic pathways associated with these compounds and their impact on the p*AOX1*. For instance, while sorbitol has been utilized to reduce methanol consumption and toxicity, its broader metabolic implications have not been thoroughly investigated. An in-depth analysis of metabolic modifications targeting the assimilation pathways of carbon and energy sources in response to non-repressing carbon sources is needed to elucidate the mechanisms behind their des repressive effects on the extensively utilized p*AOX1* induction system.

Understanding these metabolic pathways is crucial for several reasons. Firstly, it can reveal potential bottlenecks or inefficiencies in the metabolic network that could be addressed to enhance rProt production. Secondly, insights into the regulatory mechanisms of the p*AOX1* in the presence of non-repressing carbon sources could lead to more efficient induction systems, reducing reliance on methanol and its associated risks. Finally, this knowledge could enable the design of strains capable of not using methanol, thus increasing the flexibility and scalability of bioproduction processes.

Recent studies have demonstrated that methanol is not the only inducer of the p*AOX1*. The use of formate in *K. phaffii* has stood out, being a non-toxic component compared to formaldehyde or methanol. These advances highlight the potential of formate as a safer and more sustainable alternative to methanol, though further research is needed to maximize its efficacy.

Lastly, while significant progress has been made in enhancing *K. phaffii*'s metabolic capabilities, a deeper understanding of the interaction between non-repressing carbon sources and the p*AOX1* induction system is essential. The following chapters will focus on dissecting the use and regulatory networks of an inducer compound (e.g., formate) and a non-repressive carbon source (e.g., sorbitol) to improve *K. phaffii*'s potential as a versatile and efficient yeast host for recombinant protein production.

Chapter 3

Formate from THF-C1 metabolism induces the AOX1 promoter in formate dehydrogenase-deficient Komagataella phaffii

Description of Chapter 3

The previous chapters emphasized the need for research on cell engineering to enhance the profile of non-repressing compounds of the p*AOX1*, aiming to reduce methanol usage. This chapter explores how disrupting the gene encoding formate dehydrogenase (*FDH1*), a component of the Mut dissimilative pathway, enables *K. phaffii* to evolve into an effective inducible system that does not require methanol. The mechanism behind this system is described below.

This work is an original contribution adapted from:
Bustos, C., Fickers. P., & Berrios., J. (2024). "Formate from THF-C1 metabolism induces the *AOX1* promoter in formate dehydrogenase-deficient *Komagataella phaffii*". This paper was published in *Microbial Biotechnology*, ***17*** (10), e70022. (https://doi.org/10.1111/1751-7915.70022).

Chapter 3. Formate from THF-C1 metabolism induces the *AOX1* promoter in formate dehydrogenase-deficient *Komagataella phaffii*

1. Introduction

The methylotrophic yeast *Komagataella phaffii (Pichia pastoris)* is a well-established and reliable cell factory for producing recombinant proteins (rProt) (Ergün *et al.*, 2021; Barone *et al.*, 2023). The expression systems used typically and historically rely on the regulated promoter from the alcohol oxidase 1 gene (p*AOX1*). This promoter is under catabolic repression during cell growth on glycerol or glucose, while p*AOX1* induction and thus, rProt synthesis, is triggered by adding an inducer to the culture medium, typically methanol (Thorpe *et al.*, 1999; Ergün *et al.*, 2021; Bustos *et al.*, 2022) Alternative carbon sources, such as sorbitol, do not repress p*AOX1* and can be used as the sole carbon and energy source in combination with methanol to produce rProt (Inan and Meagher, 2001; Niu *et al.*, 2013). When the repressing carbon source is depleted or at low concentrations, the promoter is derepressed and expression occurs at low levels, typically at 2-4% of the fully induced state achieved with methanol (Vogl and Glieder, 2013). Three master transcription factors (TFs), namely methanol-induced transcription factor 1 (Mit1), methanol expression regulator 1 (Mxr1), and the positive regulator of methanol 1 (Trm1), promote p*AOX1* induction (Vogl *et al.*, 2018; Ata *et al.*, 2021). Derepression of p*AOX1* is mediated by Mxr1, while Trm1 and Mit1 contribute to promoter activation (Wang, Wang, *et al.*, 2016). In the presence of glucose or glycerol, the Nrg1 TF represses p*AOX1* by direct binding on p*AOX1* cis-elements. Furthermore, Mig1 and Mig2 function as catabolite repressors by preventing the expression of *MIT1* or by interacting with Mit1 (Wang *et al.*, 2017).

Although widely used, including on an industrial scale, methanol presents several technical challenges that are difficult to overcome in practice. It is highly flammable and can become toxic to cells at high concentrations due to the accumulation of toxic methanol catabolic products such as formaldehyde (Berrios *et al.*, 2022) (Fig. 2-2). Moreover, its oxidation by alcohol oxidases in peroxisomes requires oxygen, thereby increasing the cellular oxygen demand compared to other carbon sources. Additionally, methanol catabolism generates heat, which must be dissipated, thereby increasing the operational costs, especially for large-scale production processes (Krainer *et al.*, 2012; Niu *et al.*, 2013). Currently, there is a trend underscoring the critical need for alternative methanol-free systems that facilitate the development of more cost-effective and sustainable solutions for industrial rProt production. Methanol-free derepressed bioprocesses present a promising alternative in this context (Shinobu Takagi *et al.*, 2012; García-Ortega *et al.*, 2019; Ergün *et al.*, 2021).

Formate, an intermediate metabolite of the methanol dissimilation pathway (Hartner & Glieder, 2006, Fig. 2-2), has emerged as an interesting alternative inducer to methanol for rProt synthesis in *K. Phaffii*. It is produced from formaldehyde by

formaldehyde dehydrogenase (Fld) before being converted into carbon dioxide by formate dehydrogenase (Fdh). Compared to methanol, formate is a more sustainable inducer that can be efficiently produced through the electrochemical conversion of carbon dioxide (Jhong *et al.*, 2013; Cotton *et al.*, 2020). The ability of formate to induce p*AOX1* has been demonstrated (Tyurin and Kozlov, 2015; Jayachandran *et al.*, 2017; Singh and Narang, 2020). However, one of the primary limitations of formate is its poor ability to be catabolized by *K. phaffii*. To address this constraint, an engineering strategy has been developed through the co-overexpression of genes encoding *Escherichia coli* acetyl-CoA synthase, *Listeria innocua* acetaldehyde dehydrogenase, and the transcription factor Mit1. This engineering effort led to an increase in xylanase production by 59% compared to the parental strain that produces xylanase (Liu et al., 2022).

In cells, formate is also an intermediate of the tetrahydrofolate-mediated one-carbon (THF-C1) metabolism involved in several anabolic pathways, including the *de novo* synthesis of purines (Kastanos et al., 1997; Piper et al., 2000; Fig. 4-1). It is obtained from cytoplasmic serine by the action of serine hydroxymethyltransferase (Shm2), methylenetetrahydrofolate dehydrogenase & methenyltetrahydrofolate cyclohydrolase (Mis1-3) and formate-tetrahydrofolate ligase (Mis1-2), and in the mitochondrion by serine hydroxymethyltransferase (Shm1) and the trifunctional enzyme: formate-tetrahydrofolate ligase, methenyltetrahydrofolate cyclohydrolase and methylenetetrahydrofolate reductase (Mis1-1) (Mitic et al., 2023, Fig. 3-1). In the THF-C1 metabolism, formate serves as a shuttle for C1 units between the cytoplasm and the mitochondrion, as THF derivatives cannot cross the mitochondrial membrane (Kastanos *et al.*, 1997).

Herein, this chapter presents the investigation of the regulation of p*AOX1* by formate in a *FDH1* knockout (FdhKO*)* strain. From this investigation, it became evident that endogenous formate from THF-C1 metabolism was sufficient to trigger p*AOX1* induction in a FdhKO mutant grown under non-repressive culture conditions (i.e. in the presence of sorbitol) without any supplementation of inducer. In those conditions, any p*AOX1*-based expression system could be potentially converted into a self-induced one.

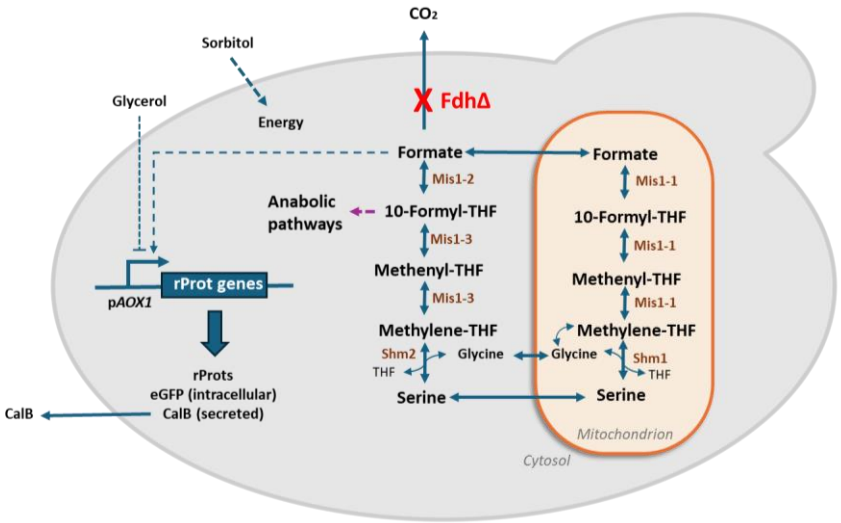

Figure 3-1. Tetrahydrofolate (THF) mediated one-carbon (THF-C1) metabolism in yeast. Fdh, formate dehydrogenase; Shm1, mitochondrial serine hydroxymethyltransferase; Shm2, cytosolic serine hydroxymethyltransferase; Mis1-2, formate-tetrahydrofolate ligase; Mis1-3, methylenetetrahydrofolate dehydrogenase & methenyltetrahydrofolate cyclohydrolase; Mis1-1, trifunctional enzyme: formate-tetrahydrofolate ligase, methenyltetrahydrofolate cyclohydrolase and methylenetetrahydrofolate reductase; THF, tetrahydrofolate; eGFP, enhance green fluorescent protein; CalB, lipase B from *Candida antarctica* . *FDH1* gene knockout is mentioned in red, and enzymes involved in pathways are shown in brown.

2. Material and methods

2.1. Strain, media and culture conditions

The *Komagataella phaffii* (*K. phaffii)* and *Escherichia coli* strains used are listed in Table 3-1, respectively. *E. coli* was cultivated at 37°C in Luria-Bertani medium (LB), supplemented with antibiotics as follows: 100 µg mL^{-1} ampicillin, 50 µg mL^{-1} kanamycin, 25 µg mL^{-1} zeocin, or 50 µg mL^{-1} hygromycin. *K. phaffii* strains were cultivated at 30°C either in YPD medium (containing 20 g L^{-1} glucose, 10 g L^{-1} Difco yeast extract, and 10 g L^{-1} Difco bacto peptone) or YNB medium (containing 1.7 g L^{-1} Difco YNB w/o ammonium chloride and amino acids, 5 g L^{-1} NH_4Cl and, 0.4 mg L^{-1} biotin, 100 mM potassium phosphate buffer, pH 6.0) supplemented with as follows: 10 g L^{-1} sorbitol and 2 g L^{-1} Difco casamino acid (YNBSC), 10 g L^{-1} sorbitol, 5.1 g L^{-1} methanol and 2 g L^{-1} Difco casamino acid (YNBSMC); 10 g L^{-1} sorbitol, 10.8 g L^{1} formate and 2 g L^{-1} Difco casamino acid (YNBSFC); 10 g L^{-1} sorbitol (YNBS); 10 g L^{-1} sorbitol and 5.1 g L^{-1} methanol (YNBSM); 10 g L^{-1} sorbitol and 10.8 g L^{-1} formate (YNBSF); 10 g L^{-1} glycerol (YNBG); 6.3 g L^{-1} methanol and 4.0 g L^{-1} sorbitol (YNBMS); 10 g L^{-1} sorbitol and 2 g L^{-1} serine (YNBSS); 10 g L^{-1} sorbitol with 2 g L^{-1} glycine (YNBSG). *K. phaffii* transformants were selected on YPD agar plates, supplemented with antibiotics as follows when requested: 25 µg mL^{-1} zeocin (YPD-

Zeo), 200 µg mL^{-1} hygromycin (YPD-Hygro), 500 µg mL^{-1} geneticin (YPD-Genet) or 100 µg mL^{-1} nourseothricin (YPD-Nat).

For all cultures, a first preculture inoculated from a single colony was performed for 12 h at 30°C and 150 rpm in a 250 mL shake flask containing 25 mL of liquid YPD medium. After centrifugation at 9000 g for 5 min, the cells were washed with phosphate-buffered saline (0.1 M, pH 6) before being used to inoculate a second preculture in the same conditions in YNB media supplemented as described above. Cultures were performed in 24-square deep well plates (System Duetz, Enzyscreen) as described elsewhere containing 1.5 mL of medium (Sassi et al. 2016), in 50 mL shake flasks (5 mL medium) or in microbioreactor (BioLector 2, m2p-labs, Baesweiler, Germany). For that purpose, 48-well Flower plates (M2P-MTP-48-B, Beckman Coulter Life Sciences, USA) containing 1 mL of medium were used. Cultures were operated for 60 h with a relative humidity of 85 %, under constant agitation at 1000 rpm. Every 10 minutes, biomass was monitored using scattered light intensity at a wavelength of 620 nm while cell fluorescence was quantified at 520 nm (excitation at 488 nm). The gain was set as 2 for biomass and 4 for fluorescence. Specific fluorescence was obtained by dividing the fluorescence value by the biomass value. It was expressed in specific fluorescence units (sFU). All cultures were seeded at an initial optical density at 600 nm of 0.5 from cells grown in the second preculture. Cultures in 24-square deep well plates and flasks were performed with three biological replicates, whereas cultures in the BioLector were performed with two biological replicates, each supported by two technical replicates, resulting in a total of four replicates.

Table 3-1. *E. coli* and *K. phaffii* strains used in the 3rd chapter

Number	Names	Genotype - Plasmid	Reference
E. coli			
A2		BB1_23	(Prielhofer *et al.*, 2017)
D12		BB3aZ_14	(Prielhofer et al., 2017)
A4		BB1_12_p*GAP*	(Prielhofer et al., 2017)
C1		BB1_34_*ScCYC1*tt	(Prielhofer et al., 2017)
E1		BB3eH_14	(Prielhofer et al., 2017)
E6		BB3aN_14	(Prielhofer et al., 2017)
RIE396		pKTAC-CRE	(Marx *et al.*, 2008)
RIE369		RIP369, pGEMTeasy, *FDH1* disruption cassette	This work
RIE465		RIP465, BB1-23-*FDH1*	This work
RIE466		RIP466, BB3eH_14, p*GAP-FDH-scCYC1tt*	This work
RIE 491		RIE491, TopoBluntII, *SHM2* disruption cassette, Zeo	This work
RIE492		RIP492, TopoBluntII, *SHM1* disruption cassette, Nat	This work
K. phaffii			
RIY232	Fdh	GS115, *HIS4*	Theron et al (2019)
RIY230	Fdh eGfp	GS115, p*AOX1-eGFP*	Velastegui et al (2019)
RIY308	Fdh CalB	GS115, p*AOX1-αMF-CalB*	Velastegui et al (2019)
RIY536	FdhKO eGfp Z+	RIY230, *fdh1*Δ, p*AOX1-eGFP*, Zeo+	This work
RIY537	FdhKO CalB Z+	RIY308, *fdh1*Δ, p*AOX1-αMF-CalB*, Zeo+	This work
RIY540	FdhKO eGfp	RIY536, *fdh1*Δ, p*AOX1-eGFP*	This work
RIY561	FdhKO CalB	RIY537, *fdh1*Δ, p*AOX1*-αMF-*CalB*	This work
RIY624	FdhKO eGfp-FdhOE	RIY540, *fdh1*Δ, p*AOX1-eGFP*, p*GAP-FDH1*, Zeo+	This work
RIY641	Fdh&Shm1KO eGfp	RIY540, *fdh1*Δ, *shm1*Δ, p*AOX1-eGFP*, Nat+	This work
RIY640	Fdh&Shm2KO eGfp	RIY540, *fdh1*Δ, *shm2*Δ, p*AOX1-eGFP*, Zeo+	This work
RIY642	Fdh&Shm1,2KO eGfp	RIY540, *fdh1*Δ, *shm1*Δ, *shm2*Δ, p*AOX1-eGFP*, Zeo+, Nat+	This work

2.2. General genetic techniques

Standard media and techniques were used for *E. coli* (Sambrook and Russell, 2001). Restriction enzymes, DNA polymerases, and T4 DNA ligase were obtained from New England Biolabs (NEB, Ipswich, MA, USA) or Thermo Scientific (Thermo Scientific, Waltham, MA USA). Primers for PCR and qPCR were synthesized by Eurogentec (Seraing, Belgium, Table A3-1. Appendix 1). Vector TopoBluntII and pGEMTeasy were from Invitrogen (Waltham, Massachusetts, United States) and Promega (Madison, Wisconsin, United States), respectively. Genomic DNA was purified using a Genomic DNA Purification kit (Thermo Scientific, Waltham, MA USA). DNA fragments were purified from agarose gels using a NucleoSpin Gel and a PCR clean-up kit (Machery-Nagel, Düren, Germany). DNA sequencing was performed by Eurofin Genomic (Eurofin, Ebersberg, Germany). Quantitative PCR (qPCR) was performed as described elsewhere with primers listed in Table A3-1. Appendix 1, using the actin gene as a reference. Total RNA was extracted using the NucleoSpin RNA Plus kit (Machery-Nagel, Düren, Germany). qPCR was performed using the Luna Universal qPCR Master Mix and the Step OnePlus Real-Time PCR system (Thermo Scientific, Waltham, MA, USA). Primers and plasmid designs were performed using the software Snapgene (Dotmatics, USA). Vectors were constructed using the GoldenPiCS Kit (Prielhofer et al., 2017, Addgene kit #1000000133). *K. phaffii* was transformed as described by Lin-Cereghino et al., (2005).

2.3. Construction of plasmids and K. phaffii strains

To construct the gene disruption cassettes, a ~ 1 kb fragment upstream of the start codon (Pro-gene) and ~ 1 kb fragment downstream of the stop codon (Term-gene) of the genes PAS_chr3_0932 (*FDH1*), PAS_chr4_0587 (*SHM1*) and PAS_chr4_0415 (*SHM2*) were PCR-amplified using *K. phaffii* GS115 genomic DNA as a template. The primer pairs used to amplify Pro-gene and Term-gene were P.fdh1-Fw/P.fdh1-Rv and T.fdh1-Fw/T.fdh1-Rv for *FDH1*, P.shm1-Fw/P.shm1-Rv and T.smh1-Fw/T.shm1-Rv for *SHM1*; and P.shm2-Fw/P.shm2-Rv and T.smh2-Fw/T.shm2-Rv for *SHM2*. The zeocin and nourseothricin selection markers were amplified from plasmids D12-BB3aZ_14 and E6-BB3aN_14 (Table S1), used as a template with primer pairs BleoR.fdh1-Fw/BleoR.fdh1-Rv, Nat.shm1-Fw/Nat.shm1-Rv and BleoR.shm2-Fw/ BleoR.shm2-Rv and subsequently used to construct the *FDH1*, *SHM1* and *SHM2* disruption cassettes, respectively. The *FDH1* disruption cassette (P_fdh1-Bleo.R-T_fdh1) was obtained by Golden Gate assembly using BsaI as restriction enzyme. The *SHM1* and *SHM2* disruption cassettes (Pro_gene-Selection Marker-Term_gene) were obtained by an overlapping PCR using the corresponding purified Pro_gene, selection marker, Term_gene fragment as templates and primer pairs P.fdh1-Fw/T.fdh1-Rv, P.shm1-Fw/T.shm1-Rv and P.shm2-Fw/T.shm2-Rv, respectively. The resulting ~ 3.2 kb fragments were cloned into the pGEMT-Easy vector or Blunt II-Topo vector to generate plasmids RIP 369 (*FDH1*), RIP491 (*SHM2*), RIP492 (*SHM1*) (Table S1). The *FDH1* disruption cassette from plasmid RIP369 was subsequently used to transform RIY230 (Fdh eGfp) and RIY308 (Fdh CalB) strains to yield RIY536 (FdhKO eGfp Z+) and RIY537 (FdhKO CalB Z+)

strains, respectively. Construction of RIY230 (Fdh eGfp) and RIY308 (Fdh CalB) strains were described in Velastegui et al., (2019). The *SMH1* and *SHM2* disruption cassettes from plasmids RIP492 and RIP491 were used to transform RIY540 (FdhKO eGfp) strain to generate the RIY640 (Fdh&Shm2KO eGfp), RIY641(Fdh&Shm1KO eGfp) and RIY642(Fdh&Shm1,2KO eGfp) strains (Table 1). The disruption cassettes were released from the corresponding plasmid by SacI restriction. Transformants were selected on YPD-Zeo and YPD-Nat, according to the corresponding marker. For marker rescue, RIY536 (FdhKO eGfp Z+), and RIY237 (FdhKO CalB Z+) strains were transformed with the replicative vector RIP396 (pKTAC-Cre) and transformants were selected on YPD-Genet. The resulting strains were RIY540 (FdhKO eGfp) and RIY561 (FdhKO CalB). To construct the *FDH1* expression vector, the GoldenPiCS system was used (Prielhofer *et al.*, 2017). Internal BpiI recognition sequence in gene PAS_chr3_0932 (*FDH1*) was removed by overlapping PCR using pairs Fdh1-Fw/Fdh1.BpiI-Rv and Fdh1.BpiI-Fw/Fdh1-Rv using *K. Phaffii GS115* genomic DNA as a template. The resulting PCR product was cloned into plasmid A2 (BB1-23) at BsaI restriction site to yield plasmid RIP465. Plasmid RIP466 (p*GAP-FDH1*-ScCYC1tt) was constructed by Golden Gate assembly from the plasmids RIP465, A4 (BB1_12_p*GAP*), C1 (BB1_34_*ScCYC1*tt) and E1. (BB3eH_14) using BpiI as the restriction enzyme. After PmeI digestion and purification, plasmid RIP466 was used to transform the RIY540 (FdhKO eGfp) strain to yield the RIY624 (FdhKO eGfp-FdhOE) strain. Transformants were selected on YPD-Hygro. Correctness of the disruption mutant genotype was confirmed by analytical PCR on the genomic DNA of the different disrupted strains. For gene disruption, the forward primers annealed upstream of the Pro-genes, namely Up.fdh1-Fw, Up.shm1-Fw, Up.shm2-Fw, for genes *FDH1, SHM1* and *SHM2*, respectively, while the reverse primers annealed within the selection marker, namely BleoR.Int-Rv for genes *FDH1* and *SHM2*, and Nat.shm1-Rv for gene *SHM1*. As further confirmation, forward primers that annealed within the selection marker BleoR.Int-Fw for gene *FDH1* and *SHM2, and* Nat.Int-Fw for gene *SHM1* and reverse primers that annealed downstream of the Term-gene, namely Dw.fdh1-Rv, Dw.shm1-Rv, Dw.shm2-Rv, for gene *FDH1, SHM1* and *SHM2*, respectively, were used. To confirm the excision of the selection marker in the RIY540 (FdhKO eGfp) strain and RIY561 (FdhKO CalB) strain, primer pairs P.fdh1-Fw/T.fdh1-Rv were used. To verify the genotype of the RIY624 strain (FdhKO eGfp-FdhOE), primers pGAp.Int-Fw and Cyc1t.Int-Rv that annealed in the p*GAP* and the *ScCYC1*tt region were used. A schematic representation of the strain genotype is presented in Fig 3-2.

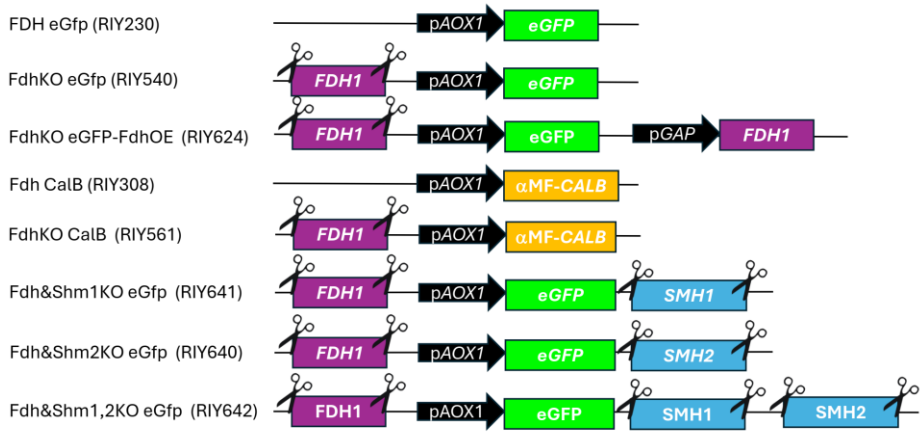

Figure 3-2. Schematic representation of the genotype of the strains presented in this chapter.

2.4. Analytical methods

A Cell growth was monitored either by optical density at 600nm (OD_{600}) or dry cell weight (DCW) as previously described (Carly *et al.*, 2016). Methanol, formate, sorbitol, and glycerol concentrations were determined by HPLC (Agilent 1100 series equipped with UV (210 nm) and RID detector, Agilent Technologies, Santa Clara, CA, USA) using an Aminex HPX-87H ion-exclusion column (300 × 7.8 mm Bio-Rad, Hercules, CA, USA). Compounds were eluted from the column at 65°C with a flow rate of 0.5 mL min^{-1} and using a 5 mM H_2SO_4 solution as the mobile phase. Formate was also quantified using the Formic acid quantification kit (K-FORM, Megazyme Inc., Bray, Ireland)

Intracellular eGFP fluorescence was quantified using a BD Accuri C6 Flow Cytometer (BD Biosciences, San Jose, CA, USA) as described elsewhere (Sassi *et al.*, 2016). For each sample, 20,000 cells were analyzed using the FL1-A and FSC channels, and FL1-A/FSC dot plots were analyzed using the CFlowPlus software (Accuri, BD Biosciences). A threshold of 5800 fluorescence units (FU) on FL1-A channel was applied to eliminate the noise for endogenous fluorescence from the cells. To calculate the total value of fluorescence in the cell population, the FL1-A median value (i.e., the eGFP fluorescence) was multiplied by the fraction of cells with eGFP fluorescence (i.e., induced cells). It was expressed in total fluorescence unit (TFU).

Spectrofluorometric analysis of eGFP was performed on SpectraMax M2 (Molecular Devises, San Jose San Jose, CA, USA) using λex and λem at 488 and 535 nm, respectively. Measurements were taken after 30 s of sample shaking. Signal gain was set to 225, and the number of light flashes was set to 30. Specific eGFP fluorescence was expressed as specific fluorescence units (sFU), i.e., as fluorescence value normalized to biomass related to optical density at 600 nm (OD_{600}) of 0.5.

The lipase activity in the culture supernatant was determined by monitoring the hydrolysis of p-nitrophenylbutyrate (p-NPB) as described elsewhere (Fickers *et al.*, 2003). The release of para-nitrophenol was monitored at 405 nm using a SpectraMax M2 (Molecular Devices, San Jose, CA, USA). All lipase activity assays were performed at least in triplicate. One unit of lipase activity was defined as the amount of enzyme releasing 1 µmol p-nitrophenol per minute at 25 °C and pH 7.2 (εPNP = 0.0148 $\mu M^{-1}.cm^{-1}$).

Fluorescence microscopy was performed with a Nikon Eclipse Ti2-E inverted automated epifluorescence microscope (Nikon Eclipse Ti2-E, Nikon France, France) equipped with a DS-Qi2 camera (Nikon camera DSQi2, Nikon France, France), and a 100× oil objective (CFI P-Apo DM Lambda 100× Oil (Ph3), Nikon France, France). The GFP-3035D cube (excitation filter: 472/30 nm, dichroic mirror: 495 nm, emission filter: 520/35 nm, Nikon France, Nikon) was used to visualize eGFP. Prior to observation, cells were washed with phosphate buffer saline and diluted at a cell concentration of 0.5 gDCW L^{-1}. For image processing, ImageJ software was used (Collins, 2007; Schneider *et al.*, 2012).

3. Results and discussion

3.1. AOX1 promoter activity is upregulated by formate

In methylotrophic yeasts, formate is an intermediate of the methanol dissimilation pathway (Hartner & Glieder, 2006, Fig. 2-2). Studies have demonstrated the efficacy of formate as both an inducer and a carbon source to produce rProt in *K. phaffii* (Singh and Narang, 2020; Liu, Li, *et al.*, 2022; Liu, Zhao, *et al.*, 2022). Herein, an enhanced green fluorescent protein (eGFP) reporter system was used to probe the regulation of the *AOX1* gene promoter (p*AOX1*) by formate. For this purpose, the RIY230 strain (*pAOX1-eGFP*, hereafter Fdh eGfp strain), (Velastegui *et al.*, 2019) was grown on sorbitol (YNBS) supplemented or not with methanol or formate (YNBSC, YNBSMC, and YNBSFC, respectively) in deep well plates. Sorbitol was selected as the carbon source since it is known to be non-repressive for p*AOX1* (Niu *et al.*, 2013). Total eGFP fluorescence was monitored in cells by flow cytometry at the end of the growth phase (i.e., 18h) and during the stationary phase (i.e., 24h). As shown in Fig. 3-3, the eGFP signals were low in the sorbitol medium (16601 and 9340 TFU, respectively). In the absence of an inducer such as methanol or formate, the low p*AOX1* induction level can be attributed to the action of the constitutively low expression of *MXR1* encoding global activator of genes involved in methanol catabolism (Ata et al., 2021). The p*AOX1* induction levels were markedly higher and within the same range for cells grown in sorbitol-methanol (61207 and 48518 TFU, respectively) or sorbitol-formate (50488 and 52960 TFU, respectively). These observations contrast with a recent report on similar experiments conducted on glycerol-based defined media (YNBG), where eGFP-specific fluorescence levels were reported as 4.1-fold lower in the presence of formate compared to methanol (Feng *et al.*, 2022). This demonstrates that formate can substitute methanol for p*AOX1* induction, at least in a sorbitol-minimal medium.

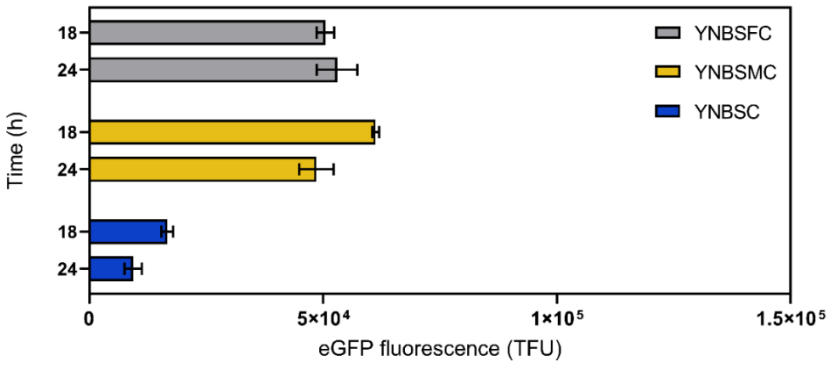

Figure 3-3. GFP fluorescence of Fdh eGfp strain after 18h and 24 h of growth in YNB minimal medium containing sorbitol and formate (YNBSFC, grey), sorbitol and methanol (YNBSMC, yellow), and sorbitol (YNBSC, blue). Fluorescence was quantified by flow cytometry on 20,000 cells and expressed as TFU (total fluorescence, see materials and method for calculation details). Data are the mean and standard deviation of triplicate cultures conducted in deep well plates.

3.2. Formate can be used as a free inducer in a FdhKO strain

In the methanol dissimilation pathway, formate is converted to carbon dioxide by formate dehydrogenase (Fdh, Fig. 2-2). In methylotrophic yeasts, including *K. phaffii*, Fdh was shown as non-essential for cell survival. However, the growth of a formate dehydrogenase knockout mutant (FdhKO) is markedly reduced in a methanol-based medium (Guo *et al.*, 2021). Moreover, a FdhKO strain exhibits a heightened sensitivity to the accumulation of formate in the medium, indicating that the primary physiological function of Fdh is more related to the detoxification of intracellular formate rather than energy generation (Sibirny *et al.*, 1990; Sakai *et al.*, 1998). Therefore, the knockout of gene *FDH1* in *K. phaffii* would render formate a free p*AOX1* inducer in non-repressive conditions (in the presence of sorbitol). For that purpose, the *FDH1* knockout RIY540 strain (*fdh1*Δ, p*AOX1-eGFP*, hereafter FdhKO eGfp strain, Table 3-1) was constructed. It was grown on sorbitol, sorbitol-methanol, or sorbitol-formate (YNBSC, YNBSMC, and YNBSFC, respectively), and the eGFP fluorescence was quantified by flow cytometry after 18 h and 24 h of culture.

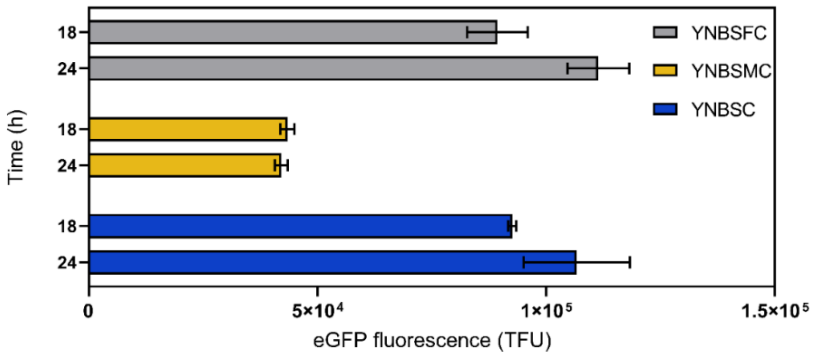

Figure 3-4. eGFP fluorescence of FdhKO eGfp strain after 18h and 24 h of growth in YNB minimal medium containing sorbitol and formate (YNBSFC, grey), sorbitol and methanol (YNBSMC, yellow), and sorbitol (YNBSC, blue). Fluorescence was quantified by flow cytometry on 20,000 cells and expressed as TFU (total fluorescence, see materials and method for calculation details). Data are the mean and standard deviation of triplicate cultures conducted in deepwell plates.

On sorbitol-methanol (YNBSMC), eGFP fluorescence signals were on average for both sampling times slightly lower for the FdhKO eGfp strain compared to the Fdh eGfp strain (i.e. 1.2-fold; 42715 and 54862 TFU, respectively; Fig. 3-3 and 3-4). This demonstrates that the knockout of *FDH1* has no outstanding impact on the strength of the p*AOX1* induction level by methanol. By contrast, on sorbitol-formate, the fluorescence signals were, on average, for both sampling times 1.9-fold higher for the FdhKO eGfp strain compared to the Fdh eGfp strain (i.e. 100359 and 51724 TFU, respectively). Therefore, preventing *K. phaffii* from dissipating formate into carbon dioxide yielded higher induction levels of p*AOX1* on formate than on methanol. More importantly, for the FdhKO eGfp strain, eGFP fluorescence signals were in the same range on sorbitol and sorbitol-formate on average for the two sampling times (i.e. 99632 and 100359 TFU, respectively). It was also 7.6-fold higher on average for the FdhKO eGfp strain compared to the Fdh eGfp strain on sorbitol (i.e., in the absence of any inducer; 99632 and 12970 TFU). The hypothesis behind this observation is presented in a following section. The lower p*AOX1* induction levels obtained for the FdhKO eGfp strain in the presence of formate-sorbitol and sorbitol-methanol compared to sorbitol can be explained by the higher concentration of formate from the medium, as well as formaldehyde and formate generated from methanol catabolism through the dissimilation pathway (Fig. 3-2). Quantification of the e*GFP* gene expression level for the FdhKO eGfp strain grown on sorbitol corroborated those results. It was increased by 2.9 and 3.2-fold in the FdhKO eGfp strain compared to the Fdh eGfp strain after 18 h and 24 h of growth, respectively (Fig. 3-5). Fluorescence microscopy also clearly showed a higher eGFP level for the knockout strain on sorbitol (i.e. without the addition of formate; Fig. 3-6).

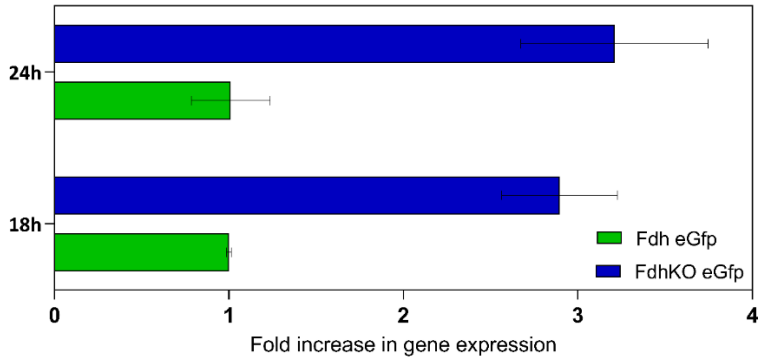

Figure 3-5. Relative expression level of eGFP gene in Fdh eGfp strain (green) and FdhKO eGfp strain (blue) in minimal medium containing sorbitol (YNBSC). Samples were collected after 18 h and 24h. Displayed values were normalized to that of the actin gene and corresponded to means and standard deviations from three independent replicates conducted in flake flasks.

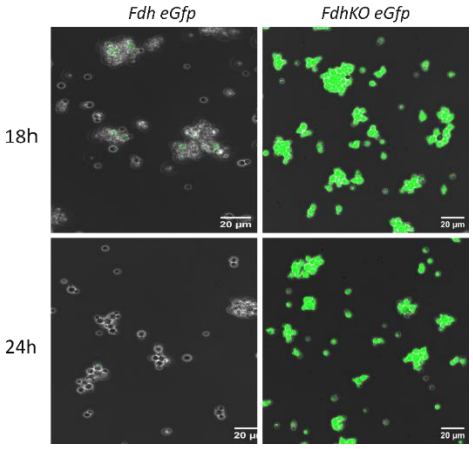

Figure 3-6. Observation of *Komagataella phaffii*, Fdh eGfp strain and FdhKO eGfp strain after 18h and 24 h of growth in minimal medium containing sorbitol (YNBSC) by fluorescent microscopy. A representative sample from the triplicate cultures conducted in flake flask are shown. Observation and image processing are detailed in material and methods.

Regarding the kinetic of cell growth for the FdhKO eGfp strain, biomass values were slightly lower in the presence of formate for both sampling times (14% on average, Table 3-2), confirming its cell toxicity. They were also slightly higher in the presence of methanol (18% on average, Table 3-2), suggesting that this carbon source

is consumed together with sorbitol, as previously reported for the wild-type strain (Niu et al., 2013; Carly et al., 2016).

Table 3-2. Biomass of RIY540 strain (FdhKO eGfp strain)

Time (h)	YNBSC (mgDCW/ml)	YNBSMC (mgDCW/ml)	YNBSFC (mgDCW/ml)
18	3.2 ± 0.1	3.9 ± 0.3	2.6 ± 0.1
24	3.6 ± 0.1	4.3 ± 0.1	3.3 ± 0.1

3.3. Complementation of the FdhKO strain restored the wild-type phenotype

To confirm that the phenotype of the FdhKO eGfp strain is related to the disruption of the gene PAS_chr3_0932, it was expressed under the control of the constitutive p*GAP* promoter in the FdhKO eGfp strain. The resulting RIY624 strain (*fdh1D*, p*AOX1-eGFP*, p*GAP-FDH*, hereafter FdhKO eGfp-FdhOE strain) was grown on sorbitol (YNBS) together with Fdh and FdhKO eGfp strains, used as negative and positive controls, respectively. The fluorescence level of the FdhKO eGfp-FdhOE strain was reduced by 24-fold on average on two sampling times (18 h and 24 h) as compared to the FdhKO eGfp strain (i.e.87218 and 3657 TFU, respectively; Fig. 3-7). This demonstrates that the disruption of the *FDH1* gene is related to the phenotype of the knockout strain.

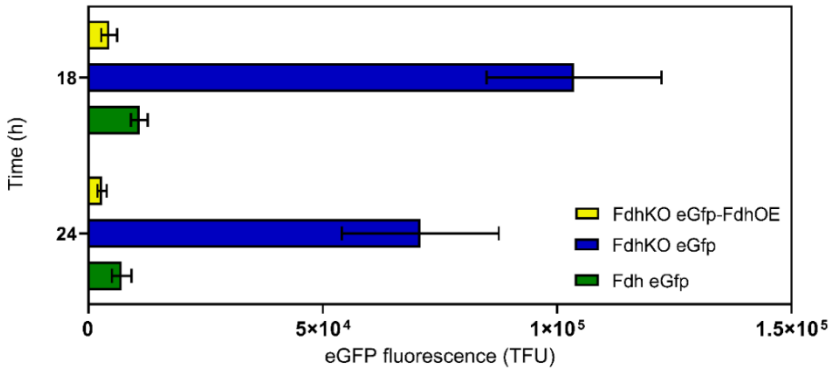

Figure 3-7. eGFP fluorescence of Fdh eGfp strain (green); FdhKO eGfp strain (blue); FdhKO eGfp-FdhOE strain (yellow) after 18h and 24 h of growth in minimal medium containing sorbitol (YNBSC). Fluorescence was quantified by flow cytometry on 20,000 cells and expressed as TFU (total fluorescence, see materials and method for calculation details). Values are the means and standard deviation from biological triplicate cultures conducted in shake flasks.

3.4. Unravelling the origins of formate in a methanol-free environment

In the FdhKO eGfp strain, a strong increase in the p*AOX1* induction level was observed under non-repressive culture conditions and in the absence of formate compared to the Fdh eGfp strain (on sorbitol medium, YNBSC). This suggests that formate is generated in an alternative metabolic pathway and somehow accumulates intracellularly in the FdhKO eGfp strain. Besides the methanol dissimilation pathway, formate is generated from cytoplasmic serine in the THF-C1 metabolism by Shm2, Mis1-3 and Mis1-2 enzymes (Fig. 3-1, (Kastanos *et al.*, 1997; Mitic *et al.*, 2023). In a *K. phaffii* wild-type strain, formate generated through that metabolism can, therefore, be consumed by formate-tetrahydrofolate ligase to form 10-formyl-THF or by formate dehydrogenase to form carbon dioxide. As the disruption of gene *FDH1* prevents this conversion into carbon dioxide, formate may somehow accumulate intracellularly in the FdhKO eGfp strain, explaining thus the induction level of p*AOX1* in non-repressive conditions. To verify this hypothesis, the expression of gene *FDH1* (as well as *FGH1* and *FLD*) was first confirmed by qPCR in cells grown on sorbitol (YNBS, Fig. 3-8).

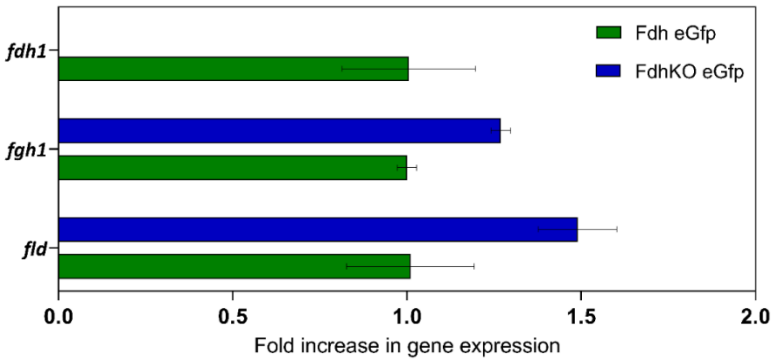

Figure 3-8. Relative expression level of genes involved in the methanol dissimilation pathway *FLD* (PAS_chr3_1028), *FGH1* (PAS_chr3_0867), *FDH1* (PAS_chr3_0932) in the Fdh eGfp strain (green) and FdhKO eGfp strain (blue) in YNBSC medium**.** Samples were collected after 18 h of culture. The displayed values were normalized to that of the actin gene and corresponded to means and standard deviations from duplicates independent replicates cultures conducted in flake flasks.

We then tried to increase the intracellular formate formation through the THF-C1 pathway indirectly by the addition of serine in the culture medium. Therefore, Fdh eGfp and FdhKO eGfp strains were grown in sorbitol-based media supplemented or not with serine (YNBS and YNBSS, respectively), and the specific fluorescence (i.e. normalized to biomass) was monitored over 60 h. For the Fdh eGfp strain, the fluorescence signal remained at a constant and low level, similar to the RIY232 strain (GS115 prototroph, hereafter Fdh), on both media and throughout the entire cultivation period (Fig. 3-9A & B). This suggests that p*AOX1* is most probably not

induced in those conditions in the Fdh eGfp strain. By contrast, the fluorescence signal and thus p*AOX1* induction level were markedly higher for the FdhKO eGfp strain, especially on a medium supplemented with serine. The specific fluorescence values for the FdhKO eGfp strain after 60 h of growth were 4.0 and 6.1-fold increased on sorbitol and sorbitol-serine, respectively, compared to the Fdh eGfp strain. Moreover, the addition of serine in the medium yielded for the FdhKO eGfp strain a 1.5-fold increased fluorescence signal compared to the non-supplemented medium. Similarly, we tried to decrease the intracellular formate formation through the THF-C1 pathway by growing the cell in the presence of glycine, as it has been reported as a Shm inhibitor (Piper *et al.*, 2000). As shown in Fig 3-9C, the addition of glycine impaired p*AOX1* induction for both strains for over 50 h. Gene PAS_chr4_0415 (*SHM2*) encoding cytoplasmic (Shm2) was also disrupted in the FdhKO eGfp strain. The resulting RIY640 strain (*fdh1*Δ, *shm2*Δ, p*AOX1-eGFP*, hereafter Fdh&Shm2KO eGfp strain) was grown on sorbitol in the presence or not of serine or glycine (YNBS, YNBSS and YNBSG, respectively). In all tested media, the specific fluorescence signal was markedly lower for Fdh&Shm2KO eGfp strain as compared to the FdhKO eGfp strain (Fig. 3-9). By contrast, disruption of genes PAS_chr4_0587 (*SHM1*) encoding mitochondrial (Shm1) did not reduce markedly the eGFP fluorescence (Fig A3-2). These findings substantiate the hypothesis that the intracellular formate is higher in the FdhKO eGfp strain, accounting for p*AOX1* induction in non-repressive culture conditions.

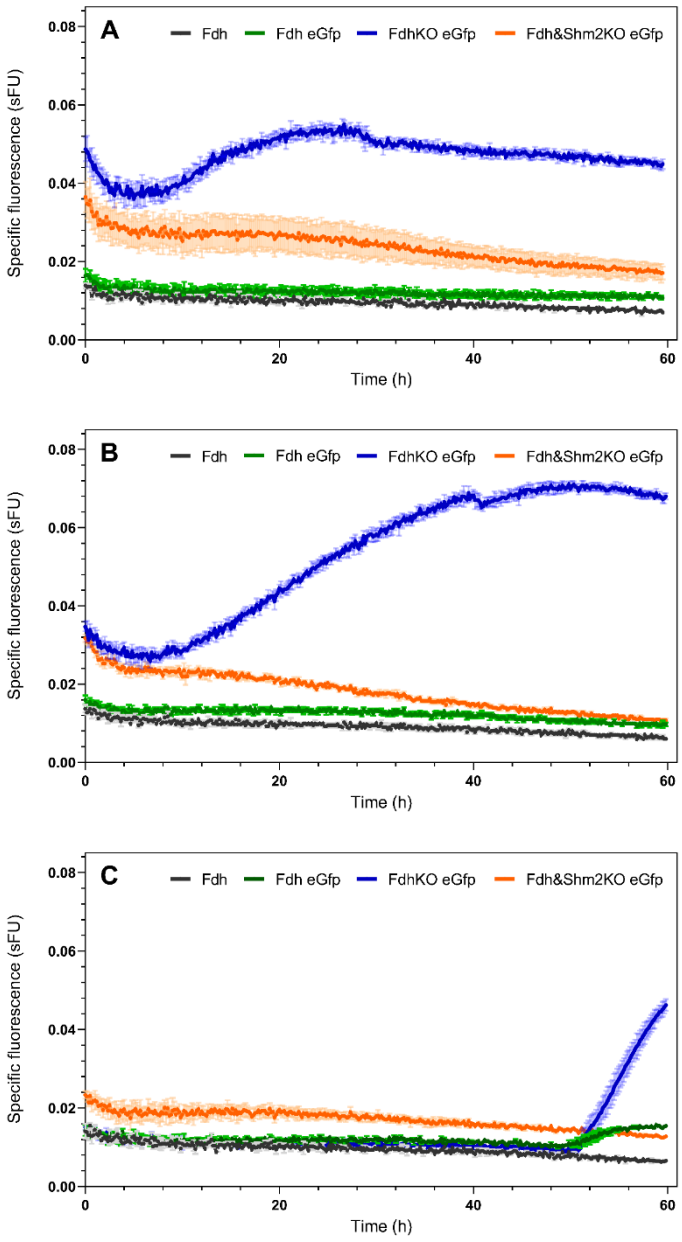

Figure 3-9. Specific eGFP fluorescence of Fdh strain (black); Fdh eGfp strain (green); FdhKO eGfp strain (blue); Fdh&Shm2KO eGfp strain (orange) strains; during growth in YNB minimal medium containing sorbitol (YNBS, panel A), sorbitol and serine (YNBSS, panel B), and sorbitol and glycine (YNBSG, panel C). Cells were grown in BioLector and specific fluorescence values are means and standard deviation on four cultures replicates. sFU: specific fluorescence unit.

3.5. Production of a secreted protein by a FdhKO mutant in sorbitol-based medium

In many rProt production processes using *K. phaffii*, glycerol is used in a first phase to generate biomass at a high cell density, to repress p*AOX1* and thus to prevent rProt synthesis. In a second phase, the carbon source is shifted to methanol or to a mixture of methanol and sorbitol to trigger rProt synthesis by induction of p*AOX1* promoter (Niu *et al.*, 2013; Carly *et al.*, 2016; Berrios *et al.*, 2017). In the rProt production phase, the purpose is to direct most of the energy from carbon sources to rProt synthesis while minimizing cell growth. Herein, the lipase B from *Candida antarctica* (CalB) was used in combination with the α-mating factor from *S. cerevisiae* as a secretory protein reporter. The CalB coding sequence was cloned under the control of the p*AOX1* promoter and integrated into the genome of the RIY232 strain, a prototroph derivative of *K. phaffii* GS115 (Velastegui *et al.*, 2019). In the resulting RIY308 strain (p*AOX1-αMF-CalB*, hereafter Fdh CalB strain), the *FDH1* encoding gene was then knocked out to yield the RIY561 strain (*fdh1*Δ, p*AOX1-αMF-CalB*, hereafter FdhKO CalB strain). Both strains were grown either on glycerol, on a mixture of methanol and sorbitol (60/40, 0.3 C-mol as in Carly et al., 2016; Niu et al., 2013), and on sorbitol (i.e., YNBG, YNBMS and YNBS, respectively). Biomass and specific lipase CalB activity were quantified at different time points over 36 h (Fig.3-10).

On glycerol, cell growth for the Fdh CalB and the FdhKO CalB strains were similar, with biomass values equal to 10.6 ± 0.1 and 10.1 ± 0.3 gDCW L^{-1}, respectively, at the end of the growth phase (i.e., 12 h, Fig 5.A). As expected, the lipase activity could not be detected during the first 12 h, then after it increased slightly upon glycerol exhaustion in the medium (i.e. in p*AOX1* derepressed condition, data not shown). On methanol (YNBSM), the biomass of the FdhKO CalB strain was markedly lower compared to the Fdh CalB strain, most probably due to the accumulation of toxic methanol catabolism byproducts (i.e., formate) as previously reported (Guo *et al.*, 2021). For both strains, the specific CalB lipase activity increased similarly over time to reach values after 30 h of 113.6 and 113.3 U $mgDCW^{-1}$ for the Fdh CalB and the FdhKO CalB strains, respectively (Fig 3-10. D). On sorbitol, both strains exhibited similar lower biomass values as compared to the glycerol medium. This could be lined with the lower uptake rate for sorbitol compared to glycerol (0.02 g $gDCW^{-1}$ h^{-1} and 0.9 g $gDCW^{-1}$ h^{-1}, respectively; data not shown). Most importantly, the maximum specific lipase activity was markedly higher for the *FDH1* disrupted strain (FdhKO CalB) compared to the non-disrupted one (i.e. 130-fold). The specific lipase CalB activity for the FdhKO CalB strain was in the same range on sorbitol and the mixture of methanol and sorbitol medium (136 U $mgDCW^{-1}$ and 113.3 U $mgDCW^{-1}$, respectively). However, it was reached 2.4 times faster on sorbitol medium (i.e. after 15 h and 36 h, respectively, Fig 3-10. F).

Ultimately, samples from cultures performed on sorbitol medium were collected after 15 h (i.e., at maximum CalB activity) and analyzed by HPLC and an enzymatic assay based on the activity of the formate dehydrogenase and quantification of the

$NADH_2$ generated at 340 nm. As shown in Fig.3-11A, formate standard solutions eluted at a retention time of 17.3 minutes. A peak at this retention time was also observed for the FdhKO CalB strain (Fig 3-11C), indicating the presence of formate, whereas it was not detected in the Fdh CalB strain (Fig 3-11B). Spiking both samples with a standard solution of formate further confirmed that the eluted compound at 17.3 minutes in the FdhKO CalB sample corresponds to formate (Fig 3-11B & C). As shown in Table 3-3, formate was only detected in the supernatant of strain FdhKO. This further confirms that formate is generated from THF-C1, accumulates in FdhKO strains, and crosses the cytoplasmic membrane probably by simple diffusion (Gabba *et al.*, 2020). In those samples, less than 5% of sorbitol has been consumed (data not shown).

Table 3-3. Format concentration in the supernatant

Strain	**Formate mM**
Fdh CalB	0
FdhKO CalB	0.09

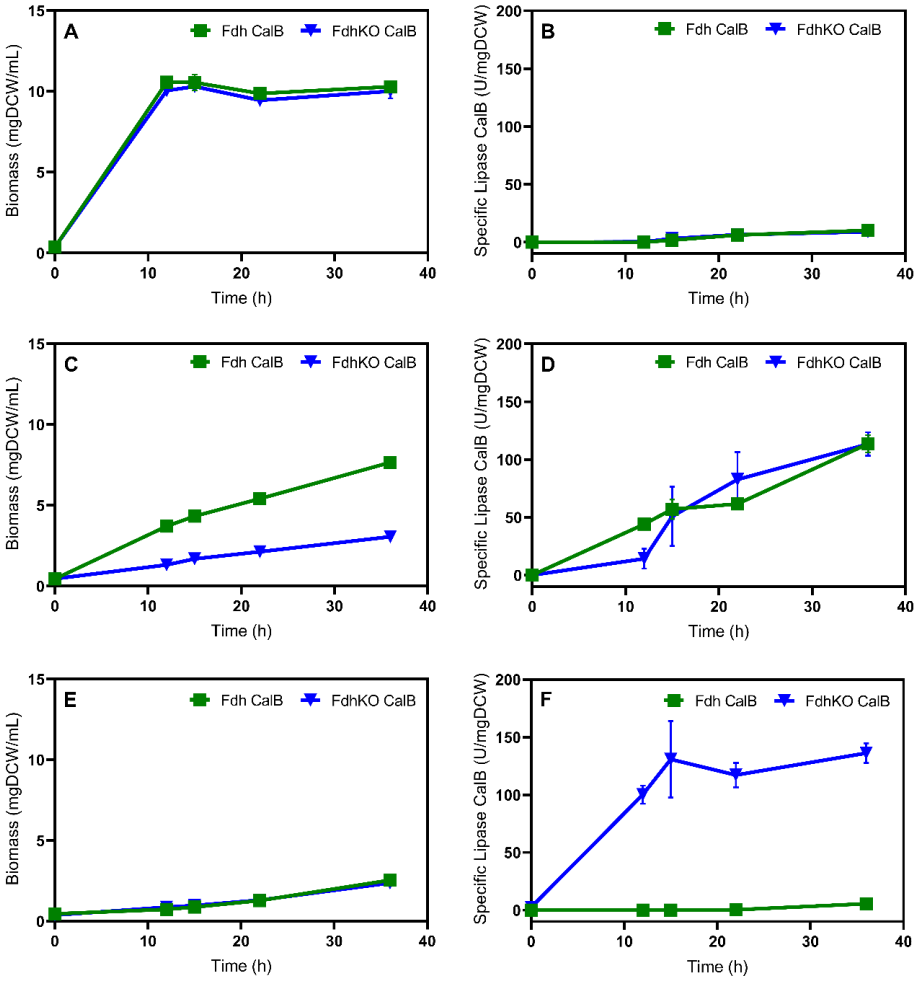

Figure 3-10. Biomass and specific lipase activity during growth of strains Fdh CalB strain (green squares) and FdhKO CalB strain (blue triangles) in the presence of glycerol (YNBG, panels A and B), methanol-sorbitol (YNBMS, panels C and D) and sorbitol (YNBS, panels E and F). Data are mean and standard deviation from cultures were performed in triplicate in shake flasks. Lipase assays were performed in triplicates.

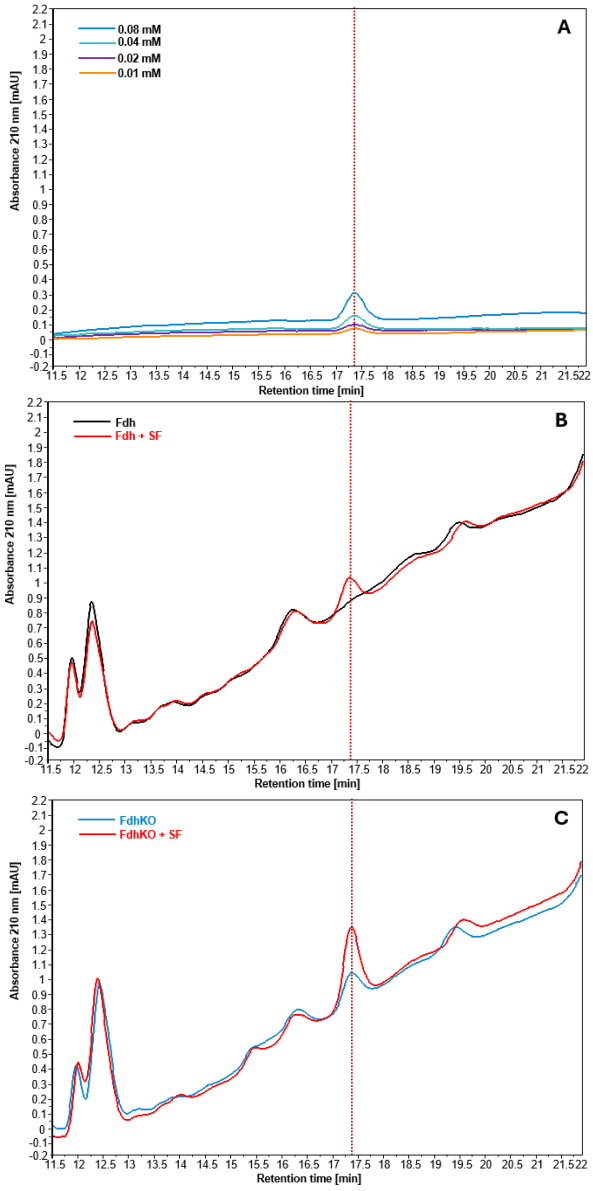

Figure 3-11. High-performance liquid chromatography (HPLC) chromatogram. Formate standard solutions at concentrations ranging from 0.01 mM to 0.08 mM (A); supernatant of Fdh CalB strain (black) and supernatant of Fdh CalB strain spiked with formate standard solution (red, 0.08 mM final concentration of spiked formate) (B); supernatant of FdhKO CalB strain (blue) and supernatant of FdhKO CalB strain spiked with formate standard solution (red, 0.08 mM final concentration of spiked formate) (C). Supernatant samples from cultures performed on sorbitol medium (YNBS) were collected after 15 hours. The absorbance value was set at zero after 11.5 min.

4. Conclusions

Herein, we have demonstrated that formate from the THF-C1 metabolism induces the p*AOX1* promoter in a FdhKO strain grown under derepressed culture conditions. This is particularly interesting for recombinant protein production processes, as adding inducers such as methanol or formate is no longer required to trigger rProt synthesis. By growing the cells in a mixture of glycerol and sorbitol, rProt synthesis is initiated upon glycerol depletion in the medium. This auto-induced system paves the way for further development of methanol-free processes for rProt synthesis in *K. phaffii*.

Chapter 4

Engineering carbon source metabolism in a formate dehydrogenase-deficient Komagataella phaffii

Description of Chapter 4

In the previous chapter, we demonstrated that deleting the *FDH1* gene allowed the accumulation of formate from the THF-C1 pathway and induction of the p*AOX1* promoter under non-repressive conditions. The results indicated that the FdhKO strain is a promising platform for producing recombinant proteins in a methanol-free medium. Following this, the study aimed to enhance the carbon source metabolism of the FdhKO strain through metabolic engineering. For this purpose, some repressive and non-repressive carbon sources for p*AOX1* regulation were tested with the FdhKO strain for cell growth and the specific rProt productivity. Among them, sorbitol was chosen for further investigation into its metabolism, and its implications regarding the induction of pAOX1. The following sections will thoroughly examine these findings.

Part of the data presented in this chapter were generated by Ing. Rocio Cozmar, PhD candidate in our research group.

Chapter 4. Engineering carbon source metabolism in a formate dehydrogenase-deficient *Komagataella phaffii*

1. Introduction

Komagataella phaffii (*K. phaffii*) can metabolize methanol as its sole carbon and energy source. In addition to methanol, *K. phaffii* can grow on various other carbon sources, including glucose, glycerol, mannitol, lactate, fructose, and sorbitol, similar to other yeast species (Çalik *et al.*, 2015). The use of glycerol and glucose has been extensively studied to enhance the performance of high-cell-density cultures in mixed substrate cultures with methanol (Zhang *et al.*, 2003; Paulová *et al.*, 2012). Moreover, the regulation of p*AOX1* depends on the response to different carbon sources; excess amounts of glucose or glycerol strongly repress p*AOX1* (Theron *et al.*, 2018). The induction of p*AOX1* is principally mediated by three master transcription factors (TFs): methanol-induced transcription factor 1 (Mit1), methanol expression regulator 1 (Mxr1), and the positive regulator of methanol 1 (Prm1) (Vogl *et al.*, 2018). In the presence of glucose or glycerol, catabolic repressors such as Mig1, Mig2, and Ngr1 do not regulate the expression of genes that are under the control of the p*AOX1* (Wang *et al.*, 2017). On the other hand, sorbitol is recognized as a non-repressive carbon source for the p*AOX1* (Inan & Meagher, 2001). Its use as a co-carbon source with methanol has been reported to have positive effects, including reducing cellular stress, oxygen consumption, and proteolytic degradation.(Azadi et al., 2017; Çelik et al., 2009; Niu et al., 2013). In recent studies, sorbitol has also been used with formate as an inducer of p*AOX1* (Liu et al., 2022a).

In Chapter 3, we demonstrated that disruption of the formate dehydrogenase gene *FDH1* led to the accumulation of intracellular formate, produced via THF-C1 metabolism. Under non-repressive conditions, such as in the presence of sorbitol, this formate was sufficient to induce the p*AOX1* promoter without the need for external inducers. However, the specific growth rate of *K. phaffii* is lower when sorbitol is used as a carbon source compared to glycerol (Berrios *et al.*, 2017).

Sorbitol catabolism requires first entry inside the cells by a specific transporter and its conversion into fructose by a specific sorbitol dehydrogenase. The activity of this specific dehydrogenase has been reported as a bottleneck for sorbitol catabolism in *Komagataella kurtzmanii* (Akentyev *et al.*, 2023).

In this chapter, the FdhKO *K. phaffii* strain is addressed through metabolic engineering to enhance the assimilation of non-repressive carbon sources, aiming to improve the productivity of this novel self-induced system. Through this investigation, sorbitol was identified as the most effective carbon source for recombinant protein production in the FdhKO strain. Consequently, sorbitol uptake was increased by overexpressing the native gene encoding sorbitol dehydrogenase (*SOR1*) (Fig. 4-1). However, this increased consumption adversely affected the rProt gene expression achieved by the FdhKO strain. Further research is needed to fully

leverage the capacity of the FdhKO strain, as it presents new challenges and opportunities for production in methanol-free media.

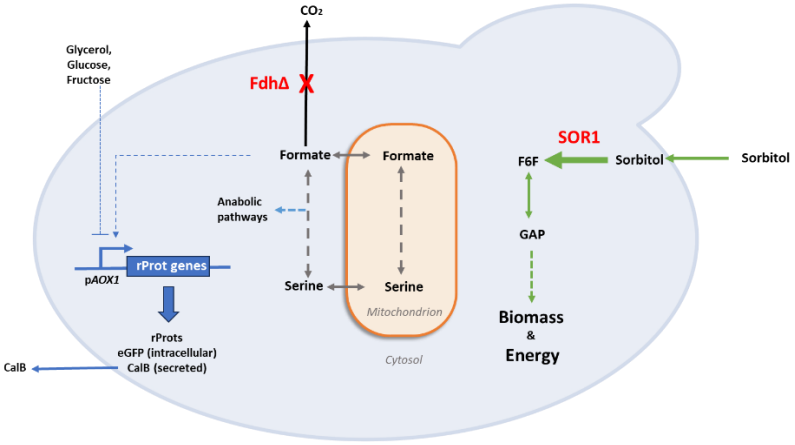

Figure 4-1. Schematic diagram illustrating the sorbitol assimilation pathway in a formate dehydrogenase-deficient *K. phaffii*. Formate from THF-C1 metabolism induces the p*AOX1*. The overexpression of the sorbitol dehydrogenase *SOR1* gene increases biomass and energy production.

2. Material and methods

2.1. Strain, media and culture conditions

The *Komagataella phaffii* (*K. phaffii)* and *Escherichia coli* strains used are listed in Table 4-1. *E. coli* was cultivated at 37°C in Luria-Bertani medium (LB), supplemented with antibiotics as follows: 100 µg mL^{-1} ampicillin, 50 µg mL^{-1} kanamycin, or 25 µg mL^{-1} zeocin. *K. phaffii* strains were cultivated at 30°C either in YPD medium (containing 20 g L^{-1} glucose, 10 g L^{-1} Difco yeast extract, and 10 g L^{-1} Difco bacto peptone) or YNB medium (containing 1.7 g L^{-1} Difco YNB w/o ammonium chloride and amino acids, 5 g L^{-1} NH_4Cl and, 0.4 mg L^{-1} biotin, 100 mM potassium phosphate buffer, pH 6.0) supplemented with as follows: 10 g L^{-1} sorbitol (YNBS); 10 g L^{-1} glycerol (YNBG); 6.3 g L^{-1} methanol and 4.0 g L^{-1} sorbitol (YNBMS); 9.9 g L^{-1} glucose (YNBGu); 9.9 g L^{-1} fructose (YNBF); 10 g L^{-1} mannitol (YNBMt); 12.33 g L^{-1} lactate (YNBL); 1 g L^{-1} glycerol (YNBG1); 1 g L^{-1} glycerol and 1 g L^{-1} sorbitol (YNBGS11); 1 g L^{-1} glycerol and 2 g L^{-1} sorbitol (YNBGS12); 1 g L^{-1} glycerol and 4g L^{-1} sorbitol (YNBGS14); 20 g L^{-1} sorbitol (YNB20S). *K.phaffii* transformants were selected on YPD agar plates, supplemented with 25 µg mL^{-1} zeocin (YPD-Zeo).

For all cultures, a first preculture inoculated from a single colony was performed for 12 h at 30°C and 150 rpm in a 250 mL shake flask containing 25 mL of liquid YPD medium. After centrifugation at 9000 g for 5 min, the cells were washed with phosphate-buffered saline (0.1 M, pH 6) before being used to inoculate a second preculture in the same conditions in YNB media supplemented as described above.

Cultures were performed in 50 mL shake flasks (5 mL medium) or in a microbioreactor (BioLector 2, m2p-labs, Baesweiler, Germany). For that purpose, 48-well Flower plates (M2P-MTP-48-B, Beckman Coulter Life Sciences, USA) containing 1 mL of medium were used. Cultures were operated for 60 h with a relative humidity of 85 %, under constant agitation at 1000 rpm. Every 10 minutes, biomass was monitored using scattered light intensity at a wavelength of 620 nm while cell fluorescence was quantified at 520 nm (excitation at 488 nm). The gain was set as 2 for biomass and 4 for fluorescence. Specific fluorescence was obtained by dividing the fluorescence value by the biomass value. It was expressed in specific fluorescence units (sFU). Cultures to reduce the cell growth based on the oxygen availability were conducted in shake-flask batches in Erlenmeyer flasks of various total volumes and constant medium volumes corresponding to K_La coefficients of 10, 50, and 100 h^{-1}. The K_La coefficients were calculated using the K_La calculator tools developed by PreSens (www.presens.de). All cultures were seeded at an initial optical density at 600 nm of 0.5 from cells grown in the second pre-culture. Cultures in flasks were performed with three biological replicates, whereas cultures in the BioLector were performed with two biological replicates, each supported by two technical replicates, resulting in a total of four replicates.

Table 4-1. *E. coli* and *K. phaffii* strains used in the 4th chapter

Number	Name	Plasmid/ Parental strain, Genotype	Reference
E. coli			
A2		BB1_23	(Prielhofer *et al.*, 2017)
D12		BB3aZ_14	(Prielhofer *et al.*, 2017)
A4		BB1_12_p*GAP*	(Prielhofer *et al.*, 2017)
C1		BB1_34_*ScCYC1*tt	(Prielhofer *et al.*, 2017)
C9		BB1_34_*RPS3*tt	(Prielhofer *et al.*, 2017)
D4		BB2_AB	(Prielhofer *et al.*, 2017)
D5		BB2_BC	(Prielhofer *et al.*, 2017)
RIE341		A2_BB1_23_*SOR1*	This work
RIE343		A2_BB1_23_Pp*HXT1*	This work
RIE354		BB3-p*GAP*- Pp*HXT1-SsCy1*tt	This work
RIE355		BB3-p*GAP-SOR1-SsCy1*tt	This work
RIE370		BB3-AC-LoxP	This work
RIE372		BB2(AB)-p*GAP-SOR1- SsCy1*tt	This work
RIE374		BB2(BC1)-P*GAP*-Pp*HXT1-RPS3*tt	This work

RIE378		BB3a-p*GAP-SOR1-SsCy1*tt, p*GAP*- Pp*HXT1-RPS3*tt	This work
K.phaffii			
RIY232	Fdh	GS115, *HIS4*	(Theron *et al.*, 2019)
RIY230	Fdh eGfp	GS115, p*AOX1-eGFP*	(Velastegui *et al.*, 2019)
RIY308	Fdh CalB	GS115, p*AOX1-αMF-CalB*	(Velastegui *et al.*, 2019)
RIY540	FdhKO eGfp	RIY536, *fdh1*Δ, p*AOX1-eGFP*	(Bustos *et al.*, 2024)
RIY561	FdhKO CalB	RIY537, *fdh1*Δ, p*AOX1*-αMF-*CalB*	(Bustos *et al.*, 2024)
RIY529	SDH	RIY232, p*GAP-SOR1- SsCy1*tt	This work
RIY530	ST	RIY232, p*GAP*-Pp*HXT1- SsCy1*tt	This work
RIY532	SDH-ST	RIY232, p*GAP-SOR1,* p*GAP*-Pp*HXT1*	This work
RIY643	FdhKO-SdOE eGfp	RIY540, *fdh1*Δ, p*AOX1-eGFP,* p*GAP-SOR1*	This work
RIY562	FdhKO-SdOE CalB	RIY561, *fdh1*Δ, p*AOX1-αMF-CalB*, p*GAP-SOR1*	This work

2.2. General genetic techniques

Standard media and techniques were used for *E. coli* (Sambrook and Russell, 2001). Restriction enzymes, DNA polymerases, and T4 DNA ligase were obtained from New England Biolabs (NEB, Ipswich, MA, USA) or Thermo Scientific (Thermo Scientific, Waltham, MA USA). Primers for PCR and qPCR were synthesized by Eurogentec (Seraing, Belgium, Table S2). Vector TopoBluntII and pGEMTeasy were from Invitrogen (Waltham, Massachusetts, United States) and Promega (Madison, Wisconsin, United States), respectively. Genomic DNA was purified using a Genomic DNA Purification kit (Thermo Scientific, Waltham, MA, USA). DNA fragments were purified from agarose gels using a NucleoSpin Gel and a PCR clean-up kit (Machery-Nagel, Düren, Germany), DNA sequencing and the synthetic gene Pp*HXt1* was performed by Eurofin Genomic (Eurofin, Ebersberg, Germany). Quantitative PCR (qPCR) was performed as described elsewhere with primers listed in Table A4-1 Appendix 3, using the actin gene as a reference. Total RNA was extracted using the NucleoSpin RNA Plus kit (Machery-Nagel, Düren, Germany). qPCR was performed using the Luna Universal qPCR Master Mix and the Step OnePlus Real-Time PCR system (Thermo Scientific, Waltham, MA, USA). Primers and plasmid designs were performed using the software Snapgene (Dotmatics, USA). Vectors were constructed using the GoldenPiCS Kit (Prielhofer et al., 2017, Addgene kit #1000000133). *K. phaffii* was transformed as described by Lin-Cereghino et al., (2005).

2.3. Construction of plasmids and K. phaffii strains

The GoldenPiCS system was used to construct the *SOR1* and Pp*HXT1* expression vectors (Prielhofer *et al.*, 2017). Internal BpiI recognition sequence in gene

PAS_chr1-1_0490 (*SOR1*) was removed by overlapping PCR using pairs SOR1-Fw/ SOR1-Rv using *K. Phaffii GS115* genomic DNA as a template. In the gene PAS_chr1-4_0570 (Pp*HXT1*) the internal BpiI and BsaI recognition sequences were removed, and the synthetic gene was generated with the addition of external BsaI sequence recognition. The resulting PCR product and synthetic gene were cloned into plasmid A2 (BB1-23) at BsaI restriction site to yield plasmids RIE341(BB1_23_*SOR1*) and RIE343(BB1_23_Pp*HXT1*), respectively, the positive construct was verified by colony and plasmid PCR with M13-Fw/M13-Rv. Plasmid RIE354 (p*GAP-SOR1*-Sc*CYC1*tt) and RIE355 (p*GAP-PpHXT1*-ScCYC1tt) were assembled by Golden Gate assembly from the plasmids, A4 (BB1_12_p*GAP*), C1 (BB1_34_*ScCYC1*tt), D12 (BB3aZ_14), with RIE341 and RIE343, respectively, using BpiI as the restriction enzyme, and verify the correct construct by colony and plasmid PCR with p*GAP*.Int-Fw/*ScCYC1*tt.Int-Rv. The expression plasmid RIE370(BB3-AC-LoxP) was ensemble at HindIII and PstI restriction site by the combination of the plasmid D12 (BB3aZ_14) and C12(BB3aK_AC). The double overexpression of *SOR1* with Pp*HXT1* was performed in three steps: first, the plasmids RIE341 was cloned separately with the plasmids A4, C1, and D4 using BsaI to yield the plasmid RIE372; second, the plasmids RIE343 was cloned with the plasmids A4, C9 and D5 using BsaI to yield the plasmid RIE374; and finally, the plasmids RIE372, RIE374, and RIE370 were ensemble with BpiI to yield the plasmid RIE378 (BB3a-p*GAP-SOR1-SsCy1*tt, p*GAP*-Pp*HXT1-RPS3*tt). The plasmids construct confirmation was performed with colony and plasmid PCR with the couple of primers p*GAP*.Int-Fw/ *ScCYC1*tt.Int-Rv, p*GAP*.Int-Fw/ Rps3tt.Int-Rv, and p*GAP*.Int-Fw/ Rps3tt.Int-Rv respectively.

Construction of RIY230 (Fdh eGfp) and RIY308 (Fdh CalB) strains were described in Velastegui et al., (2019), RIY540 (FdhKO eGfp) and RIY561 (FdhKO CalB) were described in Bustos et al. (2024). The plasmids RIE354 (p*GAP*- Pp*HXT1-SsCy1*tt), RIE355(p*GAP-SOR1-SsCy1*tt) and RIE378(p*GAP-SOR1-SsCy1*tt, p*GAP*- Pp*HXT1-RPS3*tt) were linearized with AscI and used to transform RIY232 strain to yield RIY529(p*GAP-SOR1*- *SsCy1*tt, hereafter SDH strain), RIY530(p*GAP-PpHXT1-SsCy1*tt, hereafter ST strain) and RIY532(p*GAP-SOR1*, p*GAP*-Pp*HXT1*, hereafter SDH-ST strain). The overexpression of *SOR1* in the strains RIY540 (FdhKO eGfp) and RIY561 (FdhKO CalB) was performed by transformation with the linearization of the plasmid RIE355 with AscI, to yield the strain RIY643(*fdh1*Δ, p*AOX1-eGFP*, p*GAP-SOR1*, hereafter FdhKO-SdOE eGfp strain) and RIY564(*fdh1*Δ, p*AOX1-αMF-CalB*, hereafter pGAP-SOR1).

To verify the genotype of the strains RIY529, RIY530, RIY532, RIY643 and RIY564, primers p*GAP*.Int-Fw/S*cCYC1*tt.Int-Rv, p*GAP*.Int-Fw/ Rps3tt.Int-Rv, and IntAOXtt.fw/ IntAOXtt.Rv that annealed in the p*GAP*, *ScCYC1*tt, Rps3tt, and *AOX*tt region were used. A schematic representation of the strain genotype is presented in Fig 4-2.

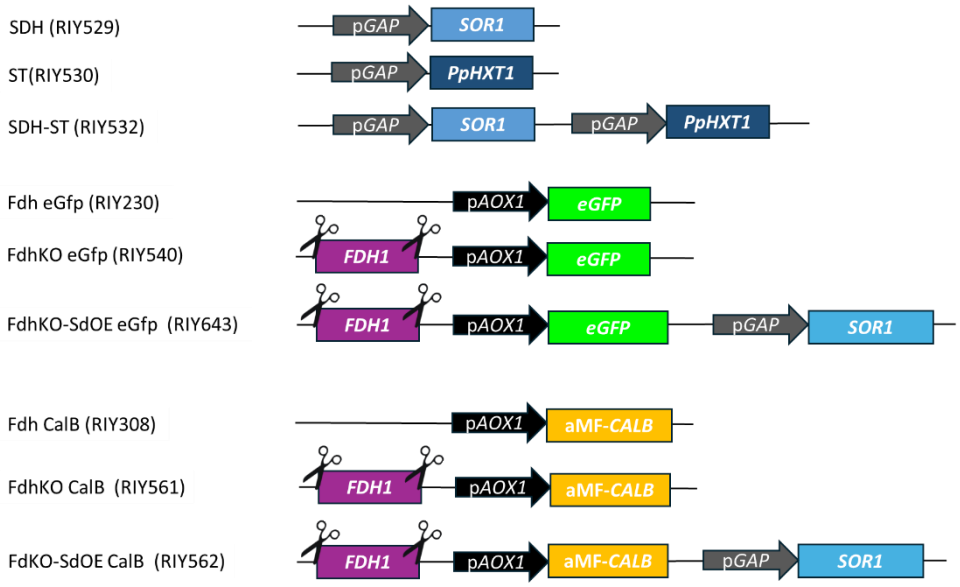

Figure 4-2. Schematic representation of the genotype of the strains presented in this chapter.

2.4. Analytical methods

Cell growth was monitored either by optical density at 600nm (OD_{600}) or dry cell weight (DCW). An OD_{600} value of 1 was found to correspond to 0.65 g DCW/L sorbitol, glycerol, glucose, fructose, mannitol, and lactate concentrations were determined by HPLC (Agilent 1100 series equipped with UV (210 nm) and RID detector, Agilent Technologies, Santa Clara, CA, USA) using an Aminex HPX-87H ion-exclusion column (300 × 7.8 mm Bio-Rad, Hercules, CA, USA). Compounds were eluted from the column at 50 °C with a flow rate of 0.5 mL min^{-1} and using a 5 mM H_2SO_4 solution as the mobile phase.

Intracellular eGfp fluorescence was quantified using a BD Accuri C6 Flow Cytometer (BD Biosciences, San Jose, CA, USA) as described elsewhere (Sassi *et al.*, 2016). For each sample, 20,000 cells were analyzed using the FL1-A and FSC channels, and FL1-A/FSC dot plots were analyzed using the CFlowPlus software (Accuri, BD Biosciences). A threshold of 5800 fluorescence units (FU) on FL1-A channel was applied to eliminate the noise for endogenous fluorescence from the cells. To calculate the total value of fluorescence in the cell population, the FL1-A median value (i.e., the eGfp fluorescence) was multiplied by the fraction of cells with eGfp fluorescence (i.e., induced cells). It was expressed in total fluorescence unit (TFU). Spectrophotometric analysis of eGfp was performed on SpectraMax M2 (Molecular Devises, San Jose San Jose, CA, USA) using λex and λem at 488 and 535 nm, respectively. Measurements were taken after 30 s of sample shaking. Signal gain was

set to 225, and the number of light flashes was set to 30. Specific eGfp fluorescence was expressed as specific fluorescence units (SFU), i.e., as fluorescence value normalized to biomass related to optical density at 600 nm (OD_{600}) of 0.5.

The formic acid assay kit (Megazyme Inc., Bray, Ireland) was used to measure formate concentrations in the supernatant samples. A total 255 µL reaction volume was measured by the manufacturer's instructions at 340 nm.

The lipase activity in the culture supernatant was determined by monitoring the hydrolysis of p-nitrophenylbutyrate (p-NPB) as described elsewhere (Fickers *et al.*, 2003). The release of para-nitrophenol was monitored at 405 nm using a SpectraMax M2 (Molecular Devices, San Jose, CA, USA). All lipase activity assays were performed at least in triplicate. One unit of lipase activity was defined as the amount of enzyme releasing 1 µmol p-nitrophenol per minute at 25 °C and pH 7.2 (εPNP = 0.0148 $\mu M^{-1}.cm^{-1}$).

3. Results and discussion

3.1. Non-repressive carbon sources and their effect on rProt production on the novel deficient formate dehydrogenase strain

Strategies involving co-feeding methanol with auxiliary carbon sources such as glycerol, sorbitol, mannitol, and lactate have been employed to mitigate the toxic effects of methanol and enhance recombinant protein expression using p*AOX1* (Berrios et al., 2017; Gu et al., 2014; Nakagawa et al., 2015; Thorpe et al., 1999; Xie et al., 2005; Zhu et al., 2019). These approaches have improved recombinant protein production in both slow methanol-utilizing strains (MutS) and high methanol-consuming (Mut+) strains (Liu et al., 2019). Studies have shown that sorbitol, mannitol, and lactate do not repress the p*AOX1*, thus reducing the need for strict control of residual substrate levels (Inan & Meagher, 2001). Additionally, (Bustos *et al.*, 2024) demonstrated that formate, derived from THF-C1 metabolism, can induce the p*AOX1* in a formate dehydrogenase-deficient (FdhKO) strain grown under derepressed culture conditions with sorbitol as the carbon source.

Herein, the FdhKO eGfp strain was grown in the presence of other carbon sources (i.e., glycerol, glucose, fructose, mannitol, lactate, and sorbitol) to evaluate the regulation of p*AOX1* on those carbon sources. The specific fluorescence level of the FdhKO strain was estimated over 24 h of cell growth. During the growth phase, the specific fluorescence levels were the lowest under p*AOX1*-repressive carbon sources, such as glycerol and glucose, with values of 7.2 and 3.4 sFU, respectively, at 12 h (Fig. 4-3B). At the end of the stationary phase, the fluorescence increased on glycerol, reaching 19.9 sFU at 24 h, while on glucose fluorescence remained at a low level (4.06 sFU). These results are consistent with the established understanding of p*AOX1* TFs catabolic repression in the presence of glycerol or glucose. The induction of p*AOX1* is mediated by the cooperative action of the TFs Mxr1, Mit1, and Trm1 (Lin-Cereghino *et al.*, 2006; Vogl *et al.*, 2018; Ata *et al.*, 2021). In the presence of glycerol,

Mig1 and Nrg1 repress the expression of Mit1, thereby preventing the induction of p*AOX1*. Nrg1 also represses p*AOX1* in the presence of glucose and glycerol by directly binding in five sites of p*AOX1*, including two binding sites of Mxr1. Additionally, in the presence of glucose, Trm1 does not bind to p*AOX1* (Wang et al., 2017; Wang et al., 2016a; Wang, et al., 2016b).

On fructose, the fluorescence in the FdhKO eGfp strain increases gradually, reaching its highest value during the stationary phase (i.e., 22.6 sFU at 24 h, Fig. 4-3B), similar to the level achieved with glycerol at the same time. As glucose and glycerol, fructose has been reported as a repressive compound for p*AOX1* (Potvin et al., 2016; Zhang et al., 2010).

Conversely, when the primary carbon source is lactate, mannitol, or sorbitol, the FdhKO strain achieves lower biomass levels (i.e., 0.3, 0.7, and 0.5 gDCW L^{-1}, respectively) compared to glycerol, glucose, or fructose (i.e., 8.3, 7.3, and 6.1 gDCW L^{-1}, respectively) (Fig. 4-3A). Despite the lower biomass, the specific fluorescence in lactate and mannitol conditions was 28.5 sFU and 39.3 sFU at 12 h, representing 8.4- and 12-fold increases, respectively, compared to the repressive glucose conditions at the same time (Fig. 4-3B).

In particular, the FdhKO strain grown on sorbitol show the highest fluorescence (eGfp) values, as reported by Bustos et al., (2024.) In this medium, the FdhKO strain shows a specific fluorescence of 70.8 sFU at 12 h, representing a remarkable 20.8- and 10-fold increase compared to the repressive glucose and glycerol conditions, respectively. Additionally, compared to mannitol and lactate, sorbitol results in a 2.24- and 1.96-fold increase in specific fluorescence, respectively (Fig. 4-3B). These results support the use of sorbitol as a carbon source and align with previous reports comparing these carbon sources in combination with methanol in *K. phaffii* strains (Carly et al., 2016; Niu et al., 2013).

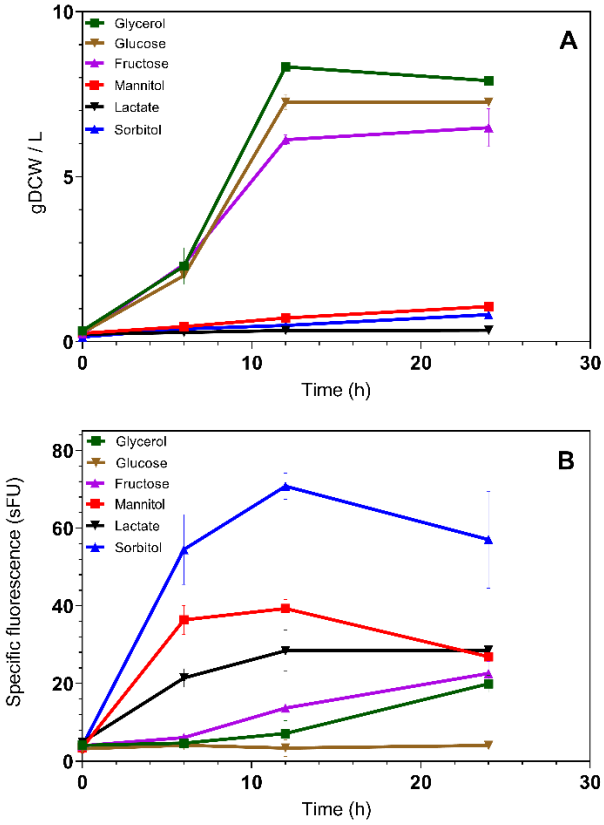

Figure 4-3. Biomass and specific fluorescence of strain RIY540 (FdhKO eGfp) in various carbon sources. Carbon sources: glycerol (green); glucose (brown); fructose (purple); Mannitol (red); Lactate (black); sorbitol (blue). Data are mean and standard deviation from cultures were performed in triplicate in shake flasks.

3.2. Enhancement of sorbitol catabolism through metabolic engineering of the sorbitol pathway

Sorbitol is one of the most widely used co-substrates for producing rProt by *K. phaffii* (Çelik *et al.*, 2009). However, the cell growth rate on sorbitol is significantly lower than that on methanol (0.04 vs. 0.1 h^{-1}, respectively, Niu et al., 2013). The bottleneck of sorbitol assimilation may depend on its transport into the cell or its conversion into fructose by sorbitol dehydrogenase (Akentyev *et al.*, 2023). So far, the gene encoding sorbitol transporter has not been characterized in *K. phaffii* (Mattanovich *et al.*, 2009; Zhang *et al.*, 2010). In *Saccharomyces cerevisiae*, the

hexose transporter Hxt15 is the most versatile polyol transporter and is related to sorbitol (Jordan *et al.*, 2016). The genes encoding sorbitol dehydrogenase (*SOR1*) have been characterized in *Saccharomyces cerevisiae* and *K. Kurtzmanii* (Toivari *et al.*, 2004; Akentyev *et al.*, 2023). The genes encoding sorbitol dehydrogenase (*SOR1*) and sorbitol transporter (*HXT15*) in *Saccharomyces cerevisiae* were used for homology search in the genome of *K. phaffii*. A BlastX search highlighted genes PAS_chr1-1_0490 and PAS_chr1-4_0570 with 55.6% and 51% identity, respectively, as a *SOR1 and PpHXT1* candidate. Those two genes were expressed under the control of the constitutive promoter p*GAP* alone or in combination in the Fdh strain, a prototroph derivative of strain GS115 (as shown in Table 4-2).

Table 4-2. *Effects of SOR1 and PpHXT1 genes overexpression on specific growth rate and the specific consumption rate of sorbitol*

Strain	**μ** **(h^{-1})**	**qs** **(g $gDCW^{-1}$ h^{-1})**
Fdh, parental strain	0.036	0.031
SDH	0.119	0.149
ST	0.042	0.049
SDH-ST	0.122	0.157

Abbreviations: μ, specific growth rate; DCW, dry cell weight; qs, sorbitol uptake rate.

In the ST strain, which overexpresses gene PAS_chr1-4_0570 (*PpHXT1*), the sorbitol uptake rate and the cell growth rate increased only slightly as compared to the parental strain (0.05 vs. 0.03 g $gDCW^{-1}$ h^{-1}, 0.042 vs. 0.036 h^{-1}, respectively). By contrast, overexpression of gene PAS_chr1-1_0490 (*SOR1*), SDH strain, yielded a marked increase in sorbitol uptake and growth rate as compared to the parental strain (0.15 vs 0.03 g $gDCW^{-1}$ h^{-1}, 0.12 vs 0.04 h^{-1}). This suggests that the gene PAS_chr1-4_0570 (Pp*HXT1*) most likely encodes a functional sorbitol transporter in *K. phaffii*. When both *SOR1* and Pp*HXT1* genes were co-expressed under the control of the p*GAP*, sorbitol uptake rate and growth rate did not significantly increase further (0.16 g $gDCW^{-1}$ h^{-1}, 0.122 h^{-1}). This indicates that the expression of the *SOR1* gene alone can alleviate the bottleneck in the flux of sorbitol assimilation by the cell. This finding aligns with reports in *K. kurtzmanii*, where the *SOR1* gene was identified as a bottleneck in sorbitol metabolism, and its overexpression improved cell growth in the *K. phaffii* GS115 strain (Akentyev *et al.*, 2023).

3.3. Overexpression of sorbitol dehydrogenase in a formate dehydrogenase-deficient strain

With the aim of evaluating p*AOX1* regulation regarding *FDH1* gene disruption and the enhancement of sorbitol catabolism, the *SOR1* gene was overexpressed under the control of the constitutive p*GAP* promoter in the RIY540 (fdh1Δ, p*AOX1*-eGFP, hereafter FdhKO eGfp) strain (Bustos *et al.*, 2024) to yield the RIY643 (fdh1Δ, p*AOX1*-e*GFP*, p*GAP-SOR1*, hereafter FdhKO-SdOE eGfp) strain. Cell growth and

fluorescence of both strains were monitored over, with culture media containing varying concentrations of sorbitol combined with glycerol (i.e., G: 1.75g L^{-1} glycerol; GS2: 1.75 g L^{-1} glycerol + 1.75 g L^{-1} sorbitol, and GS4: 1.75 g L^{-1} glycerol + 3.5 g L^{-1} sorbitol). This setup simulates conditions commonly used in bioprocess for rProt production in *K. phaffii*, where glycerol is utilized in the early stages to promote high biomass generation (Ergün *et al.*, 2022).

Under the evaluated conditions (i.e., G, GS2, and GS4), both FdhKO eGfp and FdhKO-SdOE eGfp strains exhibited diauxic growth, preferring to consume glycerol first, followed by sorbitol as demonstrated by HPLC analyses (see Figure A4-2 Appendix 5). Glycerol was depleted after 8 h of culture, at which point the FdhKO eGfp and FdhKO-SdOE eGfp strains reached similar biomass values (i.e., 14.94 vs 15.41 a.u, respectively) (Fig 4-4. A&C). As expected, glycerol exerted repression over the p*AOX1*, leading to the lowest specific fluorescence signal at this time for both strains (0.012 vs. 0.011 sFU, respectively) (Fig 4-4 B&D). Upon glycerol depletion, the sorbitol uptake rate became strain-dependent.

In the FdhKO strain, sorbitol catabolism after glycerol depletion resulted in the highest biomass levels at 24 hours in GS2 (20.2 a.u.) and 34 hours in GS4 (27.08 a.u.). The specific fluorescence signal peaked at 18 hours in both GS2 and GS4 (0.069 and 0.074 sFU, respectively), indicating that sorbitol concentration did not significantly impact the fluorescence levels achieved by the FdhKO eGfp strain (Fig. 4-4 B).

Conversely, the FdhKO-SdOE eGfp strain cultured on GS2 and GS4 media reached peak biomass levels more rapidly, within 14 hours and 18 hours, respectively, compared to the FdhKO eGfp strain. This fast growth is attributed to enhanced sorbitol uptake (Fig. 4-4 A&C). However, unexpectedly, the specific fluorescence signal of the FdhKO-SdOE eGfp strain was 1.8-fold lower than that of the FdhKO eGfp strain in both GS2 and GS4 conditions (0.039 and 0.037 sFU, respectively) (Fig. 4-4 B&D). This represents only a 1.5-fold increase in fluorescence after glycerol depletion, compared to the 3-fold increase observed in the FdhKO eGfp strain. These differences appear to be independent of sorbitol concentration, as similar fluorescence levels were observed in both GS2 and GS4.

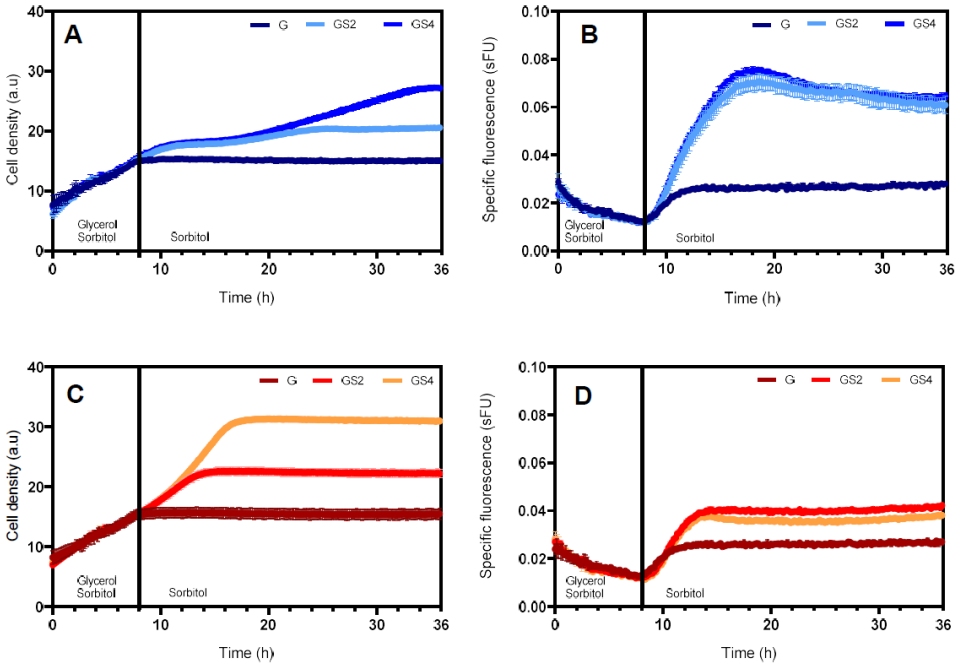

Figure 4-4. Comparative impact of enhanced sorbitol catabolism through *SOR1* gene overexpression in FdhKO eGfp strain vs. FdhKO-SdOE eGfp strain at different sorbitol concentrations. **A & B**: FdhKO eGfp strain; **C & D**: FdhKO-SdOE eGfp strain. G: 1.75g L^{-1} glycerol; GS2: 1.75 g L^{-1} glycerol + 1.75 g L^{-1} sorbitol; GS4: 1.75 g L^{-1} glycerol + 3.5 g L^{-1} sorbitol). Cells were grown in BioLector, and specific fluorescence values are the means and standard deviation of three culture replicates. sFU: specific fluorescence unit; a.u: arbitrary units.

Further research was conducted with a second recombinant protein model, the secreted protein lipase B from *Candida antarctica* (CalB), evaluated alongside the overexpression of the *SOR1* gene, resulting in the RIY564 strain (fdh1Δ, p*AOX1*-αMF-*CALB*, p*GAP*-*SOR1*; hereafter FdKO-SdOE CalB). Cell growth and lipase CalB titer were quantified at different time points over a 36 h period in a medium containing 10 g L^{-1} sorbitol (Fig. 4-5). The FdKO-SdOE CalB strain, with enhanced sorbitol assimilation, showed a 1.5-fold increase in total lipase CalB production compared to the FdhKO CalB strain (i.e., 469.6 and 322.4 U mL^{-1}, respectively) at 36 h (Fig. 4-5B). However, in terms of specific lipase CalB activity, the FdKO-SdOE CalB strain exhibited a 3.55-fold decrease compared to the FdhKO CalB strain (Fig. 4-5C), reflecting the same trend observed in the strains expressing e*GFP* (Fig. 4-4), where specific fluorescence signals decreased despite higher biomass production.

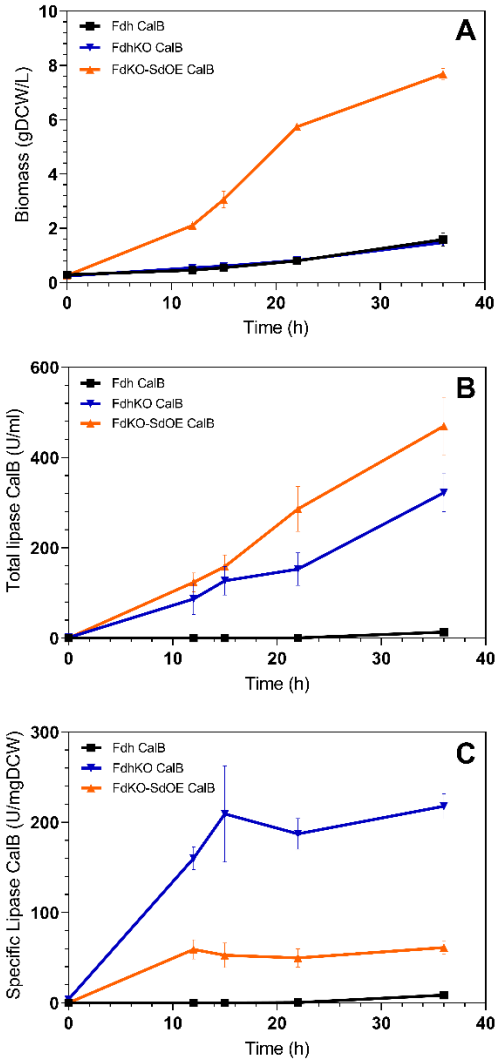

Figure 4-5. Comparative impact of enhanced sorbitol catabolism through *SOR1* gene overexpression. **A:** cell density; **B:** total lipase CalB; **C:** specific lipase CalB. Fdh CalB (black); FdhKO CalB (blue); FdhKO-SdOE CalB (orange). Data are mean and standard deviation from cultures, which were performed in triplicate in shake flasks.

It is noteworthy that the primary difference between these strain lines is in the specific growth rate, which is 0.04 h^{-1} for the FdhKO strain and 0.1 h^{-1} for the FdhKO-SdOE strain due to the overexpression of *SOR1*.

3.4. Control of the cell growth to evaluate the differences between the FdhKO and FdhKO-SdOE strains

In *K. phaffii*, low energy generation from carbon sources has been identified as a bottleneck for the synthesis of recombinant proteins in systems where formate is used as an inducer for the p*AOX1* (Feng *et al.*, 2022). Contrary to expectations, overexpression of *SOR1* in the FdhKO strain, which increased sorbitol uptake and cell growth, resulted in a reduction of specific recombinant protein productivity. We hypothesize that the higher growth rate of the FdhKO-SdOE strain prevents formate accumulation, as this C1-unit is consumed in different anabolic pathways.

To test this hypothesis, the FdhKO eGfp and FdhKO-SdOE eGfp strains were analyzed after 22 hours of growth, during which there was no limitation of the carbon source (see Figure A4-6, Appendix 6 for residual sorbitol concentration). The strains were cultured under different growth rates by modulating oxygen availability (OA) in shake-flask cultures using various K_La conditions (Fig. 4-6A). Oxygen availability was controlled by altering the headspace volume, defined as the ratio of the culture medium to the total vessel volume (Gorczyca *et al.*, 2020). Estimated K_La values of 100, 50, and 10 were used as benchmarks. As expected, when oxygen availability decreased, cell growth rates correspondingly slowed in both the FdhKO-SdOE eGfp (0.10, 0.09, and 0.06 h^{-1}) and FdhKO eGfp strains (0.05, 0.04, and 0.03 h^{-1}) (Fig. 4-6A).

Upon comparing eGfp fluorescence signals between the two strains across different growth rates, a clear inverse trend was observed: as the growth rate increased, eGfp fluorescence decreased. The eGfp fluorescence levels ranged from 105 268 TFU at a growth rate of 0.033 h^{-1} in the FdhKO eGfp strain to 2 709 TFU at 0.097 h^{-1} in the FdhKO-SdOE eGfp strain (Fig. 4-6). Experiments were conducted with both strains under comparable growth rates but different oxygen availability to further explore this trend. For instance, the FdhKO-SdOE eGfp strain at a growth rate of 0.060 h^{-1} (K_La 10) showed an eGfp level of 12 184 TFU, while the FdhKO eGfp strain at 0.050 h^{-1} (K_La 100) exhibited an eGFP level of 8 937 TFU (Fig. 4-6B).

Conversely, when both strains were grown under identical K_La (i.e., 50), the growth rates diverged: 0.04 h^{-1} for FdhKO eGfp and 0.09 h^{-1} for FdhKO-SdOE eGfp. Under these conditions, eGfp fluorescence was 8.1-fold higher in the FdhKO eGfp strain (28 255 TFU) compared to the FdhKO-SdOE eGfp strain (3 490 TFU). This supports the conclusion that growth rate, rather than oxygen availability, is the dominant factor influencing eGfp fluorescence, reinforcing our hypothesis that cell growth rate has a direct effect on the fluorescence level.

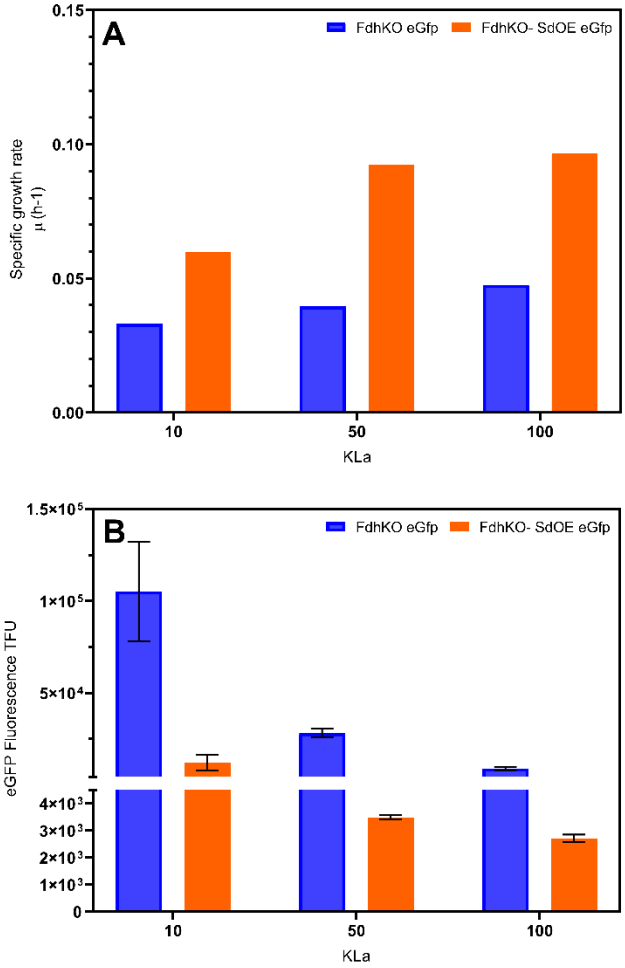

Figure 4-6. Growth rate and eGfp fluorescence in *K. phaffii* mutants cultured under different K_La values in shake-flask cultures. **A:** growth rate; **B:** eGfp fluorescence (TFU). FdhKO eGfp strain (blue), FdhKO-SdOE eGfp strain (orange). Numbers in the figure legend indicate the K_La parameter value in (h^{-1}). Data are the mean and standard deviation of biological triplicate cultures at 22 h in YNB20S.

To further assess whether increased growth rates impair formate accumulation in the FdhKO-SdOE eGfp strain compared to the FdhKO eGfp strain, culture supernatants were collected after 22 hours of growth under different conditions and analyzed using an enzymatic formic acid assay (Fig. 4-7). The formate content exhibited a trend similar to that of the observed eGfp fluorescence levels (Fig 4-7 & Fig 4-6). When the growth rates of both strains were close (i.e., 0.05 h^{-1} for FdhKO

eGfp and 0.06 h^{-1} for FdhKO-SdOE eGfp), the formate concentration differed by 4-fold (i.e., 9.4 and 2.0 µM/ gDCW· L^{-1}). This difference in formate levels could be attributed to a slight increase in the growth rate, which can impact the cell's metabolic state. Fast growth imposes greater demands for nutrients, energy, and biosynthetic precursors, including formate, essential for purine biosynthesis (Christensen and Mackenzie, 2006). Notably, at a lower growth rate (0.03 h^{-1} at KLa 10), the FdhKO eGfp strain exhibited a 98-fold higher formate concentration than the FdhKO-SdOE eGfp strain, grown at a faster rate (0.10 h^{-1} at KLa 100). These increased metabolic requirements could explain the observed variation in formate accumulation. These metabolic demands likely drive the variation in formate levels, which corresponded with significant differences in eGfp fluorescence (Fig. 4-6 B). These results support our hypothesis that higher growth rates in the FdhKO-SdOE eGfp strain limit formate accumulation, leading to reduced induction of p*AOX1* and, consequently, lower synthesis of proteins such as lipase CalB and eGfp.

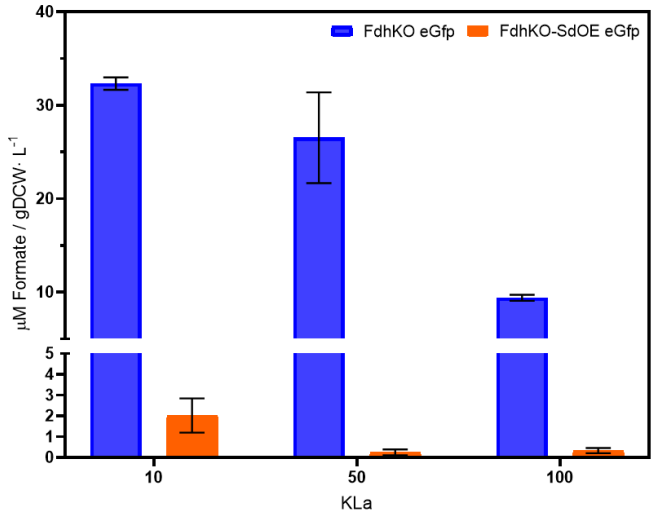

Figure 4-7. Formate concentration in the supernatant of *K. phaffii* mutants cultured under different K_La in shake flask cultures. FdhKO eGfp strain (blue), FdKO-SdOE eGfp strain (orange). Data are the mean and standard deviation from biological triplicate cultures at 22 h in YNB20S.

4. Conclusions

This study aimed to enhance recombinant protein (rProt) production in the FdhKO strain by employing metabolic engineering strategies to improve sorbitol assimilation. While the overexpression of *SOR1* successfully increased sorbitol uptake and promoted cell growth, it unexpectedly led to a decrease in specific rProt production.

Our findings indicate that the elevated growth rates in the FdhKO-SdOE eGfp strain resulted in reduced formate accumulation. This reduction subsequently limited the induction of p*AOX1*, leading to a decrease in the synthesis of recombinant proteins, such as lipase CalB and eGfp. The observed inverse correlation between growth rates and eGfp fluorescence, alongside the significant variations in formate content, supports our hypothesis that growth rate is a critical determinant of protein productivity in systems utilizing formate as an inducer.

Chapter 5

General Discussion

Chapter 5. General discussion

In *Komagataella phaffii*, the induction of the p*AOX1* promoter primarily depends on the use of methanol. However, methanol use carries several disadvantages, prompting efforts to explore alternatives to reduce or eliminate methanol dependency. Recent reports have described new inducers for the p*AOX1* as part of the shift towards methanol-free systems. Therefore, the main objective of this thesis was to develop metabolic engineering strategies in *Komagataella phaffii* that target the metabolism of non-repressor compounds of the p*AOX1* to reduce methanol requirements in recombinant protein production.

Early studies by Tyurin & Kozlov (2015) and Jayachandran et al (2017) identified formic acid and its salts as potential inducers of the p*AOX1*. In our investigation, we corroborated the potential of formate as a p*AOX1* inducer in the Fdh eGfp strain, where induction levels were similar for both formate and methanol (Fig. 3-3). These results align with the findings of Singh & Narang, (2020) and Feng et al., (2022), indicating that metabolites downstream of methanol, such as formate, can also induce p*AOX1*. Therefore, we hypothesized that knocking out the *FDH1* gene in *K. phaffii*, which metabolizes formate into CO_2, could increase intracellular formate levels and potentially enhance the induction of the p*AOX1*. Results from the FdhKO eGfp strain validated this hypothesis (Fig. 3-4), exhibiting 1.9-fold higher fluorescence signals than the Fdh eGfp strain. In contrast, when methanol was used, both strains showed the same fluorescent level, with no improvement (Figs. 3-3 and 3-4), confirming the effectiveness of formate as an inducer of p*AOX1*.

Unlike other studies that used formate along with additional energy sources such as ATP (Feng *et al.*, 2022), overexpressing transcription factors like Mit1 (Liu et al., 2022a) or introducing pathways for formate metabolism (Liu et al., 2022b), our straightforward *FDH1* gene knockout strategy achieved high p*AOX1* induction on sorbitol media. Remarkably, the induction in the FdhKO eGFp strain on sorbitol media reached levels comparable to formate induction without supplementary inducers. Moreover, the FdhKO eGfp strain showed 1.85-fold higher induction levels on sorbitol compared to methanol. This observation was validated by the relative expression levels of the *GFP* gene and fluorescence microscopy. Restoring the *FDH1* gene in the knockout strain removed the auto-induction effect, confirming the role of formate accumulation. Furthermore, the FdhKO methanol-free system was tested with the extracellular protein lipase CalB, demonstrating consistent results in recombinant (rProt) production.

Previous studies on the *FDH1* gene deletion in *Candida boidinni* and *K. phaffii* grown on methanol showed that its primary function is the detoxification of cellular formate, and it is not essential for cell survival (Sakai *et al.*, 1997; Guo *et al.*, 2021). However, further studies in methanol-free cultures have not been reported until this work. In this study, we observed that formate was produced in the FdhKO strains even in methanol-free cultures, suggesting an alternative metabolic pathway. We demonstrated that this alternative metabolic pathway involves THF-C1 metabolism, as evidenced by modulating formate levels through serine or glycine addition and

deleting enzymes in the THF-C1 metabolic pathway (Fig. 3-9). Our supernatant formate analysis proves that increased formate accumulation in the FdhKO strains enhances p*AOX1* induction.

To further optimize this FdhKO methanol-free system, we evaluated various non-repressing carbon sources. (Inan and Meagher, 2001) reported that sorbitol, mannitol, and lactate do not repress p*AOX1*. Both mannitol and sorbitol have previously been used in combination with methanol to enhance rProt production (Eskitoros & Çalık, 2014; Gu et al., 2014; Niu et al., 2013). These sugar alcohols are metabolized into fructose, with mannitol converted via mannitol dehydrogenase and sorbitol via sorbitol dehydrogenase (Çalik *et al.*, 2015). Despite their similar metabolic pathways, sorbitol has been preferred over mannitol due to its higher yields (Chen *et al.*, 2017; Yang and Zhang, 2018). Although lactate has been identified as a non-repressive compound for p*AOX1* (Xie *et al.*, 2005), sorbitol stands out over this compound based on the results presented. Furthermore, when repressive carbon sources like glucose and glycerol were tested, the fluorescence levels in the FdhKO eGfp strain significantly were reduced. This analysis further validates the selection of sorbitol as the primary carbon source in this novel methanol-free system, as it outperformed other carbon sources evaluated (Fig. 4-3).

Given the promising results with sorbitol as a primary carbon source, we further investigated ways to enhance the productivity of the FdhKO strain, specifically addressing the limitation of low energy generation associated with p*AOX1* induction using formate (Feng *et al.*, 2022). To address this, we employed metabolic engineering to enhance the growth of sorbitol media and overcome its metabolic bottleneck limitation by overexpressing the genes encoding sorbitol dehydrogenase *SOR1* and a putative transporter Pp*HXT1*. Our findings show that the overexpression of SOR1 effectively improved sorbitol uptake, resulting in a 3.3-fold increase in the FdhKO-SdOE strain's growth rate compared to the parental FdhKO strain.

Notably, the new system described in this investigation retains the inducible characteristics of p*AOX1*, in contrast with other methanol-free systems reported by (Wang *et al.*, 2017) and (Vogl *et al.*, 2018). When the FdhKO and FdhKO-SdOE strains were cultivated in mixed sorbitol-glycerol cultures, the p*AOX1* under glycerol conditions remained repressed and was only derepressed on glycerol depletion and in the presence of sorbitol. (Fig. 4-6).

However, while *SOR1* overexpression increased growth, it unexpectedly reduced rProt synthesis, with a 1.8-fold reduction in eGfp and a 3.5-fold decrease in lipase CalB synthesis. We hypothesized that the differences in the growth rate between the FdhKO and FdhKO-SdOE strains might be linked to reduced formate availability within the cells. This hypothesis is supported by the fact that at least 25% of the one-carbon units required for de novo purine synthesis are derived from formate (Christensen and Mackenzie, 2006). To examine this further, we modulated oxygen availability to control the growth rates of the FdhKO and FdhKO-SdOE strains, enabling the evaluation of the relationship between growth rate, formate levels, and eGfp synthesis and, thus indirectly, the induction of p*AOX1*. Our findings

confirmed that faster growth rates in the FdhKO-SdOE strain led to reduced intracellular formate accumulation, which in turn diminished the induction of p*AOX1* and reduced rProt synthesis. The inverse relationship between growth rate and eGfp fluorescence, along with the significant differences in formate levels under varying K_La conditions, strongly supports our hypothesis that the balance between cell growth and formate availability is a critical determinant of protein synthesis in this FdhKO system. These findings underscore a critical balance: while metabolic engineering strategies like *SOR1* overexpression can enhance biomass production by accelerating growth rates, they may concurrently reduce the availability of key metabolites, such as formate, which are essential for efficient p*AOX1* induction in the methanol-free system reported. This highlights the need for careful optimization of growth conditions and metabolic fluxes to maximize recombinant protein yields without depleting crucial inducers. Future work should explore strategies to engineer alternative formate biosynthesis pathways to overcome these limitations.

The development of this methanol-free induction system marks a significant step forward in enhancing the safety and cost-effectiveness of industrial bioprocesses, particularly in minimizing methanol use, which is crucial for large-scale production. This shift aligns with growing market demands, as evidenced by the projected increase in the global industrial enzyme market from USD 6.3–6.4 billion in 2021 to USD 8.7 billion by 2026, with a CAGR of 6.3% (Barone *et al.*, 2023). These figures highlight the rising demand for safer and more economical production methods, positioning methanol-free systems as a valuable innovation.

In summary, our study provides key insights into the metabolic dynamics of methanol-free expression systems in *K. phaffii*. It reveals that growth rate and formate availability are intricately linked to p*AOX1* induction and recombinant protein synthesis efficiency in the novel FdhKO strain. By addressing these metabolic bottlenecks, we can further optimize such systems for industrial applications, reducing the reliance on methanol and enhancing the scalability of recombinant protein production.

Chapter 6

Conclusions and perspectives

Chapter 6. Conclusions and perspectives

1. Conclusions

This investigation employed metabolic engineering to explore new strategies to reduce the methanol induction dependency in *Komagataella phaffii* and mitigate the drawbacks associated with methanol. The approach used in this study successfully achieved this goal and provided a better understanding of p*AOX1* induction, leading to the following conclusions:

The deletion of the *FDH1* gene effectively transformed *K. phaffii* into a methanol-free expression system by inhibiting the primary pathway for formate catabolism into CO_2, leading to formate accumulation. Our findings revealed that THF-C1 metabolism is a significant source of intracellular formate, which is continuously generated to support purine synthesis. This accumulated formate was identified as a suitable inducer for p*AOX1*, enabling efficient expression in the *K. phaffii*.

The novel FdhKO methanol-free system developed in this study provides a straightforward and efficient solution to the challenges associated with methanol use in p*AOX1* induction. Unlike other systems that require the introduction of complex metabolic pathways for formate metabolism or the overexpression of transcription factors, this approach eliminates those complexities while maintaining efficient p*AOX1* induction.

The FdhKO methanol-free system developed in this study retains the ability to regulate p*AOX1* induction under culture conditions with glucose or glycerol, distinguishing it from other methanol-free systems that have converted p*AOX1* into a constitutive expression system, where glucose or glycerol serves as both carbon sources and inducers.

Among the non-repressive carbon sources for p*AOX1*, sorbitol emerged as the most effective in the FdhKO methanol-free system. Metabolic engineering aimed at enhancing sorbitol utilization in *K. phaffii* revealed that the primary limitation lies in its metabolism, not transport. Thus, the overexpression of the sorbitol dehydrogenase *SOR1* gene significantly improved sorbitol metabolism, leading to a 3.3-fold increase in the growth rate of *K. phaffii*.

Contrary to expectations, overexpression of the *SOR1* gene to enhance sorbitol metabolism in the formate dehydrogenase-deficient FdhKO strain impaired p*AOX1* induction, leading to a reduction in recombinant protein (rProt) synthesis eGfp and lipase CalB.

Finally, this investigation revealed that the increased growth rate of the FdhKO-SdOE strain led to reduced formate accumulation. This decrease in formate availability subsequently limited the induction of p*AOX1*, resulting in diminished synthesis of recombinant proteins, including eGfp and lipase CalB.

2. Perspectives

This work has provided valuable insights into the development of new methanol-free p*AOX1* induction systems. It uncovers the mechanism behind formate induction on non-repressive carbon sources in a formate dehydrogenase-deficient strain and highlights the use of sorbitol as the optimal carbon source for this newly reported system.

However, several future research perspectives could further enhance this system:

This study has established that intracellular formate, generated via THF-C1 metabolism, effectively induces the p*AOX1* in the FdhKO strain. Future research could focus on enhancing intracellular formate production through metabolic engineering of alternative pathways, such as the serine cycle, which is crucial for one-carbon metabolism by converting serine into glycine and generating one-carbon units. By optimizing these pathways, it may be possible to increase cellular formate availability, thereby improving p*AOX1* induction and enhancing recombinant protein synthesis.

Uncovering the transcription factor mechanisms related to the regulation by formate induction of p*AOX1* in a sorbitol medium could benefit future developments in this strain and other methanol-free systems. Regulatory relationship predictions have been reported for methanol, glycerol, and glucose (Parua *et al.*, 2012; Shen *et al.*, 2016; Zhang *et al.*, 2020). However, no research has been reported in the literature on the use of formate and sorbitol in the same way, despite this non-repressive carbon source being widely used in combination with methanol and, in recent years, with formate (Feng *et al.*, 2022).

The study was conducted using micro-bioreactor and flask scales. The promising results presented in this thesis suggest that future research on the FdhKO and FdhKO-SdOE strains should be carried out at the bioreactor level to optimize and scale up these methanol-free systems. These studies will aim to identify the optimal parameters for enhancing recombinant protein synthesis. These investigations are crucial for refining and optimizing bioprocesses, ultimately advancing their applicability in industrial settings.

The ability to regulate p*AOX1* induction in the FdhKO strain using substrates such as glycerol and sorbitol evidences the flexibility of this system. This characteristic is particularly advantageous for the biopharmaceutical industry, where producing high-quality recombinant proteins is paramount. Future research should prioritize the evaluation and optimization of therapeutic recombinant protein production within this methanol-free system, leveraging bioreactor studies to identify optimal growth conditions and parameters. Such investigations are essential for improving yields and efficiency, ultimately facilitating the scalable production of biopharmaceuticals.

Appendix

Appendix

Appendix 1

Table A3-1. Primer list used in the 3rd chapter

Name	Sequence 5´to 3´	Restriction site
M13-Fw	GTAAAACGACGGCCAGT	
M13-RV	AACAGCTATGACCATG	
P.fdh1-Fw	GGGCAGAAGGATCAGCCTGGACGAAG	
P.fdh1-Rv	GGGGA**GGTCTC**ACCTGCGTGTTTAAGTGGGTG ATGT	BsaI
BleoR.fdh1-Fw	GGG**GGTCTC**GCAGGTCGACAACCCTTA	BsaI
BleoR.fdh1-Rv	GGGC**GGTCTC**ACTTCAGTGACAACGTTGCTGA AGCAGT	BsaI
T.fdh1-Fw	GGC**GGTCTC**TGAAGTGACTTTATGAATTCGCAA	BsaI
T.fdh1-Rv	GGGGTAGCCTCAACAATTGGCAGCTCTTC	
Up.fdh1-Fw	AGAAGAGCATCTCAACTATGCCTATG	
BleoR.Int-Rv	CATGGTTTAGTTCCTCACCTTGTC	
BleoR.Int-Fw	GGAGCAGGACTGATCAGTACTTACTGA	
Dw.fdh1-Rv	GTTCAATGACGAAAAGGTGGTGTTGG	
Fdh1-Fw	AACC**GGTCTC**ACATGAAAATCGTTCTCGTT	BsaI
Fdh1-Rv	ACC**GGTCTC**CAAGCTTTATGCGACCTTTTTG	BsaI
Fdh1.BpiI-Fw	TACTACGACTACCAAGGTCTGCCAAAAGAG	
Fdh1.BpiI-Rv	CTCTTTTGGCAGACCTTGGTAGTCGTAGTA	
pGAp.Int-Fw	CGTCGCTGGCAATAATAGCGG	
Cyc1t.Int-Rv	GGGACCTAGACTTCAGGTTGTC	
P.shm1-Fw	GCATTCCGGAAATAAATCATATGT	
P.shm1-Rv	GCGTCTTCCTTGTTGTGCTTTTCTTTCAATAGTA GAG	
Nat.shm1-Fw	AGCACAACAAGGAAGACGCCGCTCC	
Nat.shm1-Rv	CTATAGTTTAATTGTTTTCAGTGACAACGTTGCT GA	
T.shm1-Fw	AACGTTGTCACTGAAAACAATTAAACTATAGGT GCCTTACT	
T.shm1-Rv	CCTCATCACTGAACAATCTGAG	
Up.shm1-Fw	GCATTGGAAAAGATCGTTTTTATTTG	
Dw.shm1-Rv	GGTATTTGCATGATAGTTTTATCCATTTC	
Nat.Int-Fw	CTGACCAAGGTGTTCCCC	
P.shm2-Fw	TGCAACCTGAGATCTTGAGACA	

P.shm2-Rv	AGGGTTGTCGACCTTTATTTGGATAGGTGGGTA GTTTGG	
BleoR.shm2-Fw	CACCTATCCAAATAAAGGTCGACAACCCTTAAT ATAAC	
BleoR.shm2-Rv	TCACTAATTATATTCGTGGATCTGATATCACCTA ATAAC	
T.shm2-Fw	TGATATCAGATCCACGAATATAATTAGTGAACA AAAGAATATAAATAA	
T.shm2-Rv	GTAATTTCTGCTTCCGGTTCTT	
Up.shm2-Fw	CAAGGTTAACGGTTCACCTATC	
Dw.shm2-Rv	TTCAAATCTTCCAACCCAACTTC	
qAct-F	AGATGGCTCCGAGAAGTTCA	Actin
qAct-R	GTTGCTCAGAGGGCTTCAAC	Actin
qFLD-F	ATCACTGACGGAGGCTTTGA	FLD
qFLD-R	TGGCATTTGAGTACGTCCCT	FLD
qFGH-F	CCCAAATTGCAGGCTGACTT	FGH
qFGH-R	AGTGGGGTTGGAGATTGGAG	FGH
qFDH-F	GCCGATGTTGTTACCGTCAA	FDH
qFDH-R	GTCACCACCGTAACCTCTCA	FDH
qeGFP-F	ATCATGGCCGACAAGCAGAA	EGFP
qeGFP-R	TCTCGTTGGGGTCTTTGCTC	EGFP

Appendix 2

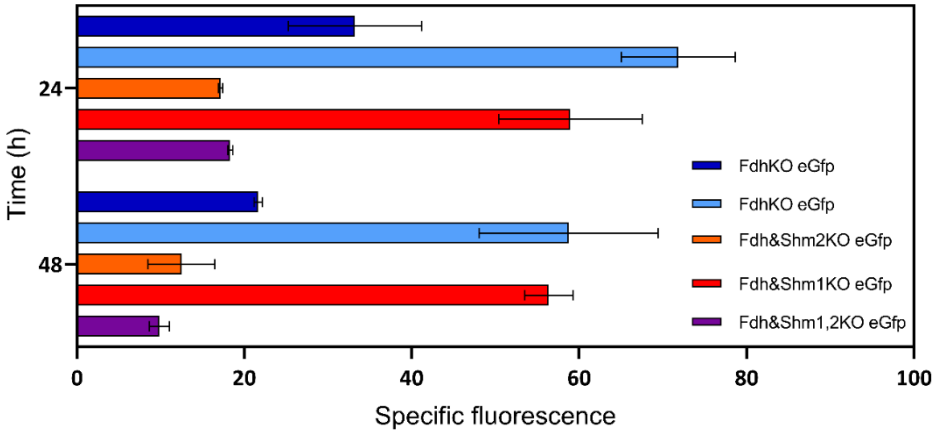

Figure. A3-2. Specific eGFP fluorescence of strain Fdh eGfp strain (growth in YNBS, blue); Fdh eGfp strain (growth in YNBSS, light blue); Fdh&Shm2KO eGfp strain (growth in YNBSS, orange); Fdh&Shm1KO eGfp strain (growth in YNBSS, red); Fdh&Shm1,2KO eGfp strain (growth in YNBSS, purple). Values are the means and standard deviation from two biological replicates conducted in shake flasks. Biomass measures and specific fluoresce unites quantification was detailed in materials and methods.

Appendix 3

Table A4-1. Primer list used in the 4th chapter

Name	Sequence 5´to 3´	Restriction site
M13-Fw	GTAAAACGACGGCCAGT	
M13-RV	AACAGCTATGACCATG	
pGAP.Int-Fw	CGTCGCTGGCAATAATAGCGG	
*ScCYC1*tt.Int-Rv	GGGACCTAGACTTCAGGTTGTC	
Rps3tt.Int-Rv	GACGAGTCCAGGGCTATCTTAAG	
SOR1-Fw	C**GGTCTC**ACATGTCCGATAACCCAAGT GTTATCTTAAAAGGATTAATGAGATTG TCATAGAAGATAGACCAATTCCAGCCA TTGAGGATCCTCACTATGTGAAAATAG CAATCAAAAGACCGGAATTTG	BsaI
SOR1-Rv	C**GGTCTC**CAAGCTTTACTCTGGGCCGT CAATGATAG	BsaI
IntAOXtt.fw	GGCATAATCTGATAGGAGGCC	
IntAOXtt.rv	CCAAGCCTGCGAAGAATGTA	

qAct-F	AGATGGCTCCGAGAAGTTCA	Actin
qAct-R	GTTGCTCAGAGGGCTTCAAC	Actin
qeGFP-F	ATCATGGCCGACAAGCAGAA	EGFP
qeGFP-R	TCTCGTTGGGGTCTTTGCTC	EGFP
ST_qPCR_Fo	CCAGGTGTTTTCGTCGTTGT	PpHxt1
ST_qPCR_Rev	AGGCGAACAGAGTACATCCC	PpHxt1
SDH_qPCR_Fo	CCCGTCTCGTTACAGCAATG	SOR1
SDH_qPCR_Rev	GCATGGACAGCAACACTCAA	SOR1

Appendix 4

Table A4-2. Kinetic parameters of the FdhKO eGfp strain: specific growth rate, substrate-to-biomass yield, and specific substrate consumption rate on various carbon sources.

Medium	μ (h^{-1})	$Y_{X/S}$ ($gDCW\ g^{-1}$)	q_S ($g\ gDCW^{-1}\ h^{-1}$)
Sorbitol	0.040	1.355	0.030
Glycerol	0.267	0.365	0.731
Glucose	0.273	0.601	0.453
Fructose	0.271	0.530	0.512
Mannitol	0.048	2.079	0.023
Lactate	0.017	1.062	0.016

Abbreviations: μ: Specific growth rate; $Y_{X/S:}$ Yield of substrate-into-biomass; q_S: specific substrate consumption rate.

Appendix 5

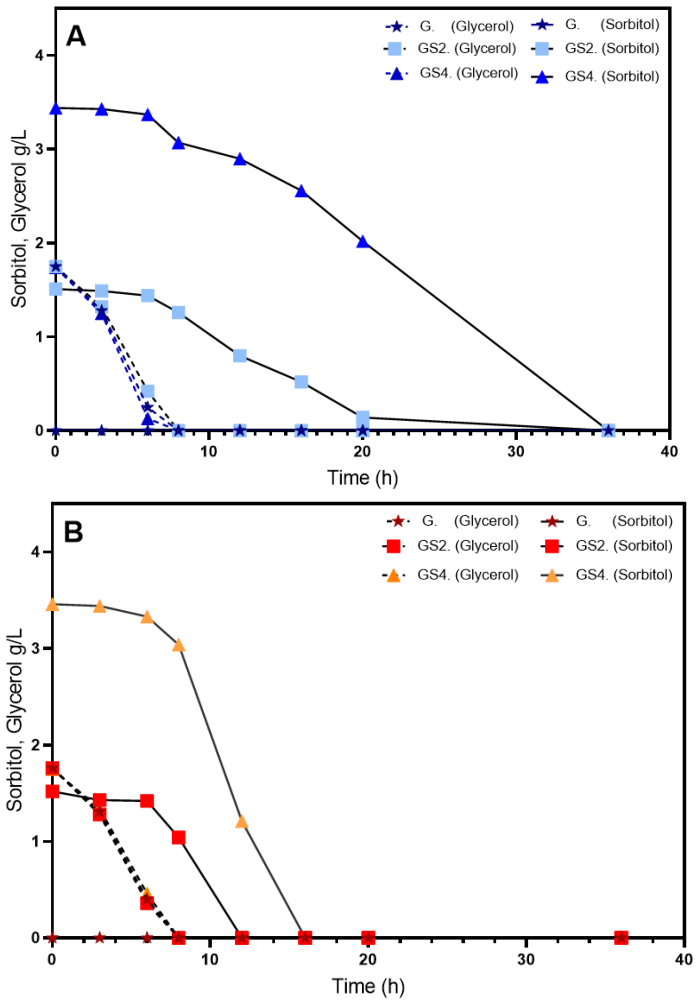

Figure. A4-2. Substrate consumption profile of FdhKO eGfp (A) and FdhKO-SdOE eGfp (B) strains in a glycerol-sorbitol mixed culture media. G: 1.75g L^{-1} glycerol; GS1: 1.75 g L^{-1} glycerol + 0.58 g L^{-1} sorbitol; GS2: 1.75 g L^{-1} glycerol + 1.75 g L^{-1} sorbitol; GS4: 1.75 g L^{-1} glycerol + 3.5 g L^{-1} sorbitol.

Appendix 6

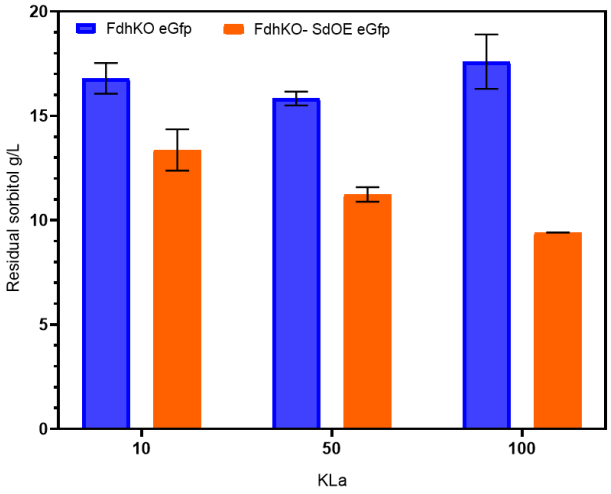

Figure A4-3. Residual sorbitol profile. FdhKO eGfp strain (blue) and FdhKO-SdOE eGfp strain (orange). Data are the mean and standard deviation from biological triplicate cultures at 22 h in YNB20S.

References

References

Ahmad, M., Hirz, M., Pichler, H., and Schwab, H. (2014) Protein expression in *Pichia pastoris*: Recent achievements and perspectives for heterologous protein production. *Appl Microbiol Biotechnol* **98**: 5301–5317.

Akentyev, P., Sokolova, D., Korzhenkov, A., Gubaidullin, I., and Kozlov, D. (2023) Expression level of *SOR1* is a bottleneck for efficient sorbitol utilization by yeast *Komagataella kurtzmanii*. *Yeast* **40**: 414–424.

Arias, C.A.D., Marques, D. de A.V., Malpiedi, L.P., Maranhão, A.Q., Parra, D.A.S., Converti, A., and Junior, A.P. (2017) Cultivation of *Pichia pastoris* carrying the scFv anti LDL (−) antibody fragment. Effect of preculture carbon source. *Brazilian Journal of Microbiology* **48**: 419.

Ata, Ö., Ergün, B.G., Fickers, P., Heistinger, L., Mattanovich, Di., Rebnegger, C., and Gasser, B. (2021) What makes *Komagataella phaffii* non-conventional? *FEMS Yeast Res* **21**: foab059.

Azadi, S., Mahboubi, A., Naghdi, N., Solaimanian, R., and Mortazavi, S.A. (2017) Evaluation of Sorbitol-Methanol Co-Feeding strategy on production of recombinant human growth hormone in *Pichia pastoris*. *Iranian Journal of Pharmaceutical Research* **16**: 1555–1564.

Barone, G.D., Emmerstorfer-Augustin, A., Biundo, A., Pisano, I., Coccetti, P., Mapelli, V., and Camattari, A. (2023) Industrial production of proteins with *Pichia pastoris —Komagataella phaffii*. *Biomolecules* **13**: 441.

Bernauer, L., Radkohl, A., Lehmayer, L.G.K., and Emmerstorfer-Augustin, A. (2021) *Komagataella phaffii* as emerging model organism in fundamental research. *Front Microbiol* **11**: 607028.

Berrios, J., Flores, M.O., Díaz-Barrera, A., Altamirano, C., Martínez, I., and Cabrera, Z. (2017) A comparative study of glycerol and sorbitol as co-substrates in methanol-induced cultures of *Pichia pastoris*: temperature effect and scale-up simulation. *J Ind Microbiol Biotechnol* **44**: 407–411.

Berrios, J., Theron, C.W., Steels, S., Ponce, B., Velastegui, E., Bustos, C., et al. (2022) Role of dissimilative pathway of *Komagataella phaffii* (*Pichia pastoris*): Formaldehyde toxicity and energy metabolism. *Microorganisms 2022, Vol 10, Page 1466* **10**: 1466.

Boehm, T., Pirie-Shepherd, S., Trinh, L.-B., Shiloach, J., and Folkman, J. (1999) Disruption of the *KEX1* gene in *Pichia pastoris* allows expression of full-length murine and human endostatin. *Yeast* **15**: 563–572.

Braun-Galleani, S., Dias, J.A., Coughlan, A.Y., Ryan, A.P., Byrne, K.P., and Wolfe, K.H. (2019) Genomic diversity and meiotic recombination among isolates of the biotech yeast *Komagataella phaffii* (*Pichia pastoris*). *Microb Cell Fact* **18**: 1–13.

Braun-Galleani, S., Henríquez, M.J., and Nesbeth, D.N. (2019) Whole cell biosynthesis of 1-methyl-3-phenylpropylamine and 2-amino-1,3,4-butanetriol

using *Komagataella phaffii* (*Pichia pastoris*) strain BG-10 engineered with a transgene encoding Chromobacterium violaceum ω-transaminase. *Heliyon* **5**: e02338.

Brierley, R.A., Bussineau, C., Kosson, R., Melton, A., and Siegel, R.S. (1990) Fermentation Revelopment of Recombinant *Pichia pastoris* Expressing the Heterologous Gene: Bovine Lysozyme. *Ann N Y Acad Sci* **589**: 350–362.

Burgard, J., Grünwald-Gruber, C., Altmann, F., Zanghellini, J., Valli, M., Mattanovich, D., and Gasser, B. (2020) The secretome of *Pichia pastoris* in fed-batch cultivations is largely independent of the carbon source but changes quantitatively over cultivation time. *Microb Biotechnol* **13**: 479–494.

Bustos, C., Berrios, J., and Fickers, P. (2024) Formate from THF-C1 metabolism induces the *AOX1* promoter in formate dehydrogenase-deficient *Komagataella phaffii*. *Microb Biotechnol* **17**: e70022.

Bustos, C., Quezada, J., Veas, R., Altamirano, C., Braun-Galleani, S., Fickers, P., and Berrios, J. (2022) Advances in cell engineering of the *Komagataella phaffii* Platform for recombinant protein production. *Metabolites* **12**: 346.

Cai, H.L., Doi, R., Shimada, M., Hayakawa, T., and Nakagawa, T. (2021) Metabolic regulation adapting to high methanol environment in the methylotrophic yeast *Ogataea methanolica*. *Microb Biotechnol* **14**: 1512–1524.

Çalik, P., Ata, Ö., Güneş, H., Massahi, A., Boy, E., Keskin, A., et al. (2015) Recombinant protein production in *Pichia pastoris* under glyceraldehyde-3-phosphate dehydrogenase promoter: From carbon source metabolism to bioreactor operation parameters. *Biochem Eng J* **95**: 20–36.

Carly, F., Niu, H., Delvigne, F., and Fickers, P. (2016) Influence of methanol/sorbitol co-feeding rate on p*AOX1* induction in a *Pichia pastoris* Mut+ strain in bioreactor with limited oxygen transfer rate. *J Ind Microbiol Biotechnol* **43**: 517–523.

Çelik, E., Çalık, P., and Oliver, S.G. (2009) Fed-batch methanol feeding strategy for recombinant protein production by *Pichia pastoris* in the presence of co-substrate sorbitol. *Yeast* **26**: 473–484.

Cereghino, J.L. and Cregg, J.M. (2000) Heterologous protein expression in the methylotrophic yeast *Pichia pastoris*. *FEMS Microbiol Rev* **24**: 45–66.

Chen, L., Mohsin, A., Chu, J., Zhuang, Y., Liu, Y., and Guo, M. (2017) Enhanced protein production by sorbitol co-feeding with methanol in recombinant *Pichia pastoris Strains*. *Biotechnology and Bioprocess Engineering* **22**: 767–773.

Chiruvolu, V., Cregg, J.M., and Meagher, M.M. (1997) Recombinant protein production in an alcohol oxidase-defective strain of *Pichia pastoris* in fedbatch fermentations. *Enzyme Microb Technol* **21**: 277–283.

Christensen, K.E. and Mackenzie, R.E. (2006) Mitochondrial one-carbon metabolism is adapted to the specific needs of yeast, plants and mammals. *BioEssays* **28**: 595–605.

Collins, T.J. (2007) ImageJ for microscopy. *Biotechniques* **43**: 25–30.

Cotton, C.A., Claassens, N.J., Benito-Vaquerizo, S., and Bar-Even, A. (2020) Renewable methanol and formate as microbial feedstocks. *Curr Opin Biotechnol* **62**: 168–180.

Diaz Arias, C.A., Molino, J.V.D., de Araújo Viana Marques, D., Queiroz Maranhão, A., Abdalla Saes Parra, D., Pessoa Junior, A., and Converti, A. (2019) Influence of carbon source on cell size and production of anti LDL (-) single-chain variable fragment by a recombinant *Pichia pastoris strain*. *Mol Biol Rep* **46**: 3257–3264.

Ergün, B.G., Berrios, J., Binay, B., and Fickers, P. (2021) Recombinant protein production in *Pichia pastoris*: from transcriptionally redesigned strains to bioprocess optimization and metabolic modelling. *FEMS Yeast Res* **21**: foab057.

Ergün, B.G., Demir, İ., Özdamar, T.H., Gasser, B., Mattanovich, D., and Çalık, P. (2020) Engineered deregulation of expression in yeast with designed hybrid-promoter architectures in coordination with discovered master regulator transcription factor. *Adv Biosyst* **4**: 1900172.

Ergün, B.G., Laçın, K., Çaloğlu, B., and Binay, B. (2022) Second generation *Pichia pastoris* strain and bioprocess designs. *Biotechnology for Biofuels and Bioproducts* **15**: 150.

Eskitoros, M.Ş. and Çalık, P. (2014) Co-substrate mannitol feeding strategy design in semi-batch production of recombinant human erythropoietin production by *Pichia pastoris*. *Journal of Chemical Technology & Biotechnology* **89**: 644–651.

Feng, A., Zhou, J., Mao, H., Zhou, H., and Zhang, J. (2022) Heterologous protein expression enhancement of *Komagataella phaffii* by ammonium formate induction based on transcriptomic analysis. *Biochem Eng J* **185**: 108503.

Fickers, P., Nicaud, J.M., Destain, J., and Thonart, P. (2003) Overproduction of lipase by *Yarrowia lipolytica* mutants. *Appl Microbiol Biotechnol* **63**: 136–142.

Gabba, M., Frallicciardi, J., van 't Klooster, J., Henderson, R., Syga, Ł., Mans, R., et al. (2020) Weak acid permeation in synthetic lipid vesicles and across the yeast plasma membrane. *Biophys J* **118**: 422–434.

Gao, J., Jiang, L., and Lian, J. (2021) Development of synthetic biology tools to engineer *Pichia pastoris* as a chassis for the production of natural products. *Synth Syst Biotechnol* **6**: 110–119.

García-Ortega, X., Cámara, E., Ferrer, P., Albiol, J., Montesinos-Seguí, J.L., and Valero, F. (2019) Rational development of bioprocess engineering strategies for recombinant protein production in *Pichia pastoris (Komagataella phaffii)* using the methanol-free GAP promoter. Where do we stand? *N Biotechnol* **53**: 24–34.

Gassler, T., Sauer, M., Gasser, B., Egermeier, M., Troyer, C., Causon, T., et al. (2020) The industrial yeast *Pichia pastoris* is converted from a heterotroph into an autotroph capable of growth on CO2. *Nat Biotechnol* **38**: 210–216.

Geertman, J.M.A., van Maris, A.J.A., van Dijken, J.P., and Pronk, J.T. (2006) Physiological and genetic engineering of cytosolic redox metabolism in *Saccharomyces cerevisiae* for improved glycerol production. *Metab Eng* **8**: 532–542.

Geier, M., Brandner, C., Strohmeier, G.A., Hall, M., Hartner, F.S., and Glieder, A. (2015) Engineering *Pichia pastoris* for improved NADH regeneration: A novel chassis strain for whole-cell catalysis. *Beilstein Journal of Organic Chemistry* **11**: 1741–1748.

Gorczyca, M., Kaźmierczak, J., Steels, S., Fickers, P., and Celińska, E. (2020) Impact of oxygen availability on heterologous gene expression and polypeptide secretion dynamics in *Yarrowia lipolytica*-based protein production platforms. *Yeast* **37**: 559–568.

Gu, L., Zhang, J., Liu, B., Du, G., and Chen, J. (2014) High-level extracellular production of glucose oxidase by recombinant *Pichia Pastoris* using a combined strategy. *Appl Biochem Biotechnol* **175**: 1429–1447.

Guo, F., Dai, Z., Peng, W., Zhang, S., Zhou, J., Ma, J., et al. (2021) Metabolic engineering of *Pichia pastoris* for malic acid production from methanol. *Biotechnol Bioeng* **118**: 357–371.

Hartner, F.S. and Glieder, A. (2006) Regulation of methanol utilisation pathway genes in yeasts. *Microb Cell Fact* **5**: 39.

Hazeu, W. and Donker, R.A. (1983) A continuous culture study of methanol and formate utilization by the yeast *Pichia pastoris*. *Biotechnol Lett* **5**: 399–404.

He, H., Wu, S., Mei, M., Ning, J., Li, C., Ma, L., et al. (2020) A combinational strategy for effective heterologous production of functional human lysozyme in *Pichia pastoris*. *Front Bioeng Biotechnol* **8**: 118.

Heistinger, L., Gasser, B., and Mattanovich, D. (2018) Creation of stable heterothallic strains of *Komagataella phaffii* enables dissection of mating gene regulation. *Mol Cell Biol* **38**: e00398-17.

Heistinger, L., Gasser, B., and Mattanovich, D. (2020) Microbe profile: *Komagataella phaffii*: A methanol devouring biotech yeast formerly known as *Pichia pastoris*. *Microbiology (United Kingdom)* **166**: 614–616.

Henríquez, M.J., Braun-Galleani, S., and Nesbeth, D.N. (2020) Whole cell biosynthetic activity of *Komagataella phaffii* (*Pichia pastoris*) GS115 strains engineered with transgenes encoding *Chromobacterium violaceum* ω-transaminase alone or combined with native transketolase. *Biotechnol Prog* **36**: e2893.

Inan, M. and Meagher, M.M. (2001) Non-repressing carbon sources for alcohol oxidase (*AOX1*) promoter of *Pichia pastoris*. *J Biosci Bioeng* **92**: 585–589.

Jayachandran, C., Palanisamy Athiyaman, B., and Sankaranarayanan, M. (2017) Formate co-feeding improved *Candida antarctica* Lipase B activity in *Pichia pastoris*. *Res J Biotechnol* **12**: 29–36.

Jhong, H.R.M., Ma, S., and Kenis, P.J. (2013) Electrochemical conversion of CO2 to useful chemicals: current status, remaining challenges, and future opportunities. *Curr Opin Chem Eng* **2**: 191–199.

Jia, L., Li, T., Wu, Y., Wu, C., Li, H., and Huang, A. (2021) Enhanced human lysozyme production by *Pichia pastoris* via periodic glycerol and dissolved oxygen concentrations control. *Appl Microbiol Biotechnol* **105**: 1041–1050.

Jia, L., Mpofu, E., Tu, T., Huai, Q., Sun, J., Chen, S., et al. (2017) Transcriptional analysis for carbon metabolism and kinetic modeling for heterologous proteins productions by *Pichia pastoris* in induction process with methanol/sorbitol co-feeding. *Process Biochemistry* **59**: 159–166.

Jordan, P., Choe, J.Y., Boles, E., and Oreb, M. (2016) Hxt13, Hxt15, Hxt16 and Hxt17 from *Saccharomyces cerevisiae* represent a novel type of polyol transporters. *Sci Rep* **6**: 23502.

Juturu, V. and Wu, J.C. (2018) Heterologous protein expression in *Pichia pastoris*: Latest research progress and applications. *ChemBioChem* **19**: 7–21.

Kafri, M., Metzl-Raz, E., Jona, G., and Barkai, N. (2016) The cost of protein production. *Cell Rep* **14**: 22–31.

Kastanos, E.K., Woldman, Y.Y., and Appling, D.R. (1997) Role of mitochondrial and cytoplasmic serine hydroxymethyltransferase isozymes in de Novo purine synthesis in *Saccharomyces* cerevisiae. *Biochemistry* **36**: 14956–14964.

Khlebodarova, T.M., Bogacheva, N. V., Zadorozhny, A. V., Bryanskaya, A. V., Vasilieva, A.R., Chesnokov, D.O., et al. (2024) *Komagataella phaffii* as a platform for heterologous expression of enzymes used for industry. *Microorganisms 2024, Vol 12, Page 346* **12**: 346.

Kickenweiz, T., Glieder, A., and Wu, J.C. (2018) Construction of a cellulose-metabolizing *Komagataella phaffii* (*Pichia pastoris*) by co-expressing glucanases and β-glucosidase. *Appl Microbiol Biotechnol* **102**: 1297–1306.

Kim, S. and Hahn, J.S. (2015) Efficient production of 2,3-butanediol in *Saccharomyces cerevisiae* by eliminating ethanol and glycerol production and redox rebalancing. *Metab Eng* **31**: 94–101.

Krainer, F.W., Dietzsch, C., Hajek, T., Herwig, C., Spadiut, O., and Glieder, A. (2012) Recombinant protein expression in *Pichia pastoris* strains with an engineered methanol utilization pathway. *Microb Cell Fact* **11**: 22.

Kurtzman, C.P. (2009) Biotechnological strains of *Komagataella* (*Pichia*) *pastoris* are *Komagataella phaffii* as determined from multigene sequence analysis. *J Ind Microbiol Biotechnol* **36**: 1435–1438.

Li, P., Sun, H., Chen, Z., Li, Y., and Zhu, T. (2015) Construction of efficient xylose utilizing *Pichia pastoris* for industrial enzyme production. *Microb Cell Fact* **14**: 1–10.

Lin-Cereghino, G.P., Godfrey, L., Cruz, B.J. de la, Johnson, S., Khuongsathiene, S., Tolstorukov, I., et al. (2006) Mxr1p, a key regulator of the methanol utilization pathway and peroxisomal genes in *Pichia pastoris*. *Mol Cell Biol* **26**: 883.

Lin-Cereghino, J., Wong, W.W., Xiong, S., Giang, W., Luong, L.T., Vu, J., et al. (2005) Condensed protocol for competent cell preparation and transformation of the methylotrophic yeast *Pichia pastoris*. *Biotechniques* **38**: 44–48.

Liu, B., Li, H., Zhou, H., and Zhang, J. (2022) Enhancing xylanase expression by *Komagataella phaffii* by formate as carbon source and inducer. *Appl Microbiol Biotechnol* **106**: 7819–7829.

Liu, B., Zhao, Y., Zhou, H., and Zhang, J. (2022) Enhancing xylanase expression of *Komagataella phaffii* induced by formate through Mit1 co-expression. *Bioprocess Biosyst Eng* **45**: 1515–1525.

Liu, T., Liu, B., Zhou, H., and Zhang, J. (2021) Knockout of the *DAS* gene increases *S* -adenosylmethionine production in *Komagataella phaffii*. *Biotechnology & Biotechnological Equipment* **35**: 29–36.

Liu, T., Zhao, Y., Zhang, Jianguo, and Zhang, Jining (2019) Enhancement of xylanase expression by *Komagataella phaffii* through pexophagy inhibition. *Biotechnology and Biotechnological Equipment* **33**: 855–862.

Liu, W. cang, Zhou, F., Xia, D., and Shiloach, J. (2019) Expression of multidrug transporter P-glycoprotein in *Pichia pastoris* affects the host's methanol metabolism. *Microb Biotechnol* **12**: 1226–1236.

Liu, W., Xiang, H., Zhang, T., Pang, X., Su, J., Liu, H., et al. (2020) Development of a new high-cell density fermentation strategy for enhanced production of a fungus β-glucosidase in *Pichia pastoris*. *Front Microbiol* **11**: 549751.

Liu, W.C., Inwood, S., Gong, T., Sharma, A., Yu, L.Y., and Zhu, P. (2019) Fed-batch high-cell-density fermentation strategies for *Pichia pastoris* growth and production. *Crit Rev Biotechnol* **39**: 258–271.

Macauley-Patrick, S., Fazenda, M.L., McNeil, B., and Harvey, L.M. (2005) Heterologous protein production using the *Pichia pastoris* expression system. *Yeast* **22**: 249–270.

Maccani, A., Landes, N., Stadlmayr, G., Maresch, D., Leitner, C., Maurer, M., et al. (2014) *Pichia pastoris* secretes recombinant proteins less efficiently than Chinese hamster ovary cells but allows higher space-time yields for less complex proteins. *Biotechnol J* **9**: 526–537.

Marx, H., Mattanovich, D., and Sauer, M. (2008) Overexpression of the riboflavin biosynthetic pathway in *Pichia pastoris*. *Microb Cell Fact* **7**: 1–11.

Mattanovich, D., Graf, A., Stadlmann, J., Dragosits, M., Redl, A., Maurer, M., et al. (2009) Genome, secretome and glucose transport highlight unique features of the protein production host *Pichia pastoris*. *Microb Cell Fact* **8**: 1–13.

Mitic, B.M., Troyer, C., Lutz, L., Baumschabl, M., Hann, S., and Mattanovich, D. (2023) The oxygen-tolerant reductive glycine pathway assimilates methanol, formate and CO2 in the yeast *Komagataella phaffii*. *Nature Communications 2023 14:1* **14**: 1–13.

Nakagawa, T., Wakayama, K., and Hayakawa, T. (2015) Selection of suitably non-repressing carbon sources for expression of alcohol oxidase isozyme promoters in the methylotrophic yeast *Pichia methanolica*. *J Biosci Bioeng* **120**: 41–44.

Nieto-Taype, M.A., Garcia-Ortega, X., Albiol, J., Montesinos-Seguí, J.L., and Valero, F. (2020) Continuous cultivation as a tool toward the rational bioprocess development with *Pichia Pastoris* Cell factory. *Front Bioeng Biotechnol* **8**: 632.

Niu, H., Jost, L., Pirlot, N., Sassi, H., Daukandt, M., Rodriguez, C., and Fickers, P. (2013) A quantitative study of methanol/sorbitol co-feeding process of a *Pichia pastoris* Mut+/pAOX1-lacZ strain. *Microb Cell Fact* **12**: 33.

Nocon, J., Steiger, M., Mairinger, T., Hohlweg, J., Rußmayer, H., Hann, S., et al. (2016) Increasing pentose phosphate pathway flux enhances recombinant protein production in *Pichia pastoris*. *Appl Microbiol Biotechnol* **100**: 5955–5963.

O'Flaherty, R., Bergin, A., Flampouri, E., Mota, L.M., Obaidi, I., Quigley, A., et al. (2020) Mammalian cell culture for production of recombinant proteins: A review of the critical steps in their biomanufacturing. *Biotechnol Adv* **43**: 107552.

Park, Y.R., Su, X.D., Shrestha, S.K., Yang, S.Y., and Soh, Y. (2022) 2E-Decene-4,6-diyn-1-ol-acetate inhibits osteoclastogenesis through mitogen-activated protein kinase-c-Fos-NFATc1 signalling pathways. *Clin Exp Pharmacol Physiol* **49**: 341–349.

Parua, P.K., Ryan, P.M., Trang, K., and Young, E.T. (2012) *Pichia pastoris* 14-3-3 regulates transcriptional activity of the methanol inducible transcription factor Mxr1 by direct interaction. *Mol Microbiol* **85**: 282–298.

Paulová, L., Hyka, P., Branská, B., Melzoch, K., and Kovar, K. (2012) Use of a mixture of glucose and methanol as substrates for the production of recombinant trypsinogen in continuous cultures with *Pichia pastoris* Mut+. *J Biotechnol* **157**: 180–188.

Peña, D.A., Gasser, B., Zanghellini, J., Steiger, M.G., and Mattanovich, D. (2018) Metabolic engineering of *Pichia pastoris*. *Metab Eng* **50**: 2–15.

Phaff, H.J., Miller, M.W., and Shifrine, M. (1956) The taxonomy of yeasts isolated from *Drosophila* in the Yosemite region of California. *Antonie Van Leeuwenhoek* **22**: 145–161.

Piper, M.D., Hong, S.P., Ball, G.E., and Dawes, I.W. (2000) Regulation of the balance of one-carbon metabolism in *Saccharomyces cerevisiae*. *Journal of Biological Chemistry* **275**: 30987–30995.

Potvin, G., Zhang, Z., Defela, A., and Lam, H. (2016) Screening of alternative carbon sources for recombinant protein production in *Pichia pastoris*. *International Journal of Chemical Reactor Engineering* **14**: 251–257.

Prabhu, A.A. and Veeranki, V.D. (2018) Metabolic engineering of *Pichia pastoris* GS115 for enhanced pentose phosphate pathway (PPP) flux toward recombinant human interferon gamma (hIFN-γ) production. *Mol Biol Rep* **45**: 961–972.

Prielhofer, R., Barrero, J.J., Steuer, S., Gassler, T., Zahrl, R., Baumann, K., et al. (2017) GoldenPiCS: a Golden Gate-derived modular cloning system for applied synthetic biology in the yeast *Pichia pastoris*. *BMC Syst Biol* **11**: 123.

Raschmanová, H., Weninger, A., Knejzlík, Z., Melzoch, K., and Kovar, K. (2021) Engineering of the unfolded protein response pathway in *Pichia pastoris*: enhancing production of secreted recombinant proteins. *Applied Microbiology and Biotechnology 2021 105:11* **105**: 4397–4414.

Raza, A., Pothula, R., Abdelgaffar, H., Bashir, S., and Jurat-Fuentes, J.L. (2020) Identification and functional characterization of a β-glucosidase from *Bacillus*

tequelensis BD69 expressed in bacterial and yeast heterologous systems. *PeerJ* **2020**: e8792.

Rebnegger, C., Coltman, B.L., Kowarz, V., Peña, D.A., Mentler, A., Troyer, C., et al. (2024) Protein production dynamics and physiological adaptation of recombinant *Komagataella phaffii* at near-zero growth rates. *Microb Cell Fact* **23**: 1–20.

Riley, R., Haridas, S., Wolfe, K.H., Lopes, M.R., Hittinger, C.T., Göker, M., et al. (2016) Comparative genomics of biotechnologically important yeasts. *Proc Natl Acad Sci U S A* **113**: 9882–7.

Rußmayer, H., Buchetics, M., Mattanovich, M., Neubauer, S., Steiger, M., Graf, A.B., et al. (2023) Customizing amino acid metabolism of *Pichia pastoris* for recombinant protein production. *Biotechnol J* **18**: 2300033.

Sakai, Y., Murdanoto, A.P., Konishi, T., Iwamatsu, A., and Kato, N. (1997) Regulation of the formate dehydrogenase gene, *FDH1*, in the methylotrophic yeast *Candida boidinii* and growth characteristics of an FDH1- disrupted strain on methanol, methylamine, and choline. *J Bacteriol* **179**: 4480–4485.

Sakai, Y., Nakagawa, T., Shimase, M., and Kato, N. (1998) Regulation and physiological role of the *DAS1* gene, encoding dihydroxyacetone synthase, in the methylotrophic yeast *Candida boidinii*. *J Bacteriol* **180**: 5885–5890.

Sales-Vallverdú, A., Gasset, A., Requena-Moreno, G., Valero, F., Montesinos-Seguí, J.L., and Garcia-Ortega, X. (2024) Synergic kinetic and physiological control to improve the efficiency of *Komagataella phaffii* recombinant protein production bioprocesses. *Microb Biotechnol* **17**: e14411.

Sambrook, J. and Russell, D.W. (2001) Molecular cloning: a laboratory manual, 3rd Edition. New York: Cold Spring Harbor Laboratory Press.

Sassi, H., Delvigne, F., Kar, T., Nicaud, J.M., Coq, A.M.C. Le, Steels, S., and Fickers, P. (2016) Deciphering how *LIP2* and *POX2* promoters can optimally regulate recombinant protein production in the yeast *Yarrowia lipolytica*. *Microb Cell Fact* **15**: 159.

Schneider, C.A., Rasband, W.S., and Eliceiri, K.W. (2012) NIH Image to ImageJ: 25 years of image analysis. *Nature Methods 2012 9:7* **9**: 671–675.

Schwarzhans, J.P., Luttermann, T., Geier, M., Kalinowski, J., and Friehs, K. (2017) Towards systems metabolic engineering in *Pichia pastoris*. *Biotechnol Adv* **35**: 681–710.

Shen, W., Xue, Y., Liu, Y., Kong, C., Wang, X., Huang, M., et al. (2016) A novel methanol-free *Pichia pastoris* system for recombinant protein expression. *Microb Cell Fact* **15**: 1–11.

Shinobu Takagi, Noriko Tsutsumi, Yuji Terui, and XiangYu Kong (2012) Method for methanol independent induction from methanol inducible promoters in *Pichia*.

Sibirny, A.A., Ubiyvovk, V.M., Gonchar, M. V., Titorenko, V.I., Voronovsky, A.Y., Kapultsevich, Y.G., and Bliznik, K.M. (1990) Reactions of direct formaldehyde oxidation to CO2 are non-essential for energy supply of yeast methylotrophic growth. *Arch Microbiol* **154**: 566–575.

Singh, A. and Narang, A. (2023) PAOX1 expression in mixed-substrate continuous cultures of Komagataella phaffii (Pichia pastoris) is completely determined by methanol consumption regardless of the secondary carbon source. *Front Bioeng Biotechnol* **11**: 1123703.

Singh, A. and Narang, A. (2020) The Mut+ strain of *Komagataella phaffii* (*Pichia pastoris*) expresses P*AOX1* 5 and 10 times faster than Muts and Mut− strains: evidence that formaldehyde or/and formate are true inducers of P*AOX1*. *Appl Microbiol Biotechnol* **104**: 7801–7814.

Theron, C.W., Berrios, J., Delvigne, F., and Fickers, P. (2018) Integrating metabolic modeling and population heterogeneity analysis into optimizing recombinant protein production by *Komagataella (Pichia) pastoris*. *Appl Microbiol Biotechnol* **102**: 63–80.

Theron, C.W., Berrios, J., Steels, S., Telek, S., Lecler, R., Rodriguez, C., and Fickers, P. (2019) Expression of recombinant enhanced green fluorescent protein provides insight into foreign gene-expression differences between Mut+ and MutS strains of *Pichia pastoris*. *Yeast* **36**: 285–296.

Thorpe, E.D., D'Anjou, M.C., and Daugulis, A.J. (1999) Sorbitol as a non-repressing carbon source for fed-batch fermentation of recombinant *Pichia pastoris*. *Biotechnol Lett* **21**: 669–672.

Toivari, M.H., Salusjärvi, L., Ruohonen, L., and Penttilä, M. (2004) Endogenous xylose pathway in *Saccharomyces cerevisiae*. *Appl Environ Microbiol* **70**: 3681–3686.

Tomàs-Gamisans, M., Andrade, M., Maresca, C., Monforte, F., Ferrer, S., and Albiol, P. (2020) Redox engineering by ectopic overexpression of NADH kinase in recombinant *Pichia pastoris* (*Komagataella phaffii*): Impact on cell physiology and recombinant production of secreted proteins.

Türkanoğlu Özçelik, A., Yılmaz, S., and Inan, M. (2019) *Pichia pastoris* promoters. *Methods in Molecular Biology* **1923**: 97–112.

Tyurin, O. V. and Kozlov, D.G. (2015) Deletion of the *FLD* gene in methylotrophic yeasts *Komagataella phaffii* and *Komagataella kurtzmanii* results in enhanced induction of the *AOX1* promoter in response to either methanol or formate. *Microbiology (Russian Federation)* **84**: 408–411.

Velastegui, E., Theron, C., Berrios, J., and Fickers, P. (2019) Downregulation by organic nitrogen of *AOX1* promoter used for controlled expression of foreign genes in the yeast *Pichia pastoris*. *Yeast* **36**: 297–304.

Vogl, T. and Glieder, A. (2013) Regulation of *Pichia pastoris* promoters and its consequences for protein production. *N Biotechnol* **30**: 385–404.

Vogl, T., Sturmberger, L., Fauland, P.C., Hyden, P., Fischer, J.E., Schmid, C., et al. (2018) Methanol independent induction in *Pichia pastoris* by simple derepressed overexpression of single transcription factors. *Biotechnol Bioeng* **115**: 1037–1050.

Wang, J., Wang, X., Shi, L., Qi, F., Zhang, P., Zhang, Y., et al. (2017) Methanol-independent protein expression by *AOX1* promoter with trans-acting elements

engineering and glucose-glycerol-shift Induction in *Pichia pastoris*. *Scientific Reports 2017 7:1* **7**: 1–12.

Wang, X., Cai, M., Shi, L., Wang, Q., Zhu, J., Wang, J., et al. (2016) PpNrg1 is a transcriptional repressor for glucose and glycerol repression of *AOX1* promoter in methylotrophic yeast *Pichia pastoris*. *Biotechnol Lett* **38**: 291–298.

Wang, X., Wang, Q., Wang, J., Bai, P., Shi, L., Shen, W., et al. (2016) Mit1 Transcription factor mediates methanol signaling and regulates the alcohol oxidase 1 (*AOX1*) promoter in *Pichia pastoris*. *Journal of Biological Chemistry* **291**: 6245–6261.

Wang, Y., Li, J., Zhao, F., Zhang, Y., Yang, X., Lin, Y., and Han, S. (2022) Methanol oxidase from *Hansenula polymorpha* shows activity in peroxisome-deficient *Pichia pastoris*. *Biochem Eng J* **180**: 108369.

Xia, W., Hu, M., Pan, Y., Wu, D., and Wu, J. (2021) Improved production of streptomyces sp. Fa1 xylanase in a dual-plasmid *Pichia pastoris* system. *Curr Issues Mol Biol* **43**: 2289–2304.

Xie, J., Zhou, Q., Du, P., Gan, R., and Ye, Q. (2005) Use of different carbon sources in cultivation of recombinant *Pichia pastoris* for angiostatin production. *Enzyme Microb Technol* **36**: 210–216.

Xu, Q., Bai, C., Liu, Y., Song, L., Tian, L., Yan, Y., et al. (2019) Modulation of acetate utilization in *Komagataella phaffii* by metabolic engineering of tolerance and metabolism. *Biotechnol Biofuels* **12**: 1–14.

Yang, Z. and Zhang, Z. (2018) Engineering strategies for enhanced production of protein and bio-products in *Pichia pastoris*: A review. *Biotechnol Adv* **36**: 182–195.

Zavec, D., Gasser, B., and Mattanovich, D. (2020) Characterization of methanol utilization negative *Pichia pastoris* for secreted protein production: New cultivation strategies for current and future applications. *Biotechnol Bioeng* **117**: 1394–1405.

Zavec, D., Troyer, C., Maresch, D., Altmann, F., Hann, S., Gasser, B., and Mattanovich, D. (2021) Beyond alcohol oxidase: the methylotrophic yeast *Komagataella phaffii* utilizes methanol also with its native alcohol dehydrogenase Adh2. *FEMS Yeast Res* **21**: foab009.

Zepeda, A.B., Pessoa, A., and Farías, J.G. (2018) Carbon metabolism influenced for promoters and temperature used in the heterologous protein production using *Pichia pastoris* yeast. *Brazilian Journal of Microbiology* **49**: 119–127.

Zhang, C., Ma, Y., Miao, H., Tang, X., Xu, B., Wu, Q., et al. (2020) Transcriptomic analysis of *Pichia pastoris* (*Komagataella phaffii*) GS115 during heterologous protein production using a high-cell-density Fed-Batch cultivation strategy. *Front Microbiol* **11**: 463.

Zhang, P., Zhang, W., Zhou, X., Bai, P., Cregg, J.M., and Zhang, Y. (2010) Catabolite Repression of Aox in *Pichia pastoris* is dependent on hexose transporter PpHxt1 and pexophagy. *Appl Environ Microbiol* **76**: 6108–6118.

Zhang, W., Hywood Potter, K.J., Plantz, B.A., Schlegel, V.L., Smith, L.A., and Meagher, M.M. (2003) *Pichia pastoris* fermentation with mixed-feeds of glycerol and methanol: growth kinetics and production improvement. *J Ind Microbiol Biotechnol* **30**: 210–215.

Zhu, T., Sun, H., Wang, M., and Li, Y. (2019) *Pichia pastoris* as a Versatile Cell Factory for the Production of Industrial Enzymes and Chemicals: Current Status and Future Perspectives. *Biotechnol J* **14**: 1–13.